Department of Aeronautics and Astronautics
Stanford University
Stanford, California

MINIMUM-FUEL ATTITUDE CONTROL OF A RIGID BODY IN ORBIT BY AN EXTENDED METHOD OF STEEPEST-DESCENT

by

K. A. Hales

and

I. Flügge-Lotz

ACKNOWLEDGEMENT

SUMMARY

It is desired to compute the minimum-fuel attitude control of a rigid body in orbit with bounds on the control components. The control components enter the system differential equations linearly. Application of the maximum principle of Pontryagin indicates that the form of the control is a series of pulses. An extended version of the method of steepest-descent is derived which enables the switching times of the control pulses to be moved until an extremum value of the cost functional is approximated.

The attitude acquisition problem of a satellite in an elliptical orbit is selected as a potential application of this extended method of steepest-descent. Trajectories computed by this method are compared both with true optimal trajectories and with trajectories generated by an idealized feedback control scheme.

The major benefits derived from the solution of the spacecraft acquisition problem by the present method are that (1) a great deal is learned about the effectiveness of the method in solving optimization problems where the switching times of the bounded control components are treated as control parameters, and (2) state trajectories for the acquisition problem are generated which may be used for comparison purposes when considering the worth of sub-optimal feedback control schemes.

TABLE OF CONTENTS

Table of Contents (Continued)

LIST OF TABLES

LIST OF ILLUSTRATIONS

vii

List of Illustrations (Continued)

List of Illustrations (Continued)

LIST OF SYMBOLS

A	see expression (A-10)
$C(t_o)$	see expression (B-8)
$D(t_o)$	see expression (B-17)
$F(t)$, $G(t)$	see expression (5-3)
G	the universal gravitational constant
G_i	matrix $G(t)$ at $t = t_i$
H	Hamiltonian function -- see expression (2-5)
I	identity matrix
I_x, I_y, I_z	satellite centroidal principal moments of inertia
J	cost functional
J'	see Figure 6-10
K_x, K_y, K_z	inertia parameters -- see expression (A-13)
$L_1(t), L_2(t_o)$	see expression (B-11)
M	the mass of P
$M(t)$	see expression (A-24)
$N_1(t_i), N_2(t_o)$	see expression (B-20)
N_x, N_y, N_z	components of external torque in body coordinates
N_{xg}, N_{yg}, N_{zg}	components of the gravity gradient torque -- see expression (A-21)
P, P*	see Figure A-1
R, V	see expression (A-2)
S, E_i	see expression (A-26)
T_i	weighting matrix -- see expression (5-25)

U_i	see expression (1-1)
V	"mean-square" variation in control -- see expression (5-15)
V^*	augmented functional -- see expression (B-4)
W_i	Euler parameters -- see expression (A-15)
$W(\tau)$	weighting matrix -- see expression (5-15)
a	major semidiameter of ellipse
a_{ij}	direction cosines, elements of rotation matrix A -- see expression (A-10)
d_i	see expression (1-1)
$\bar{e}$	eigenvector of the transformation matrix A corresponding to the eigenvalue of $+1$. (e_x, e_y, e_z) are the components.
$\bar{f}(\bar{x}, \bar{u}, t)$	right-hand side of vector differential equation
k_1, k_2, k_3, k_p	rate and position gains -- see expression (6-1)
m	number of components in $\bar{u}$
$M(t)$	see expression (A-24)
m_{ij}	components of m(t) -- see expression (A-24)
n	normalization constant -- see expressions (A-1) to (A-2)
n	number of components in $\bar{x}$, nominally
$\bar{n}_{xb}, \bar{n}_{yb}, \bar{n}_{zb}$	unit vectors defining the (x_b, y_b, z_b) coordinate frame (typical)
p	number of elements in ψ vector
r	number of samples or discrete values of t_i
$\bar{r}$	the radius vector from P to P* with magnitude r .
s	Laplace transform variable

t	independent variable
t_i, t_k	specific times
t_o, t_f	initial and final time
u_x, u_y, u_z	see expression (4-3)
$\bar{u}$	control vector
$\bar{u}*, \bar{x}*, \bar{\lambda}*$	optimal control, and corresponding state and adjoint vectors
(x_r, y_r, z_r)	reference coordinate axes -- see Figures A-1 and A-2 for definition of coordinate frames
$\bar{x}$	general state vector -- see expression (4-2)
$\bar{x}_e(t_f)$	instantaneous equilibrium point
$\bar{x}_n, \bar{u}_n$	nominal or initial state and control vectors
$\bar{x}_o, \bar{x}_f, \bar{x}_{nf}$	see expressions (4-1) and (5-9)
$\delta\bar{\psi}, \delta\bar{x}_f, \delta\emptyset, \delta V*$	small variations in vector or scalar quantities
$\delta(\delta\bar{u})$	small variation in quantity $\delta\bar{u}$ -- see expression (B-5)
δt_d	variation in control time -- see Figure 5-1
δt_i	variation in control time -- see expression (5-21)
$\delta\bar{x}, \delta\bar{u}$	deviation from nominal $\bar{x}_n$ and $\bar{u}_n$ -- see expression (5-2)
ϵ	orbital eccentricity
θ', θ''	see expression (A-4)
θ_o	see expression (A-3)
$\bar{\lambda}$	adjoint vector

μ a $(p + 1)$ vector of constants -- see expression (B-4)

τ normalized time $(\tau = nt)$

τ_o, τ_f initial and final normalized time

$\emptyset_d$ desired value of cost functional -- see expression (5-1)

$\emptyset[\bar{x}(t_f)]$ see expression (5-1)

ψ total equivalent rotation -- see expression (A-15)

ψ_I total equivalent rotation with respect to inertial space

ψ_R total equivalent rotation with respect to the orbital reference frame

$\bar{\omega}^B$ inertial angular velocity of the satellite

$\bar{\omega}^R$ inertial angular velocity of the (x_r, y_r, z_r) coordinate frame

$\bar{\omega}^{B/R}$ angular velocity of the body with respect to the orbital reference frame

$\omega_x^B, \omega_y^B, \omega_z^B$ see expression (A-6)

$\Lambda(t, \tau)$ see expression (5-11)

$\Phi(t, \tau)$ state transition matrix -- see expressions (5-4) to (5-8)

$\nabla_x \bar{\psi}$ see expression (5-10)

I. INTRODUCTION

A. OUTLINE OF THE PROBLEM

The solutions of optimization problems can be found by a variety of techniques. However, only a few of the known techniques are applicable to problems which are nonlinear and of high-order. The present study is concerned with the construction of the optimal control for such a problem, and it is assumed that the components of the control vector, u_i , are bounded and that the cost functional which is to be minimized may be written as

$$J[\overline{u}] = \int_{t_o}^{t_f} \sum_{i=1}^{m} d_i |u_i| dt \qquad (1-1)$$

where t_o, t_f are fixed, $d_i > 0$ and $|u_i| \leq U_i$ for $i = 1, \ldots, m$. The performance index (1-1) measures the consumption of control effort. A further assumption is that the control components enter the system differential equations linearly.

The form of the optimal control for the above complex system may be deduced from the maximum principle of Pontryagin. Each of the control components is seen to possess cycles of the following form: a time interval of maximum effort of either polarity is followed by a time interval of zero effort. The timing of these control pulses by selecting the switching times at the beginning and at the end of each pulse is studied in what follows.

A potentially effective means of solving this problem is provided by the method of steepest-descent. This computational technique improves

1

on an initial guess of a nominal control time history until the problem has been solved to a sufficiently high degree of accuracy. However, care must be taken, because this method does not guarantee convergence to an extremal trajectory in state space. Also, only a local extremum value of the functional, rather than the desired global minimum, may be reached.

The manner in which the method of steepest-descent is used is influenced by the selection of the form of the nominal control time history. If, on one hand, the form of the control history is taken as some continuous curve which satisfies the bounds on the control component magnitudes, then one of the existing methods of steepest-descent may be used. If, on the other hand, one takes advantage of the application of the maximum principle to structure the form of the control history as a series of pulses, and uses the switching times as control parameters, then an extension to the existing method of steepest-descent must be made. The development of such an extended method of steepest-descent will be found in this report. Furthermore, various procedures for improving convergence with this extended method are developed.

The minimum-fuel control of a spacecraft during attitude acquisition presents a problem of the above kind. It is assumed that the spacecraft is moving in an elliptical orbit. The task of the attitude control system consists of orienting the spacecraft with respect to a specified set of reference directions, starting from large initial deviations in the spacecraft attitude and from bounded, but arbitrary, tumbling rates. Since large attitude excursions and angular rates must be taken into account the sixth-order system of dynamical equations describing the

spacecraft attitude motions may not be linearized. (These equations are derived in Chapter IV and in Appendix A.) Once acquisition has been achieved, it is assumed that another means of control will be used for "station keeping". This latter control means will not be considered here.

B. SUMMARY OF RELATED WORK

Minimum-fuel optimization problems have received wide attention in the literature in recent years. The systems that are examined are usually linear and of low order. Scalar versions of the performance index (1-1) are most commonly considered. The problem of designing a single-axis rigid-body attitude controller to minimize control fuel consumption is treated in Ref. 1-1. The problem of minimal-fuel thrust programming for the vertical descent phase of a lunar soft landing mission is considered in Ref. 1-2. Fuel-optimal control of a nonlinear second order system is discussed in Ref. 1-3. The cost functional which is minimized in the latter reference is

$$J[u] = \int_0^T \{k + |u(t)|\} dt$$

where the response time T is not fixed and k is greater than zero.

Kelley and Bryson have independently developed the gradient technique or method of steepest-descent for optimization problems [Ref. 1-4, 1-5]. This approach has been used in reentry or boost vehicle-trajectory optimization studies where precomputation of an open-loop control is required.

Recent publications on the spacecraft acquisition problem have dealt with active or passive means of acquiring a desired orientation with

emphasis on stability. Magnetic attitude control of a spinning symmetric satellite is presented in Ref. 2-2. The stable control law which is developed in the reference is compared with a minimum-time optimal control. Passive damping of the tumbling motion of a satellite is considered in Ref. 3-2. The optimal attitude control of a tumbling satellite has been treated by first optimally stopping the motion of the satellite so that it has random orientation [Ref. 1-6] and then acquiring the desired orientation by a control that is not necessarily optimal. A sub-optimal control for the attitude acquisition problem is devised in Ref. 3-1. There a control law is presented which contains several free parameters whose values are optimized.

C. CONTRIBUTIONS

The following are the principal contributions of this study:

1. An extended version of the method of steepest-descent is derived in Chapter V and Appendix B. This technique is useful in solving optimization problems where the control components are bounded in magnitude. The form that each solution takes on is a control time history for each control component.

2. The effectiveness of this extended method of steepest-descent is demonstrated. Chapter VII contains comparison between true optimal trajectories and those generated by the modified steepest-descent technique. Computational considerations which are unique to this class of optimization problem are reported in Chapter VI and Appendix B.

3. A number of solutions to the minimum-fuel, attitude acquisition problem are presented in Chapter VI and VII. By using these approximately

optimal solutions as design goals it is possible for the control engineer

to synthesize a satisfactory sub-optimal state-feedback control law.

II. OPTIMAL CONTROL PROBLEM

A. PROBLEM FORMULATION

It is desired to select a piecewise-continuous "admissible" control $\bar{u}(t)$ subject to the constraints $u_i \leq U_i$, $i = 1, \ldots, m$ for the stationary, continuous system*

$$\dot{x}_i = f_i(x_1, \ldots, x_n, u_1, \ldots, u_m) , \quad i = 1, \ldots, n \qquad (2\text{-}1)$$

starting at the initial state $\bar{x}(t_o)$ at time t_o and finishing at the final state $\bar{x}(t_f)$ at the time t_f while minimizing a performance index

$$J = \int_{t_o}^{t_f} f_o(x_1, \ldots, x_n, u_1, \ldots, u_m)dt \qquad (2\text{-}2)$$

where $\bar{u}$ is an m vector and J is a scalar functional. If $\bar{u}(t)$ can be found to meet these requirements, then $\bar{u}(t)$ is said to be the optimal control. By defining an additional state, x_o, the problem may be restated as a problem of Mayer, where

$$\dot{x}_o = f_o(x_1, \ldots, x_n, u_1, \ldots, u_m) \qquad (2\text{-}3)$$

with the initial condition $x_o(t_o) = 0$. Define an $(n+1)$ vector $\bar{x}$ with the components $x_o, x_1, \ldots, x_n$. Now minimize $x_o(t_f)$ by selecting an admissible control $\bar{u}(t)$ for the system of $(n+1)$ first-order equations:

$$\dot{x}_i = f_i(x_1, \ldots, x_n, u_1, \ldots, u_m) , \quad i = 0, 1, \ldots, n \qquad (2\text{-}4)$$

---

*What is stated here applies as well to a non-autonomous system $\dot{x}_i = f_i(x_1, \ldots, x_n, u_1, \ldots, u_m, t)$ by defining another state $x_{n+1} = t$ and using this state in the non-autonomous system [Ref. 2-1].

which satisfies the initial and terminal boundary conditions.

In order to obtain the solution, define a vector $\bar{\lambda}$ with $n+1$ components $\lambda_0, \lambda_1, \ldots, \lambda_n$ and a scalar function, the Hamiltonian, by

$$H(\bar{\lambda}, \bar{x}, \bar{u}) = \sum_{i=0}^{n} \lambda_i f_i \tag{2-5}$$

where the state variables $x_0, \ldots, x_n$ and the adjoint variables $\lambda_0, \lambda_1, \ldots, \lambda_n$ satisfy the Hamiltonian system:

$$\dot{x}_i = \partial H / \partial \lambda_i \; ; \quad \dot{\lambda}_i = - \partial H / \partial x_i \tag{2-6}$$

for $i = 0, 1, \ldots, n$. Note that since H is independent of x_0, $\dot{\lambda}_0 = 0$ which implies that λ_0 is constant. As in Ref. 2-3, λ_0 will be chosen as $\lambda_0 = -1$. Equation (2-6) represents $2n$ first-order differential equations (omitting x_0 and λ_0). For the problem under consideration, n initial and n final conditions are specified on the states x_i. The boundary conditions on λ_i are not known, but must be chosen such that the boundary conditions on the states are met [Ref. 2-1]. The vector functions $\bar{x}(t)$ and $\bar{\lambda}(t)$ are continuous, and have continuous derivatives with respect to t, except at a finite number of points.

The maximum principle states that, if $\bar{u}^*(t)$ is the optimal control, and $\bar{x}^*(t)$ is the corresponding solution, then it is necessary that there exist a nonzero vector function $\bar{\lambda}^*(t)$ such that $H(\bar{\lambda}^*, \bar{x}^*, \bar{u}^*) \geq H(\bar{\lambda}^*, \bar{x}^*, \bar{u})$ for any admissible $\bar{u}^*$ and $\bar{u}$. However, the maximum principle gives only necessary, but not sufficient, conditions.

B. FORM OF OPTIMAL CONTROL

For the performance index and the class of systems investigated here, the form of the optimal control may exhibit well defined behavior when the maximum principle is applied; however, there exists a possibility of irregular behavior which must be considered as well.

1. Regular Form

Since this study is concerned with a minimum-fuel problem where $\bar{u}$ is a three-dimensional vector,

$$f_o = \sum_{i=1}^{3} d_i |u_i| \qquad (2\text{-}7)$$

where

$$d_i > 0, \quad |u_i| \leq U_i \quad \text{for} \quad i = 1,2,3 .$$

For this problem the Hamiltonian (2-5) is written

$$H = \sum_{i=1}^{3} (-d_i |u_i| + \lambda_i u_i) + \dots \qquad (2\text{-}8)$$

where the fact that $\lambda_o = -1$ has been used and terms independent of u_i have been dropped.*

Applying the maximum principle to the control components in (2-8) leads to the control law [Ref. 2-3] :

---

*The differential equations of the system, developed below, (4-4) or (4-6), have been incorporated into the Hamiltonian with an appropriate re-indexing so that the $x_1, \dots, x_{n+1}$ numbering of Chapter IV will be compatible with $x_o, x_1, \dots, x_n$ system of Chapter II.

$$u_i(t) = \begin{cases} U_i \, \text{sgn}(\lambda_i) \, , & \text{for} \;\; |\lambda_i| \geq d_i \\ 0 \, , & \text{for} \;\; |\lambda_i| < d_i \end{cases} \qquad\qquad (2\text{-}9)^*$$

A typical time history of one of the control components might look like that in Figure. 2-1.
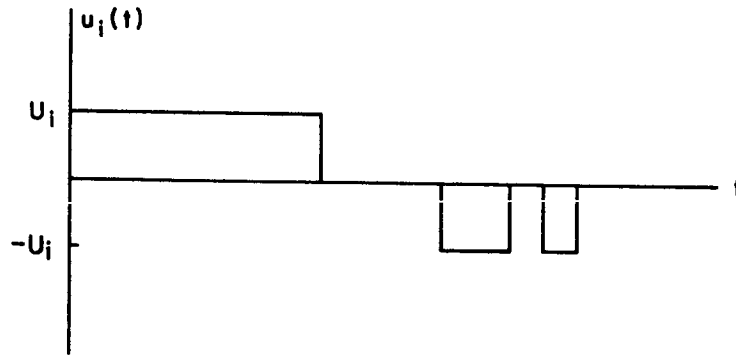
FIGURE 2-1. TYPICAL TIME HISTORY OF
A CONTROL COMPONENT

2. Singular Control

Certain classes of problems which appear to possess a bang-bang form for the optimal control after application of the necessary conditions of the maximum principle may actually require intervals of variable control effort (called "singular" control) for an optimum to be reached [Ref. 2-4]. For example, in the minimum-fuel problem characterized by the Hamiltonian of expression (2-8) a singular control may exist. If for some finite interval $t_1 \leq t \leq t_2$ one of the adjoint variables $\lambda_i(t) \equiv d_i$, then H will be a maximum for any $u_i(t)$ in the interval $0 \leq u_i(t) \leq U_i$. The control law (2-9) should then be modified to include this possibility; however, in this study only nonsingular controls will will be considered.

---

*The function $\text{sgn}(x)$ (read signum of x) is defined as $\text{sgn}(x) \equiv \dfrac{x}{|x|}$.

9

3. Indifference Regions

Attitude control problems, such as the one to be considered, may involve periodic state variables, these describing the rotation of the rigid body. If, for instance, the rotation of a shaft were to be controlled about its longitudinal axis so that some mark on the surface pointed upward, and if the rotation of the shaft about its axis were selected as a state x_1, then a desired terminal value for x_1 would be $\pm 2\pi n, (n=0,1,\ldots)$. Since there exist many acceptable terminal states, there exist many alternative control histories which satisfy the form dictated by the maximum principle and also lead to the desired terminal states [Ref. 2-5]. Further analysis must be performed to see which one of these alternative control histories minimizes the cost functional. Indeed, there exist some regions of initial conditions, called indifference regions, for which the choice of optimal control is not unique. To avoid the possibility of encountering such regions in this analysis, the range of initial conditions will be kept reasonably small, though not so small as to preclude the need for the full nonlinear dynamical equations.

C. SYNTHESIS OF CONTROLLER

Application of the maximum principle usually results in an open-loop control $\bar{u} = \bar{u}(t)$. Additional work is required to obtain the more desirable feedback control law $\bar{u} = \bar{u}(\bar{x})$. However, the optimal controller may be too complex. As a result, a simpler feedback control law which performs in a near optimal fashion may be an acceptable alternative.

The open-loop optimal control $\bar{u} = \bar{u}(t)$ can be obtained by numerically solving the two-point boundary-value problem on a high-speed digital

computer. This solution may or may not be optimal, depending upon convergence properties of the chosen computational scheme. This general technique applies to many of the most complex optimization problems. The method of steepest-descent has been selected as the most feasible method of solving by iteration the problems considered in this text.

If these systems are simple enough, an optimal feedback control law $\bar{u} = \bar{u}(\bar{x})$ can be obtained by examining the general solution to the adjoint differential equations and the form of the switching surfaces which are generated in state space [Ref. 2-1, 2-3]. Sub-optimal feedback control laws may be deduced for linear, low-order, time-invariant systems. A linear function of the states, or a piecewise approximation of the switching surfaces, or a polynomial approximation of the adjoint vector obtained from a simplified version of the cost functional have been tried with success [Ref. 2-6, 2-7, 2-8, 2-9, 2-10].

A common technique of control law synthesis is to postulate a simple control law which contains several free parameters [Ref. 2-11] . The control parameters are varied until an extremum value of the cost functional is reached.

11

III. AN APPLICATION OF OPTIMAL CONTROL THEORY

The minimum-fuel acquisition problem, which is for the most part unsolved, possesses the desired characteristics for the application of the extended method of steepest-descent. The mathematical model of the satellite is highly nonlinear, is of high-order, possesses time varying coefficients in some cases, and has bounds on the control component magnitudes. When using the method of steepest-descent, a stopping condition is required. Final time provides a logical and simple stopping condition for forward integration of the differential equations in this text. If it were desired to use this technique for minimum-time problems where the final time was not known, it would be much more difficult to express the stopping condition.

The essential purpose of this study is first to gain insight into the steepest-descent method of solving a high-order nonlinear optimization problem and second to obtain further understanding of the optimal control systems design for spacecraft acquisition. It is certainly not feasible at present to compute the attitude control on-board the spacecraft as would be required by the method of steepest-descent; however, in the future with larger spacecraft, and with higher-capacity, higher-speed digital computers such a scheme may prove feasible. One distinct and important benefit of applying the method of steepest-descent to this problem is that optimal trajectories may be generated in the initial design phase for a finite set of representative initial conditions and that these optimal solutions may be used as goals or standards which the designer could attempt to meet when synthesizing a sub-optimal control scheme.

12

IV. SYSTEM EQUATIONS

In Appendix A, coordinate systems are introduced and the equations of motion of a satellite are derived. In addition, the cost functional for optimal control is discussed and the adjoint equations are developed. Since the attitude maneuvers during acquisition will be large, the dynamical equations will be retained in their nonlinear form. Elliptical orbits for this study may possess arbitrary values of eccentricity within the limits $0 < \epsilon < 1$; and therefore, no linearization of the orbit equations will be attemped. Two distinct cases, which result in markedly different equations, will be considered: 1) the control torque is assumed of the order of magnitude of the gravity gradient disturbance torque and the assumed goal of the acquisition control is to steer to a rotating orbital reference frame; 2) the control torque is assumed high enough so that the gravity gradient torque may be ignored, and the time of acquistion is so short due to the high control torque that for all practical purposes the orbital reference frame can be considered inertially fixed. These two sets of equations are summarized in the following paragraphs.

For convenience the state-space notation is adopted in this chapter, where the set of differential equations is written in a first-order vector differential equation form:

$$\dot{\overline{x}} = \overline{f}(\overline{x}, \overline{u}, t)$$

with initial and terminal conditions on all of the states at t_o and t_f specified. By defining the orbital parameters as states for the purpose of numerical integration, the matrix equation above may be written in

autonomous form as:

$$\dot{\bar{x}} = \bar{f}(\bar{x}, \bar{u}) \quad , \quad \bar{x}(t_o) = \bar{x}_o \quad , \quad \bar{x}(t_f) = \bar{x}_f \quad . \tag{4-1}$$

In this representation the following definitions are used:

$$\bar{x} = \begin{bmatrix} x_1 \\ x_2 \\ x_3 \\ x_4 \\ x_5 \\ x_6 \\ x_7 \\ x_8 \\ x_9 \\ x_{10} \end{bmatrix} = \begin{bmatrix} J \\ x_2 \\ x_3 \\ x_4 \\ W_1 \\ W_2 \\ W_3 \\ W_4 \\ V \\ R \end{bmatrix} \tag{4-2}$$

J is the cost functional, and V and R the orbital parameters [see (A-2)]. J and x_2, x_3, x_4 have been conveniently time normalized by (A-1). In addition:

$$\bar{u} = \begin{bmatrix} u_1 \\ u_2 \\ u_3 \end{bmatrix} = u_x \bar{n}_{xb} + u_y \bar{n}_{yb} + u_z \bar{n}_{zb} \quad , \tag{4-3}$$

so that

$$u_1 = u_x \quad , \quad u_2 = u_y \quad \text{and} \quad u_3 = u_z \quad .$$

14

A. LOW TORQUE ROTATING ORBITAL REFERENCE FRAME

Two sets of equations are to be written, as discussed in the introductory remarks in this chapter. For the low torque, rotating orbital-reference-frame case the following equations are obtained upon changing the time variable and using (A-14), (A-18), (A-19), (A-22) and (4-3):

$$x_1' = d_1|u_1| + d_2|u_2| + d_3|u_3|$$

$$x_2' = u_1 + \frac{3}{(x_{10})^3} K_x a_{21} a_{31} - \theta'' a_{13} + \theta'(a_{33}x_3 - a_{23}x_4)$$
$$- K_x(x_3 + \theta'a_{23})(x_4 + \theta'a_{33})$$

$$x_3' = u_2 + \frac{3}{(x_{10})^3} K_y a_{11} a_{31} - \theta'' a_{23} + \theta'(a_{13}x_4 - a_{33}x_2)$$
$$- K_y(x_4 + \theta'a_{33})(x_2 + \theta'a_{13})$$

$$x_4' = u_3 + \frac{3}{(x_{10})^3} K_z a_{11} a_{21} - \theta'' a_{33} + \theta'(a_{23}x_2 - a_{13}x_3) \quad (4\text{-}4)$$
$$- K_z(x_2 + \theta'a_{13})(x_3 + \theta'a_{23})$$

$$x_5' = 1/2(x_2x_8 - x_3x_7 + x_4x_6)$$

$$x_6' = 1/2(x_2x_7 + x_3x_8 - x_4x_5)$$

$$x_7' = 1/2(-x_2x_6 + x_3x_5 + x_4x_8)$$

$$x_8' = 1/2(-x_2x_5 - x_3x_6 - x_4x_7)$$

$$x_9' = -1/(x_{10})^2 + (1 - \epsilon^2)/(x_{10})^3$$

$$x_{10}' = x_9$$

15

Initial conditions $\bar{x}(\tau_o) = \bar{x}_o$ are arbitrary with the exception of:

$x_1(\tau_o) = 0$; $x_8(\tau_o)$ subject to the constraint (A-16) which is rewritten

$$\boxed{\sum_{i=5}^{8} x_i^2 = 4 \quad ;}$$ (4-5)

and the orbital parameters $x_9(\tau_o)$ and $x_{10}(\tau_o)$ having to satisfy (A-3).

In most cases desired terminal conditions at $\tau = \tau_f$ are for $x_1(\tau_f)$ to be a minimum; and for $x_2(\tau_f) = ,\ldots, = x_7(\tau_f) = 0$; for $x_8(\tau_f) = 2$; and for $x_9(\tau_f)$ and $x_{10}(\tau_f)$ to be as determined by the above mentioned orbital quations.

The quantities θ', θ'' and a_{ij} in (4-4) are expressed in terms of the states by (A-4) and (A-17).

B. HIGH TORQUE, INERTIAL ORBITAL REFERENCE FRAME

The equations for the high torque case are considerably simpler since the expressions for the gravity gradient may be ignored, the need for orbital parameters dropped, and the terms which describe the rotation of the orbital reference frame in (A-14) ignored. Instead of the ten-element state vector in (4-2) an eight-element vector containing all but the last two elements may be considered for this case. By making use of the new state vector the following time normalized equations may be written:

16

$$x_1' = d_1|u_1| + d_2|u_2| + d_3|u_3|$$

$$x_2' = u_1 - K_x x_3 x_4$$

$$x_3' = u_2 - K_y x_2 x_4$$

$$x_4' = u_3 - K_z x_3 x_2$$

$$x_5' = 1/2(x_2 x_8 - x_3 x_7 + x_4 x_6)$$

$$x_6' = 1/2(x_2 x_7 + x_3 x_8 - x_4 x_5)$$

$$x_7' = 1/2(-x_2 x_6 + x_3 x_5 + x_4 x_8)$$

$$x_8' = 1/2(-x_2 x_5 - x_3 x_6 - x_4 x_7)$$

(4-6)

The initial conditions and terminal conditions are indentical with those for the prior set of equations (4-4), but this time for the eight-element state vector.

V. METHOD OF STEEPEST-DESCENT

This chapter presents a brief summary of the method of steepest-descent. Conventionally, this method, based on the first variation, is used to find by iteration a solution of a two-point boundary value problem in the calculus of variations. The solution will usually be in the form of a control history as a function of time which will achieve a local extremum of some performance functional while meeting specific constraints. An advantage of this method is that even though a relatively poor guess is made for the control history, convergence to near optimum may be achieved after some iterations.

There are many variations on the method of steepest-descent due to the system models considered and to the manner in which the method can be applied. In this chapter several ways will be discussed in which the method can be used for solving problems with no constraints on the state or control variables. Also the required modifications will be discussed when bounds on the control variables are encountered and use is to be made of the knowledge that the form of the control is a series of pulses.

A. PRELIMINARY DEVELOPMENTS

First, expressions are derived which relate the effect of a small variation in the initial state and the effect of variations in the control history upon the terminal constraints. As will be seen, the notion of influence functions or adjoint variables will play an integral role here. Small variations in an unbounded control as well as a

finite number of "strong" variations* in a bounded control history over a short time period will be considered in arriving at the desired expression. In addition an expression for the mean square variation of the control variable will be written down.

The Mayer formulation of the optimization problem is to determine the control $\bar{u}(t)$ which minimizes, in the interval $t_o \leq t \leq t_f$, the cost functional

$$J = \emptyset[\bar{x}(t_f)] \tag{5-1}$$

while satisfying the system equations $\dot{\bar{x}} = \bar{f}(\bar{x},\bar{u},t)$ for t in the interval $t_o \leq t \leq t_f$, and the constraint equations $\bar{\psi} = \bar{\psi}[x(t_f)] = 0$ with the quantities $\bar{x}(t_o)$, t_o and t_f** given. In this description

$$\bar{u}(t) = \begin{bmatrix} u_1(t) \\ \cdot \\ \cdot \\ \cdot \\ u_m(t) \end{bmatrix}$$

is an m-vector of control variables which may be freely chosen within an open or a closed set,

$$\bar{x}(t) = \begin{bmatrix} x_1(t) \\ \cdot \\ \cdot \\ \cdot \\ x_n(t) \end{bmatrix}$$

---

*Discontinuities in the control time history will be allowed. When these "strong" variations in control occur it will not be possible to differentiate and form such expressions as $\partial f_i(\bar{x},\bar{u},t)/\partial u_j$.

**The assumption that t_f is fixed is made here to simplify the analysis. This assumption is not restrictive for this study as minimum-fuel problems are to be considered, which require a fixed t_f .

is an n-vector of state variable histories which result from given values $\bar{x}(t_o)$ and a choice of $\bar{u}(t)$,

$$\bar{f} = \begin{bmatrix} f_1 \\ \cdot \\ \cdot \\ \cdot \\ f_n \end{bmatrix}$$

is an n-vector of known functions of $\bar{x}(t)$, $u(t)$ and t , assumed everywhere differentiable with respect to $\bar{x}$ and $\bar{u}$, when $\bar{u}$ lies in an open set, and assumed everywhere differentiable with respect to $\bar{x}$ only, when $\bar{u}$ lies in a closed set,

$\emptyset$ = the performance index and is a known function of $\bar{x}(t)$,

$$\bar{\psi} = \begin{bmatrix} \psi_1 \\ \cdot \\ \cdot \\ \cdot \\ \psi_p \end{bmatrix}$$

is a p-vector of terminal constraint functions, each of which is a known function of $\bar{x}(t_f)$ and is assumed everywhere differentiable with respect to $\bar{x}$, with $p \le n$.

1. Unbounded Control

It is appropriate first to consider the case where $\bar{u}$ is not bounded. Introducing the deviation from the nominal (chosen) $\bar{x}_n$ and $\bar{u}_n$ by:

$$\delta\bar{x} = \bar{x} - \bar{x}_n \quad , \quad \delta\bar{u} = \bar{u} - \bar{u}_n \quad , \tag{5-2}$$

the differential equation $\dot{\bar{x}} = \bar{f}$ in (5-1) may be linearized about $\bar{x}_n$, $\bar{u}_n$ and written as

$$\delta\dot{\bar{x}} = F(t)\delta\bar{x} + G(t)\delta\bar{u} \tag{5-3}$$

where

$$F(t) = \nabla_x \bar{f}\big|_{\bar{x}_n} = \begin{bmatrix} \partial f_1/\partial x_1 & \cdots & \partial f_1/\partial x_n \\ \vdots & & \\ \partial f_n/\partial x_1 & \cdots & \partial f_n/\partial x_n \end{bmatrix}\Bigg|_{\bar{x}_n}$$

is an $n \times n$ matrix of partial derivatives evaluated on the nominal state trajectory $\bar{x}_n$

$$G(t) = \nabla_u \bar{f}\big|_{\bar{x}_n} = \begin{bmatrix} \partial f_1/\partial u_1 & \cdots & \partial f_1/\partial u_m \\ \vdots & & \\ \partial f_n/\partial u_1 & \cdots & \partial f_n/\partial u_m \end{bmatrix}\Bigg|_{\bar{x}_n}$$

is an $m \times n$ matrix of partial derivatives evaluated on $\bar{x}_n$. As stated in [Ref. 5-1] the solution to (5-3) may be written as

$$\delta\bar{x}(t) = \Phi(t,t_o)\delta\bar{x}(t_o) + \int_{t_o}^{t} \Phi(t,\tau)G(\tau)\delta\bar{u}(\tau)d\tau \tag{5-4}$$

where $\Phi(t,t_o)$ is called the state transition matrix. $\Phi(.\,,\,.)$ exhibits the following pertinent properties:

21

$$\frac{d\Phi(t,\tau)}{dt} = F(t)\Phi(t,\tau) \quad , \tag{5-5}$$

$$\frac{d\Phi(\tau,t)}{dt} = -\Phi(\tau,t)F(t) \quad , \tag{5-6}$$

$$\Phi(t,t) = I \quad , \tag{5-7}$$

$$\Phi(t,\xi)\Phi(\xi,\tau) = \Phi(t,\tau) \quad . \tag{5-8}$$

An expression relating the effect of a small variation in state and control to the final variation in state is next required. By letting $t = t_f$, and $t_o = t$ (t is a running variable) in (5-4), one is lead to

$$\delta\overline{x}_f = \Phi(t_f,t)\delta\overline{x}(t) + \int_t^{t_f} \Phi(t_f,\tau)G(\tau)\delta\overline{u}(\tau)d\tau \quad , \tag{5-9}$$

A small variation, $\delta\overline{\psi}$, in the terminal constraint leads to the expression

$$\delta\overline{\psi} = (\nabla_x\overline{\psi})|_{\overline{x}_{nf}} \delta\overline{x}_f \tag{5-10}$$

where

$$\nabla_x\overline{\psi} = \begin{bmatrix} \partial\psi_1/\partial x_1 \cdots \partial\psi_1/\partial x_n \\ \vdots \\ \partial\psi_p/\partial x_1 \cdots \partial\psi_p/\partial x_n \end{bmatrix}$$

Let us define

$$\boxed{\Lambda^T(t_f,t) \equiv (\nabla_x\overline{\psi})|_{\overline{x}_{nf}} \Phi(t_f,t)} \tag{5-11}$$

where $(\ )^T =$ the transpose operation and

$$\Lambda^T(t_f, t) \ = \ a \ (p \times n) \quad \begin{array}{c} \text{matrix called "the influence matrix"} \\ \text{or} \\ \text{"matrix of influence coefficients".} \end{array}$$

Upon differentiating (5-11) with respect to t , and using (5-6) and (5-11), the following set of adjoint differential equations is obtained:

$$\dot{\Lambda}^T(t_f, t) \ = \ - \ \Lambda^T(t_f, t)F(t) \tag{5-12}$$

with the boundary conditions at $t = t_f$ from (5-11) and (5-7):

$$\Lambda^T(t_f, t_f) \ = \ (\nabla_x \bar{\psi}) \Big|_{x_{nf}} \tag{5-13}$$

The adjoint equations (5-12) may be integrated in reverse time from $t = t_f$ with the boundary conditions (5-13).

Finally, the desired sensitivity relationship between $\delta\bar{x}, \delta\bar{u}$ and $\delta\bar{\psi}$ is formed by using (5-9), (5-10) and (5-11):

$$\delta\bar{\psi} \ = \ \Lambda^T(t_f, t)\delta\bar{x}(t) + \int_t^{t_f} \Lambda^T(t_f, \tau)G(\tau)\delta\bar{u}(\tau)d\tau \quad . \tag{5-14}$$

The variable t could be set equal to t_o (in which case $\delta\bar{x}(t_o) \equiv 0$ from (5-1)), it could be a continuous running variable, or t could possess discrete values t_k , $k = 1,\dots,r$ where t_k is contained in $t_o \leq t_k < t_f$. Allowing t to be a continuous or a "sampled" variable may improve convergence when using the method of steepest-descent. Recommendations based on results are presented in Chapter VI concerning this possibility.

An equation for the "mean-square" variation in control V is written as:

$$V(t_o) = \int_{t_o}^{t_f} \delta \bar{u}^T W(\tau) \delta \bar{u} d\tau \qquad (5\text{-}15)$$

where $W(t)$ is an arbitrary symmetric positive definite matrix. If the value of V is "small" then the variations in control are "small" and all of the above assumptions which prompted the development of the sensitivity relationships will remain valid. The selection of how $W(t)$ changes as a function of time is important for some problems where parameters change widely over the range of the problem solution [Ref. 5-2]. In the case of more than one control variable it must be decided how to weight relatively the different control variable changes at a given instant in time as well [Ref. 5-10].

2. Bounded Control

Many problems contain bounds on the magnitude of the components of the control vector. For this study it is assumed that $|u_i| \leq U_i$, $i = 1,2,3$. For certain cost functionals, e.g., minimum-fuel or certain forms of the minimum-fuel problem, the necessary conditions of the maximum principle state that u_i will be discontinuous, and will be on full in a plus or minus direction, or off. Components of the differential "constraint" $\dot{\bar{x}} = \bar{f}$ in (5-1) will contain terms such as $|u_i|$ and will therefore not be differentiable in those arguments. The concept of the strong variation is introduced here where a finite number of large changes in u_i are allowed, each change occuring over a short time δt_d . The variations in u_i will cause large variations in the

24

slope of the state trajectories.

The first step in the following derivation is to obtain an expression similar to (5-4) which relates a variation in $\bar{x}_n(t_o)$ and a large variation in control, $\overline{\delta u}$, to the variation in $\bar{x}_n(t)$. First consider the variation in $\bar{x}_n$ resulting <u>only</u> from a single large variation in control, $\overline{\delta u}$, occuring between t_d and $(t_d + \delta t_d)$. As a result of this variation in control the new trajectory $\bar{x}$ might be generated as in Figure 5-1.
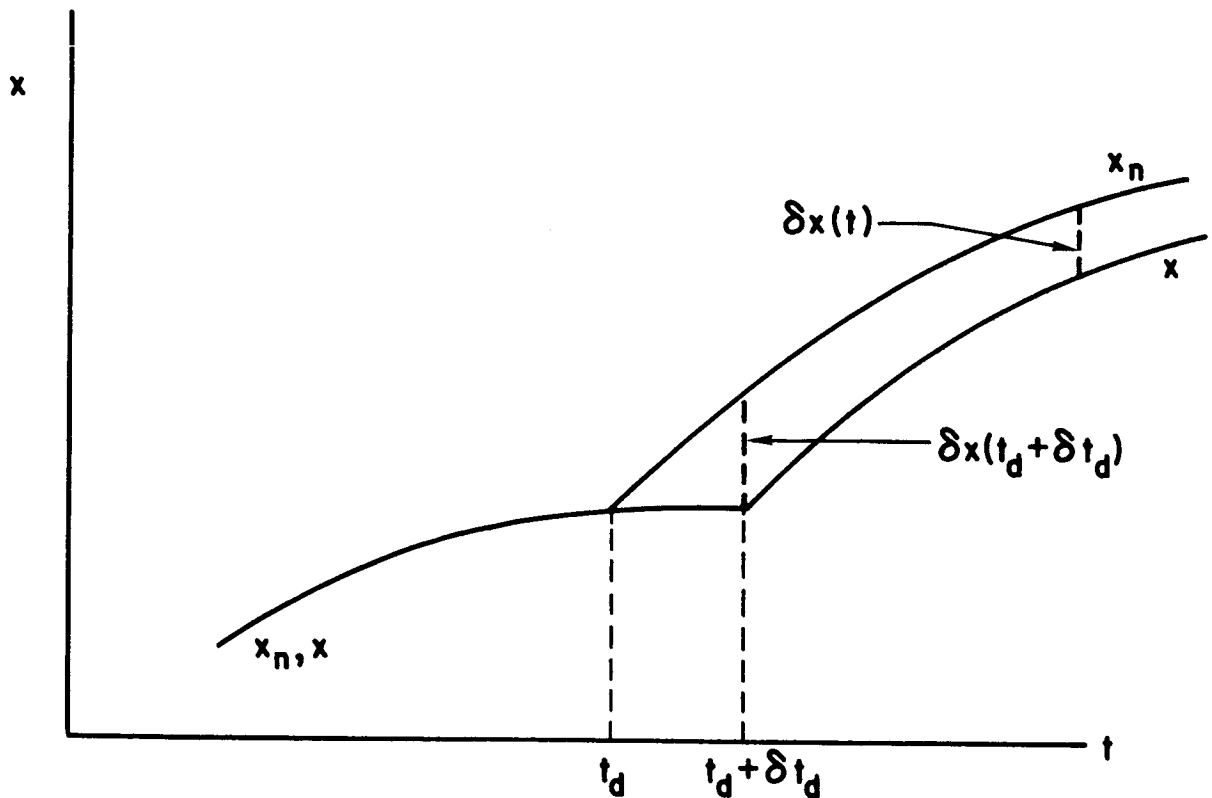
FIGURE 5-1. VARIATION IN STATE RESULTING FROM STRONG VARIATION IN CONTROL FOR THE SCALAR CASE

The nominal control switching time which occurs at $t = t_d$ and causes the discontinuous slope in $\bar{x}_n$ is changed to $t = t_d + \delta t_d$. This new switching time represents a new control $\bar{u}(t)$ and generates the new

trajectory $\overline{x}(t)$. Up to $t = t_d$ the variation in $\overline{x}_n$ is zero. As seen from the figure, the expression for $\delta \overline{x}$ at $t = t_d + \delta t_d$, to first order, may be written as

$$\delta \overline{x}(t_d + \delta t_d) = [\overline{f}(\overline{x}_n, \overline{u}_n(t_d^-), t_d) - \overline{f}(\overline{x}_n, \overline{u}_n(t_d^+), td)]\delta t_d \quad . \qquad (5\text{-}16)$$

Since no further variations in control are encountered, $\delta \overline{x}$ at $t = t_d + \delta t_d$ will be transmitted through time by the state transition matrix in the following form:

$$\delta \overline{x}(t) = \Phi(t, t_d + \delta t_d)\delta \overline{x}(t_d + \delta t_d) \quad , \text{ for } t \geq t_d + \delta t_d \quad . \quad (5\text{-}17)$$

Since the state trajectories $\overline{x}(t)$ or $\overline{x}_n(t)$ are continuous and δt_d is small, equation (5-17) may be written as:

$$\delta \overline{x}(t) = \Phi(t, t_d)\delta \overline{x}(t_d + \delta t_d) \qquad (5\text{-}18)$$

Combining (5-16) and (5-18), an expression is obtained which relates a single strong variation in control to $\delta \overline{x}(t)$:

$$\delta \overline{x}(t) = \Phi(t, t_d)[\overline{f}^- - \overline{f}^+]\delta t_d \qquad (5\text{-}19)$$

where use has been made of the following definition:

$$\boxed{\overline{f}^{\pm} = \overline{f}[\overline{x}_n, \overline{u}_n(t_d^{\pm}), t_d]} \qquad (5\text{-}20)$$

Next, by assuming that more strong variations in control exist, as well as a variation in the initial conditions at $t = t_o$, an equation similar to (5-4) is written:

$$\delta \overline{x}(t) = \Phi(t, t_o)\delta \overline{x}(t_o) + \sum_i \Phi(t, t_i)[\overline{f}^- - \overline{f}^+]\delta t_i \quad , \qquad (5\text{-}21)$$

26

where the summation is taken over each of the switching points of the control, with $t_o \leq t_i \leq t$.

An expression similar to (5-9), which relates the effect of a small variation in state and strong variations in control, is derived by letting $t = t_f$ and $t_o = t$ in (5-21):

$$\delta \overline{x}_f = \Phi(t_f, t)\delta \overline{x}(t) + \sum_i \Phi(t_f, t_i)G(t_i)\delta \overline{u}(t_i) \tag{5-22}$$

where $t \leq t_i \leq t_f$. The identify

$$\boxed{G(t_i)\delta \overline{u}(t_i) \equiv [\overline{f}^- - \overline{f}^+]\delta t_i} \tag{5-23}$$

has been introduced for analytical and computational convenience.* This identity should be used for computing $G(t_i)$.

The last step in the present derivation is to write the desired sensitivity relationship, similar to (5-14), for the bounded control case. Premultiplying (5-22) by $(\nabla_x \overline{\psi})|_{\overline{x}_{nf}}$ and using (5-10) and (5-11) one obtains:

$$\boxed{\delta \overline{\psi} = \Lambda^T(t_f, t)\delta \overline{x}(t) + \sum_i \Lambda^T(t_f, t_i)G(t_i)\delta \overline{u}(t_i)} \tag{5-24}$$

The presence of the strong variations in $\delta \overline{u}$ is reflected in the above summation.

An equation for the "mean-square" variation in control similar to (5-17) is written as

---

*The details of digital simulation are not discussed in this study.

$$V(t_o) = \sum_i \delta\bar{u}^T(t_i) T_i \delta\bar{u}(t_i) \qquad (5\text{-}25)$$

where $T_i = T(t_i)$ and where the summation extends over all switching times in interval $t_o \leq t \leq t_f$.

B. STEEPEST-DESCENT TECHNIQUES

Various ways are described here in which the basic sensitivity relationships developed above may be used to derive equations which indicate how the control history is to be changed in order to meet a desired terminal constraint while minimizing a specific cost functional.

Several alternative paths are followed in this development. The technique introduced by Kelley incorporates a penalty function treatment of the terminal constraints [Ref. 5-3]. The new functional that is to be minimized is written

$$J^* = \emptyset[\bar{x}(t_f)] + \sum_{i=1}^{p} \nu_i \psi_i^2 \qquad (5\text{-}26)$$

where ν is a $(p \times 1)$ vector of positive constants. Kelley then minimizes J^* subject to a given value of an integral similar to $V(t_o)$ of expression (5-15). This technique will satisfy the terminal constraint $\bar{\psi}$ only approximately. Bryson and Denham minimize the first variation of the original functional $\emptyset$ subject to a specific value of $V(t_o)$ in equation (5-15) and to a specific value of $\delta\bar{\psi}$ [Ref. 5-4]. The success of this latter method, as measured by the rate of convergence to a solution of the boundary value problem, is strongly influenced by the choice of $V(t_o)$.

28

A further development by Bryson and Denham and a modification by Rosenbaum seem to offer the most promise and will be followed in this study [Ref. 5-5 and 5-6]. The integral $V(t_o)$ is minimized subject to the constraint $\delta\bar{\psi}$, where the vector $\bar{\psi}$ has been augmented by adding the cost functional $\emptyset$. Experience has lead to the recommendation that no attempt be made to improve the cost functional during the first few iterations until the terminal constraints are met [Ref. 5-6]. Upon satisfaction of the terminal constraint a reduction or increase in the cost functional may be specified and further iterations performed until a satisfactory problem solution is found. The derivation of the desired control equations is found in Appendix B. In addition a computational algorithm is presented in Appendix B.

Several authors have touched on problems with bounded control and some of these have considered moving the switching times preserving the original "bang-bang" form of the control time history [Ref. 5-3, 5-7, and 5-8]*. One auther [Ref. 5-8] assumes that the derivatives $\partial f_i/\partial u_j$ exist while one [Ref. 5-3] makes no such assumption. An important set of obervations is made in Ref. 5-8: if the switching times are to be treated as control parameters then there must exist at least as many switching times as the $p + 1$ elements of the augmented constraint vector $\bar{\psi}$. There must also exist at least as many switching times as in the optimal solution. If two switching times become equal in the limit then the total number of assumed switching times may become less than the optimal number which will create an uncontrollable situation.

---

*[Ref. 5-9] has recently been received. The presentation in this reference is quite similar to some of the analytical developments in this report.

Also, by choosing the switching times as control parameters, the possibility of finding singular solutions to the two-point boundary-value problem is precluded. To be able to search out a singular solution a form of the control consistent with singular sub-arcs must be assumed. This latter alternative will not be followed in this study.

Potential difficulties arise with the computation of the inverse matrices in (B-12) and (B-21). If t_o is allowed to become a running variable t, and t approaches t_f then these matrices will become singular. In addition, as an extremal solution is reached then these matrices _may_ become singular implying from (B-12) and (B-21) that it would take an infinite amount of control variation to improve the extremum value of the cost function [Ref. 5-5]. The matrix $D(t_o)$ of (B-21) will in most cases _not_ become singular when the optimal solution is reached* because the control has been simulated by a series of pulses, and each of the switching times are required to occur at $t = t_i$ where $t_o \leq t_i \leq t_f$. More will be said about this characteristic in Chapter VII.

---

*Even if the _exact_ optimal switching times are reached, $D(t_o)$ _may not_ become singular.

VI. ACQUISITION PROBLEM: HIGH CONTROL TORQUE, INERTIAL REFERENCE FRAME

The mathematical model of the system studied in this chapter is described by equation (4-6) and in Table (A-27). The control torque levels are high enough to ignore all other disturbances such as gravity gradient.

A. IDEALIZED PROPORTIONAL CONTROL

An idealized feedback control law, the performance of which will be compared with that of an open-loop minimum-fuel control generated by the method of steepest-descent, is found in Ref. 3-1. This control law is written in scalar form with the state space notation of (4-2) and (4-3) as:

$$u_1 = -k_1 x_2 - (2k_p/x_8^3)(x_5/I_x^2)$$
$$u_2 = -k_2 x_3 - (2k_p/x_8^3)(x_6/I_y^2) \qquad\qquad (6\text{-}1)$$
$$u_3 = -k_3 x_4 - (2k_p/x_8^3)(x_7/I_z^2)$$

where k_i, $i = 1,2,3$ are the rate gains and k_p is the position gain. It is assumed that there exist no bounds on the magnitudes of the components of control torque for this idealized control law. When the total equivalent rotation ψ equals 180 degrees, then $x_8 = 0$ and the magnitude of the control vector $\bar{u}$ becomes infinite. In this report initial values will be chosen which have sufficiently small magnitudes so that the state trajectories will avoid the singularity in equations (6-1). It has been shown that if the rate gains k_1, k_2, k_3 and the position gain k_p are all greater than zero, then the equilibrium point

$(x_2 = \ldots = x_7 = 0)$ of the system of equations (4-6) and (6-1) is asymptotically stable in the large [Ref. 3-1]*. This desirable stability feature of control law (6-1) makes it an excellent choice for a preliminary design.

Satellite parameters, based on a preliminary model of the OGO Spacecraft [Ref. 6-2] are found in Table I:

Principle Moments of Inertia, slug ft^2	Inertia Parameters
$I_x = 800$	$K_x = -.35125$
$I_y = 581$	$K_y = .86058$
$I_z = 300$	$K_z = -.73000$

Table I. OGO Spacecraft Parameters

The four gains k_1, k_2, k_3 and k_p are selected such that the transient response of the system to a set of initial conditions will bring the satellite to within an acceptable distance of the desired equilibrium point in approximately 300 seconds.** This acceptable distance from the equilibrium point is taken as

$$\left(\sum_{i=2}^{7} x_i^2 \right)^{1/2} \leq 10^{-2} \tag{6-2}$$

where the three rates x_2, x_3, x_4 are in deg/sec.

---

*See [Ref. 6-1] for a discussion of stability definitions.
**An orbit of this satellite will take about 100 minutes.

To select values for the gains the system and control equations are linearized about the desired equilibrium point, resulting in three uncoupled, damped escillators. The three damping ratios are chosen as .707. Using the moments of inertia in Table I, the desired settling time of 300 seconds and the above damping ratios, one calculates the four gains which are listed in Table II.

Gains	
Position	Rate
k_p = 1730 lb^2 sec^2 ft^2	k_1 = .0258 sec^{-1}
	k_2 = .0355 sec^{-1}
	k_3 = .0685 sec^{-1}

Table II. Control Gains for Equation (6-1)

Certain bounds are placed on the range of initial conditions. Each of the three initial rates shall have a magnitude less than or equal to one degree per second. These rates represent typical design specifications for the acquisition phase [Ref. 6-3]. The maximum initial rotation $\psi(t_o)$ is selected to be less than or equal to 75 degrees. This is done so that preliminary guesses on the control time history for the method of steepest-descent will only occasionally approach the singularity which occurs when $\psi(t) = 180$ deg. A search was made over the range of these allowable initial conditions and it was found that the norm of the maximum initial control vector was equal to:

$$\| \bar{u}(t_o) \| = .715 \text{ deg/sec}^2 \qquad\qquad (6\text{-}3)$$

when using the gains in Table II. This initial magnitude (6-3) is about eight times larger than the actual, bounded control vector magnitude on the OGO spacecraft. The weights d_1, d_2, d_3 in the first equation of (4-6) are taken to be equal to one.

A number of sets of initial conditions were selected within the above limits and runs were made on the digital computer, using the differential equations (4-6) and the control law (6-1). These runs are summarized in Table III, where the initial conditions are listed, as well as the initial rotation $\psi(t_o)$. The norm of the control vector at $t = t_o$ has been included in this table for comparison purposes with the maximum figure stated in (6-3). The value of the cost functional in rad/sec is listed at $t = t_f$, where t_f is the time at which the norm of the state vector has settled to within the value in (6-2).

Response curves are plotted for Runs R-1 and R-2 in Table III and are found in Figures 6-1 and 6-7. The same dimensions will be found on each of the response curves in this text, and are summarized in Table IV. In addition to the response curves in each of the figures, a scheme is included to portray the orientation of the spacecraft at three times during the transient response. As an example see Figure 6-1b. The location of the center of the three circles above the T axis indicates the time at which each of the three orientations are described. The three times chosen in this example are therefore 0, 90, and 180 sec. Each of the circles represent unit circles lying in the plane of the orbit, centered at the center of mass of the satellite. Directions are important on these circles; to the right (parallel to the T axis)

34

Table III. Summary of Runs with Control Law (6-1).

Run	R-1	R-2	R-3	R-4	R-5
$\bar{x}(t_o)$:					
x_1 , sec^{-1}	0	0	0	0	0
x_2 , deg/sec	1	.5	0	0	1
x_3 , deg/sec	1	.5	0	0	1
x_4 , deg/sec	1	.5	0	0	1
x_5	.4	.5	0	.4	0
x_6	.8	.5	0	.8	0
x_7	.8	.5	1.2	.8	0
x_8	1.6	1.8	1.6	1.6	2
$\psi(t_o)$, deg	73.8	51.8	73.8	73.8	0
$\|\bar{u}(t_o)\|$, deg/sec^2	.524	.236	.644	.445	.081
t_o , sec	0	0	0	0	0
t_f , sec	288	360	180	276	372
$x_1(t_f)$, sec^{-1}	.260	.142	.158	.175	.0954
Plot in Figure:	6-1	6-7	-	-	-

Table IV. Notation and Dimensions for Response Curves

Plot Nomenclature	Original Sumbols	State Notation	Dimensions
T	t	t	sec
OMEGA 1	x_2	x_2	deg/sec
OMEGA 2	x_3	x_3	deg/sec
OMEGA 3	x_4	x_4	deg/sec
W1	W_1	x_5	-
W2	W_2	x_6	-
W3	W_3	x_7	-
J	J	x_1	sec^{-1}
W4	W_4	x_8	-
UV1	u_x	u_1	deg/sec^2
UV2	u_y	u_2	deg/sec^2
UV3	u_z	u_3	deg/sec^2

corresponds to the direction of the x_r axis of Figure 4-1; toward the top of the paper, (parallel to the UV1 axis) corresponds to the direction of the y_r axis; and upward out of the paper corresponds to the direction of the z_r axis. The projections of the three body fixed unit vectors $\bar{n}_{xb}$, $\bar{n}_{yb}$ and $\bar{n}_{zb}$ onto the plane of the unit circle are shown in each of the figures, with a vector being projected from above or lying in the plane of the unit circle being denoted by a solid

36

line, and being projected from below by a dashed line. The three unit vectors are identified by: a circle for $\overline{n}_{xb}$, an x for $\overline{n}_{yb}$, and a triangle for $\overline{n}_{zb}$. No identification is given to a vector if its projection is small, as seen in the middle circle in Figure 6-1b. The projections of the unit vectors on the circle on the right in Figure 6-1b indicate that the desired orientation has almost been achieved at t = 180 sec., since the $\overline{n}_{xb}$ unit vector has nearly approached the x_r direction and the $\overline{n}_{yb}$ vector has nearly approached the y_r direction.

B. STEEPEST-DESCENT

1. Results

The extended method of steepest-descent was used to iterate as close as possible to a minimum-fuel solution for the sets of initial conditions described in Table III. The weights d_i , for i = 1,2,3 , are taken as one.   The bounds on the components of the control vector were chosen initially to provide equal acceleration levels. It was decided to select the norm of the control vector to be of the same magnitude as (6-3) and so each of the three bounds were set at .412 deg/ sec^2. The $\overline{\psi}$ vector of (B-1) is written for this problem as

$$
\overline{\psi} = \begin{bmatrix} x_1(t_f) - \phi_d \\ x_2(t_f) \\ \cdot \\ \cdot \\ \cdot \\ x_7(t_f) \end{bmatrix} = 0
$$

therefore, the terminal conditions for the adjoint system (5-14) may be
written as the 7×7 matrix

$$\Lambda^T(t_f, t_f) = \begin{bmatrix} 1 & & & & & & 0 \\ & 1 & & & & & \\ & & \cdot & & & & \\ & & & \cdot & & & \\ & & & & \cdot & & \\ & & & & & \cdot & \\ 0 & & & & & & 1 \end{bmatrix} .$$

Various computer runs were made using the method of steepest-
descent. Since no proof of convergence is available for the solution of
the acquisition problem by the method of steepest-descent, many different
cases will be examined. By selecting a wide variety of cases a great
deal will be learned about the convergence properties. The initial
conditions of Run R-1, Table III were used as the basis for a number of
the following runs: Figures 6-2 shows the response of the system to an
initial, arbitrary guess of the switching times with $t_o = 0$ and
$t_f = 60$ sec. Nineteen iterations later* the response in Figure 6-3 is
obtained with a fuel consumption of .1617 sec^{-1} . Figure 6-4 shows
the response after 15 iterations when the bounds on the control components
are set equal to .206 deg/sec^2 and $t_f = 60$ sec . The fuel consumption
is .1595 sec^{-1} , which is within 1.4% of the above fuel consumption.
Comparison of Figures 6-3 and 6-4 shows that the response curves are
almost identical. Even though different sets of initial control time
histories were used to generate the steepest descent solutions of
Figures 6-3 and 6-4, the solutions converged to the same extremum value
of $J(t_f)$. Perhaps some other relative extremum value existed; however,
no indication of this possibility was found.

_____

*An iteration takes approximately 30 sec on the Burroughs B-5500
digital computer for the mathematical model considered in this chapter.

38

Using the lower set of control bounds two more responses are obtained: Table V, coupled with Figure 6-5 show that after 26 iterations with $t_f = 45$ sec the fuel consumption is .1969 sec^{-1}, and with Figure 6-6 that after 11 iterations and $t_f = 120$ sec, .1024 sec^{-1} fuel is consumed. These quantities of fuel consumption are normalized with respect to the value .260 sec^{-1}, and plotted in Figure 6-10, curve B as a function of t_f. The quantity .260 sec^{-1} is the amount of fuel consumed by the idealized proportional control which has "settled" at $t_f = 288$ sec. See Table V for a summary of this data. The shape of this curve is as expected [Ref. 2-3, 2-8]. As can be seen from this curve of fuel consumption vs. t_f, the minimum-fuel solution at $t_f = 120$ sec uses only 40% of the amount of fuel consumed by the idealized proportional control. Comparing the relative angular rates between the idealized proportional control scheme of Figure 6-1 and the minimum-fuel solutions of Figure 6-4, 6-5 and 6-6 indicates that they are approximately equal if $t_f = 45$ sec and are much lower in the minimum-fuel solution if $t_f = 120$ sec.

To examine the effectiveness of the method of steepest-descent under an off-nominal design condition a different set of initial conditions are chosen (see Run R-2, Table III), as well as a set of unequal acceleration bounds. These bounds are:

$$|u_1|_{max} = .552 \text{ deg/sec}^2$$

$$|u_2|_{max} = .403 \text{ deg/sec}^2$$

$$|u_3|_{max} = .207 \text{ deg/sec}^2$$

The norm of the maximum control vector is again .715 deg/sec^2 .

Figure 6-8 shows the response to an initial guess of control switching times with $t_f = 60$ sec . After 18 iterations, the solution may be found in Figure 6-9, where the fuel consumption is .1075 sec^{-1} . The method of steepest-descent appears to work as well for this off-nominal system as for the system which has equal control bounds. A curve of fuel consumption vs. t_f is generated for this set of initial conditions and is normalized with respect to the fuel-consumption in Run R-2 of Table III of .142 sec^{-1} in 360 sec . This curve is plotted in Figure 6-10, Curve A. As long as $t_f > 39$ sec the minimum-fuel solution will consume less fuel than the idealized proportional control scheme. The data for this curve are summarized in Table V.

Several more sets of initial conditions are examined using the method of steepest-descent with $t_f = 60$ sec and the bounds on each of the control components equal to .206 deg/sec^2 . These additional cases were prompted by the desire to gain deeper insight into the convergence properties of the method. Figure 6-11 represents the response to a _first guess_ of control switching times starting from the initial conditions $x_i = 0$ for $i = 1,...,7$. The solution to this problem is, of course, that no control should be applied and that the states will remain identically equal to zero. After 4 iterations the pulses have been collapsed, the state vector remains at the origin, and no fuel is consumed. The resulting zero states and the zero-width control pulses are _not_ presented in a figure. Figure 6-12 represents the response from the initial conditions of Run R-3 Table III after 13 iterations. The fuel consumption is .0546 sec^{-1} vs. .158 sec^{-1} as in the idealized

40

Table V. Data for Curves A and B in Figure 6-10.

Curve	t_f, sec	30	45	60	90	120
A	$x_1(t_f)$, sec^{-1}	.1809	.1299	.1075	.0915	.0769
A	$x_1(t_f)/.142$	1.275	.915	.757	.645	.541
A	No. of Iterations	20	13	18	11	14
B	$x_1(t_f)$, sec^{-1}		.1969	.1595		.1024
B	$x_1(t_f)/.260$		.756	.614		.394
B	No. of Iterations		26	15		11

proportional control case. Notice that no control is required in two
of the three axes. Figure 6-13 indicates the response from the initial
conditions of Run R-4, Table III after 15 iterations. Fuel consumption
is .0906 sec^{-1} vs. .175 sec^{-1} . The final Figure 6-14 indicates the
response from initial conditions of Run R-5, Table III after 15 iter-
ations. Fuel consumption is .0705 sec^{-1} vs. .0954 sec^{-1} . In each
of the above runs which use the idealized proportional control it takes
at least 180 seconds to acquire the desired orientation within acceptable
bounds.

By examining the solutions generated by the method of steepest-
descent one finds that the control components are usually off at
$t = t_o^+$ and at $t = t_f^-$. Experience has shown that the true optimal
solutions usually contain control components which are on at $t = t_o$
and $t = t_f$. The solutions generated by the extended method of
steepest descent seem to apply to problems with the same constraints
but with shorter time periods, $(t_f - t_o)$, than the problems which

are being studied. It is not clear how to influence the leading and trailing switching times to more closely approach $t = t_o$ and $t = t_f$ when they should approach these times.

2. Computational Considerations

There are a number of important aspects which must be considered when using the extended method of steepest-descent. The minimum-fuel, scalar control of the "$1/s^2$ plant" was studied extensively by means of the extended method of steepest-descent. The specific results will not be discussed here; however, the bases for many of the computational considerations presented below were formed as a result of this preliminary study. The success of the method depends to a large degree upon qualitative characteristics of the first guess of the switching times. After a period of trial and error it was decided to use a total of twelve switching times (six pulses of alternating polarity) in each of the three control channels as the basic form of the control time history. It is better to start with too many pulses for they can be collapsed by further iterations; whereas, if too few pulses were chosen convergence would become impossible since no provision has been made to create new impulses. In most cases, the polarity of the first pulse in each axis should be specified with a sign opposite to the sign of the initial rate about that axis. If the initial rate is zero then the polarity of the first pulse should be specified with a sign opposite to the sign of the Euler parameters corresponding to that axis. This recommendation is summarized by:

$$\text{sgn(first pulse of } u_i) = \begin{cases} - \text{sgn}[x_{i+1}(t_o)], & \text{if } x_{i+1}(t_o) \neq 0 \\ - \text{sgn}[x_{i+4}(t_o)], & \text{otherwise} \end{cases}$$

for $i = 1,2,3$. This recommendation was formed as a result of the study of the $1/s^2$ plant, and was found to be most important for the systems studied in this text. The reason for the importance of choosing the initial polarity is that when the above recommendation is followed the initial pulse has only to be widened or narrowed by subsequent iterations; whereas, if the polarity is chosen in the opposite sense then the first pulse has to be removed by iteratively moving the first two switching times until they are equal to t_o, and then widening or narrowing and and shifting the second pulse. This latter choice requires many more iterations for convergence; indeed, convergence may not be possible. This recommendation has an intuitive basis: if one is leaving the origin or is located away from the origin then the first logical action is to oppose this situation.

It was also found that an initial equal distribution of relatively narrow pulses as in Figure 6-2b offered the best initial guess of switching times for most cases. In several cases this standard initial guess of the switching times drove the state vector through the singularity at $\psi(t) = 180 \text{ deg}$. Since values of $\bar{x}_n$ are stored at a finite set of times, the chance of storing a zero value for x_8 is small; however, it was decided not to take this chance. The initial guess was then slightly modified by making the initial pulses on each control channel a little wider; thereby avoiding the singularity.

As can be seen from a comparison of Figures 6-2 and 6-3 as well as Figures 6-8 and 6-9, it is not important to obtain an initial trajectory which in any way satisfies the terminal constraints; the extended method of steepest-descent may converge to the desired terminal constraint in as few as 6 iterations.

Experience in using the method of steepest-descent to solve the acquisition problem leads to several recommendations concerning the digital simulation:

i. As discussed in Chapter V and Appendix B, t_o appearing in (B-21) may become equal to t and take on discrete values between t_o and t_f . It was found that although this "sampling" technique reduced the number of iterations required for satisfactory convergence, the additional time to perform each iteration more than overshadowed the reduction in iterations. The additional time for each iteration was due to an additional matrix inversion for each sample time. The sampling technique was not used for the majority of runs.

ii. If the magnitude of any of the components of the $\overline{\delta\psi}$ vector of (B-3) becomes too large due to an initial bad guess on the control time history then convergence is not possible. It was found that by limiting each of the components of $\overline{\delta\psi}$ to some nominal value (.5 deg/sec for the rates and .5 for the Euler parameters) then for most cases practical convergence is assured.

iii. The cost-weighting matrices, T_i , must be specified. Since the parameters of the problem do not change markedly over the period of solution the T_i and T_j , matrices are assumed equal. For the off nominal design featured in Figures 6-8 and 6-9, where the control

44

I

accelerations are unequal, speed of convergence was tested for the case where the elements of each T_i were chosen either to weight the change in total control impulse or to weight the change in switching times. The latter means of weighting provided the most rapid convergence and so for all runs the T_i matrices were specified as unit matrices.

The convergence procedure for the method of steepest-descent which proved most effective was to ignore the cost functional in the constraint $\bar{\psi}$ of (B-1) for the first iterations until the terminal constraints were met. Typically this took 6 iterations. Then a desired value of the cost functional, $\emptyset_d$, was selected which was about 50% of the value of the functional resulting from the above set of iterations, and about 4 more iterations made. The value of $\emptyset_d$ was purposely set low enough to be well below the optimum value. It was found that the constraint on the states could not be met, and that some value of the cost functional was reached, $\emptyset_{da}$, which was above the $\emptyset_d$ value. Next the $\emptyset_d$ value was ignored in the $\bar{\psi}$ vector and the only constraint that was attemped to be met was that on the states. This final set of iterations (usually about six) then achieved convergence to the terminal constraint while giving a value to the cost functional $\emptyset$ close to $\emptyset_{da}$. The final trajectory was then taken as an "optimal trajectory" as computed by the method of steepest-descent.

Convergence to a desired trajectory was difficult when the value of the interval $t_f - t_o$ approached to within 50% of the time for the minimum-time solution. It took 26 iterations to give the response in Figure 6-5 when $t_f = 45$ sec vs. 11 iterations for the response in Figure 6-6 when $t_f = 120$ sec . Similarly for a fixed t_f , when the

bounds were reduced on the control components the minimum-time solution was approached and convergence became much more difficult. It is not clear why this approach to the minimum-time solution causes these convergence difficulties.
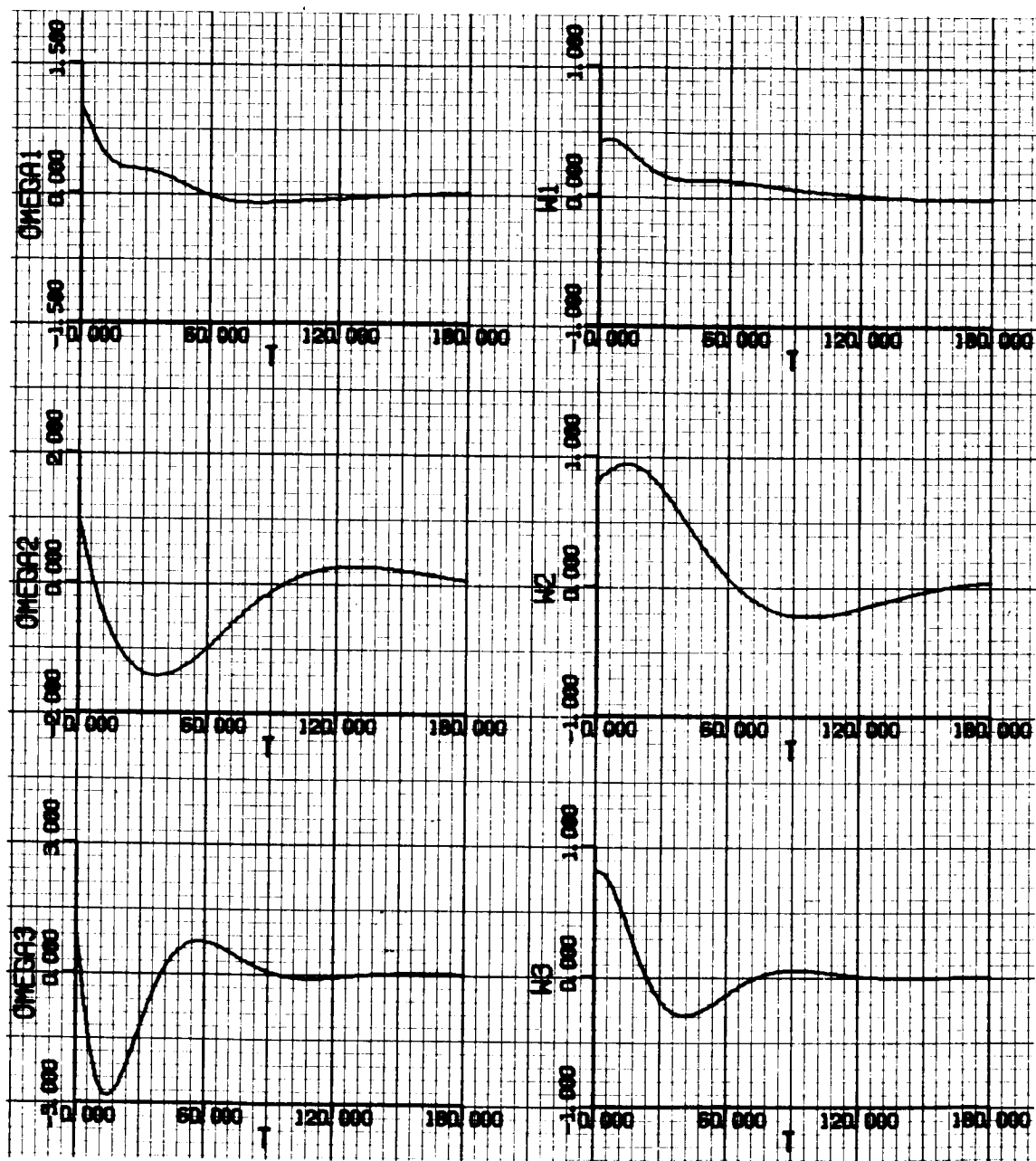
NOTE: See Table IV and Section VI-A for an explanation of
the format and dimensions of the Response Curves.

Figure 6-1a. Response Curves with Idealized Proportional Control for
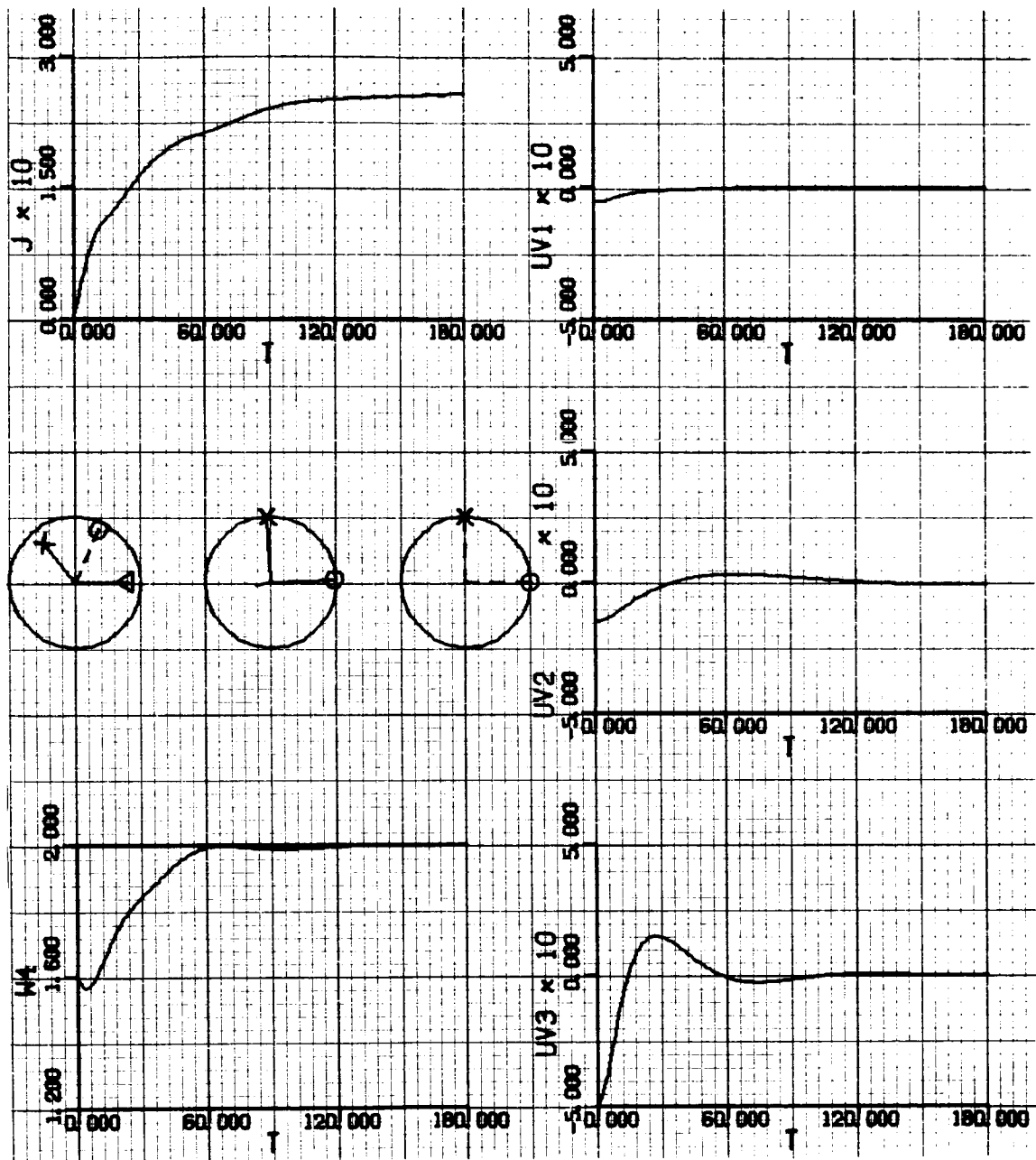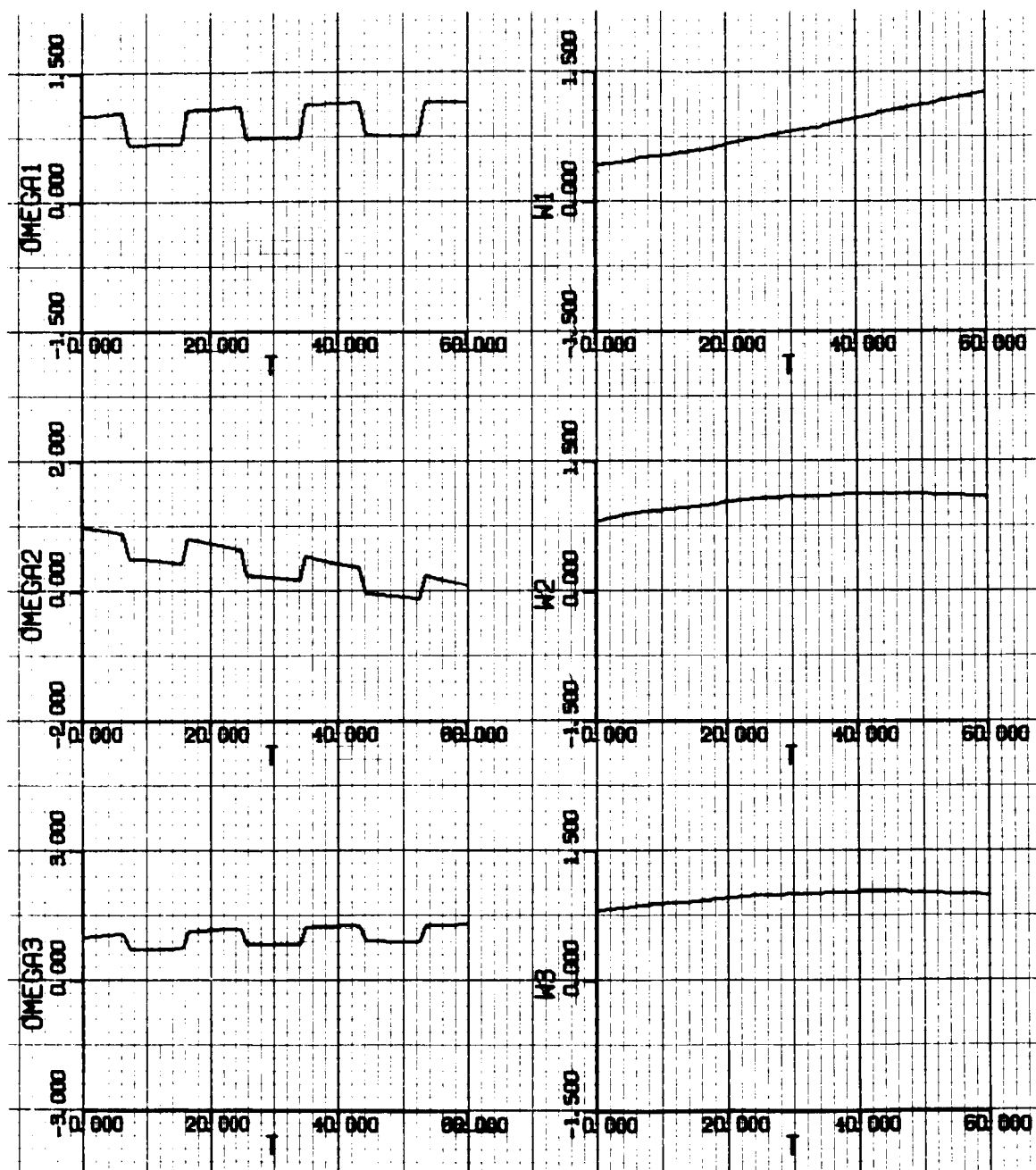Initial Conditions of Run R-1. (Table III)

48

Figure 6-1b

49

Figure 6-2a. Response to an Initial Guess of Control Time History.
Initial Conditions of Run R-1. $|u_i| \leq .412$ deg/sec^2 .
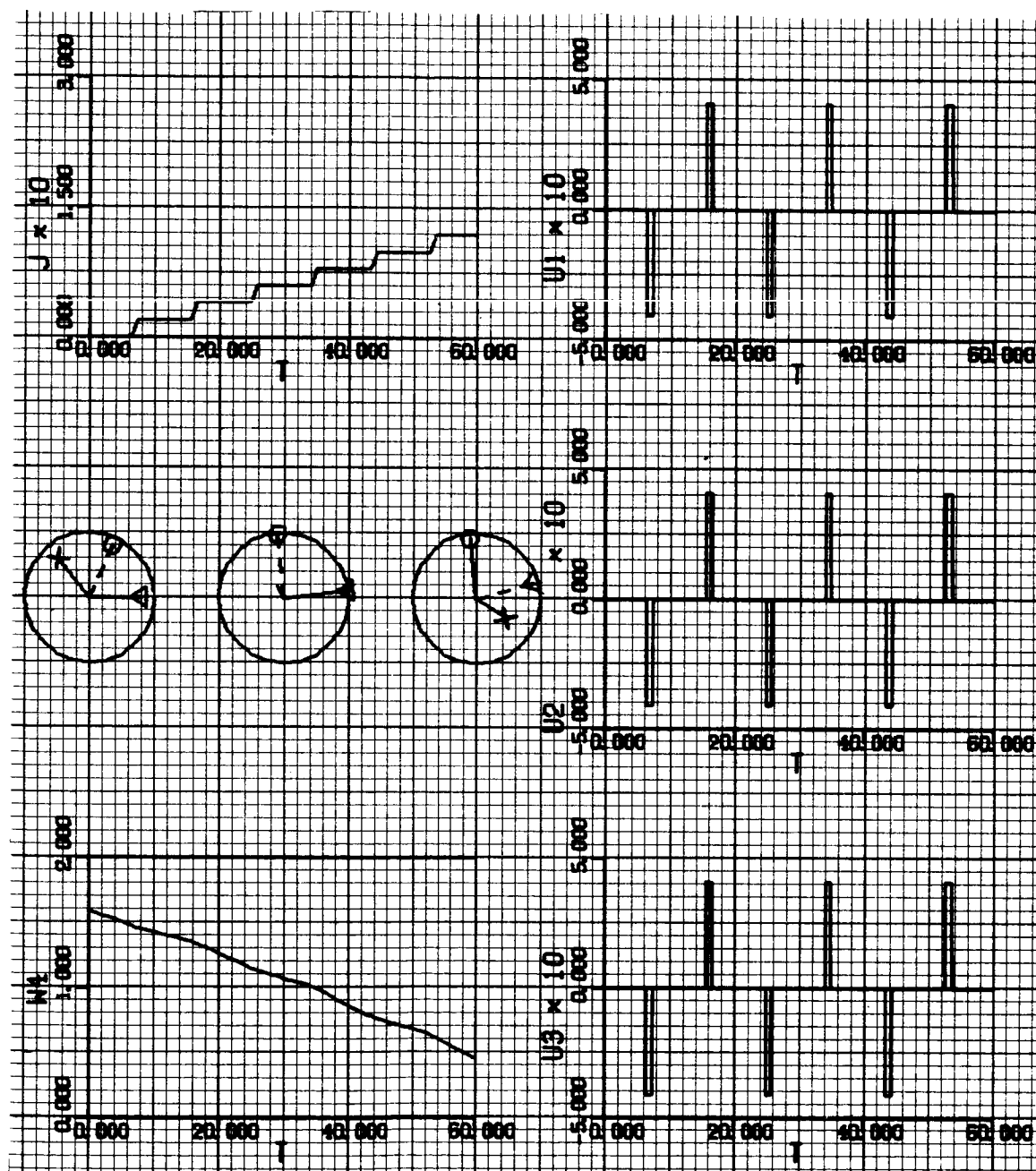
Figure 6-2b.
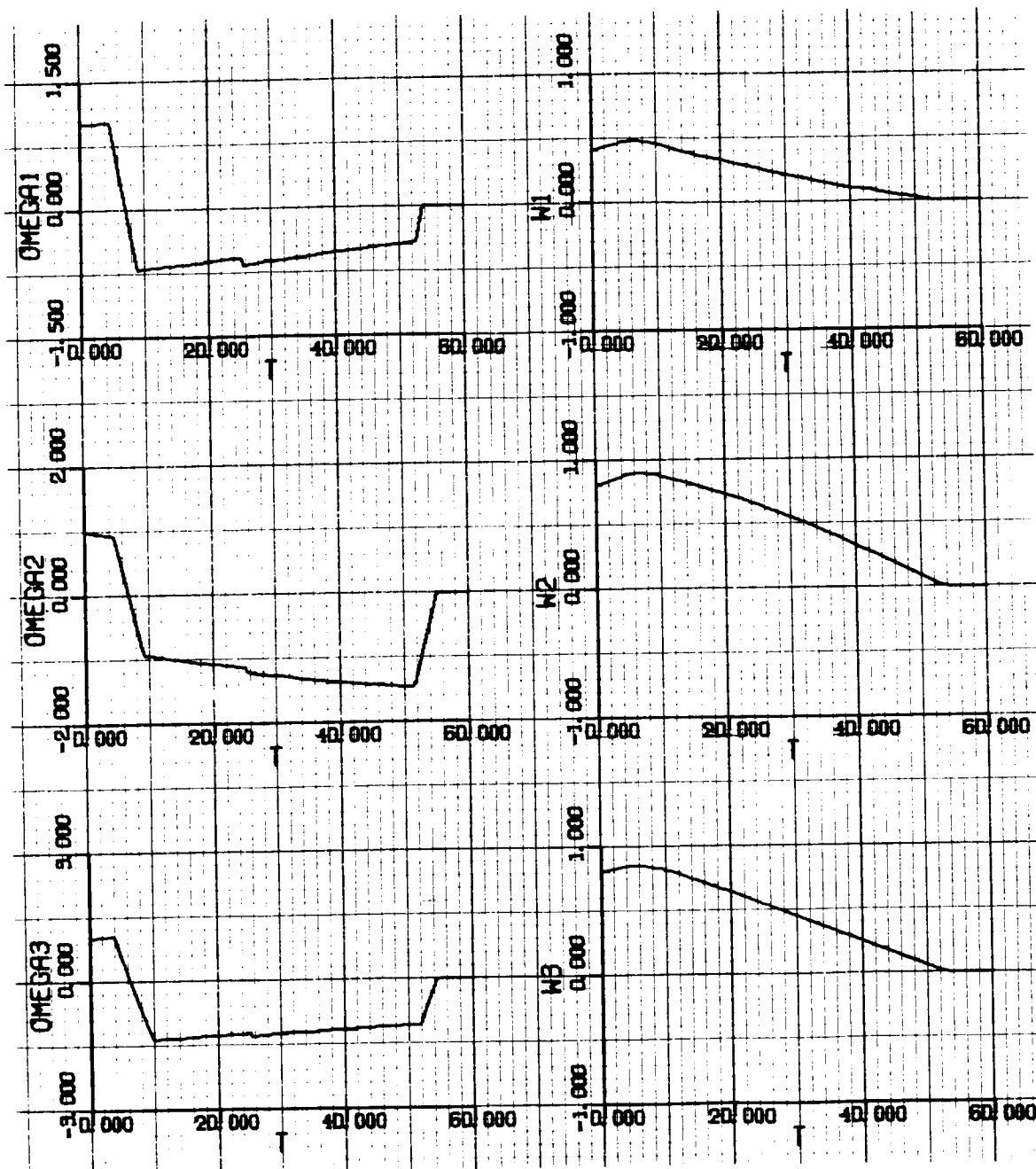
Figure 6-3a. Response Curves Generated by Method of Steepest-Descent from the Initial Guess Demonstrated in Figure 6-2.
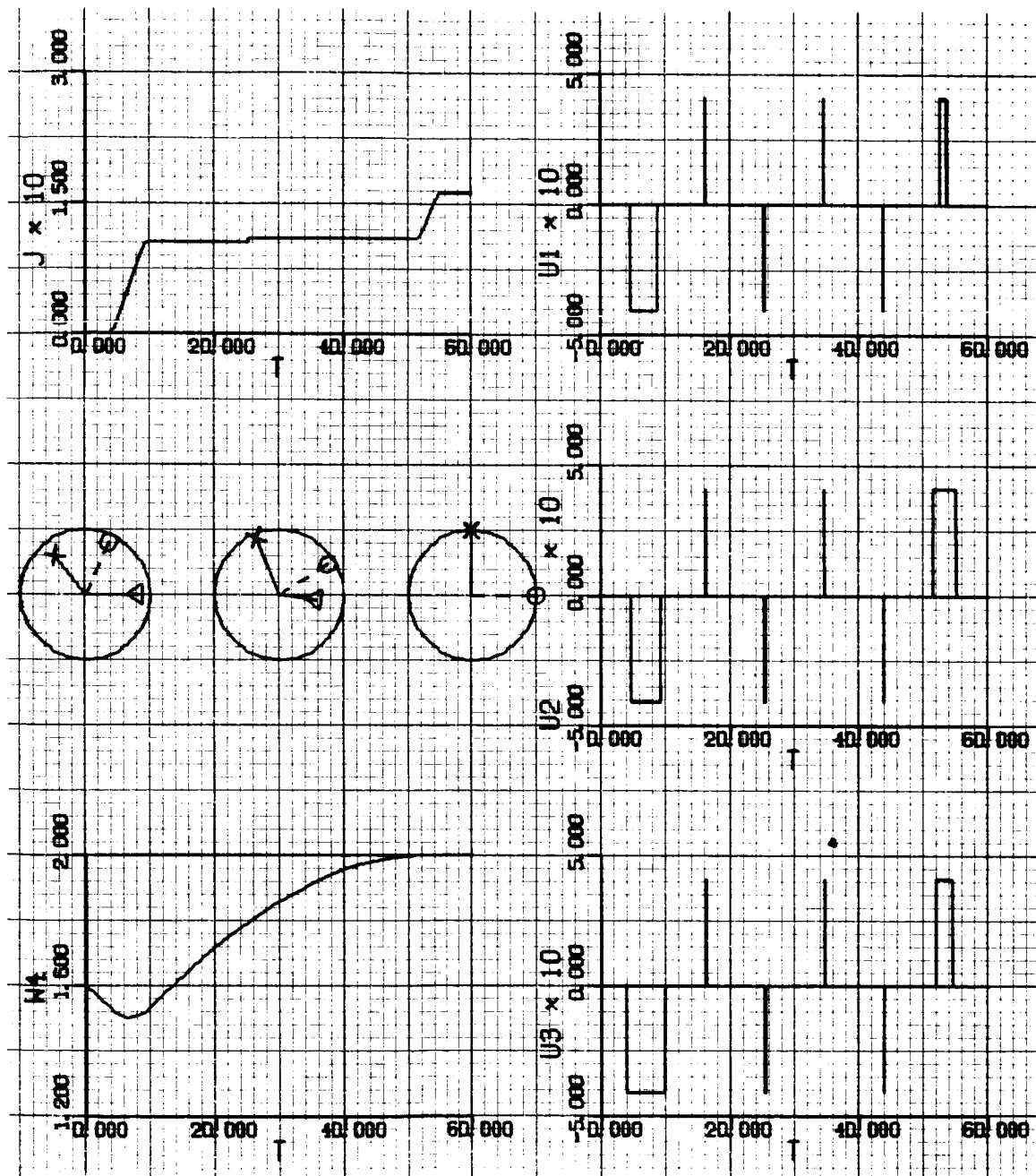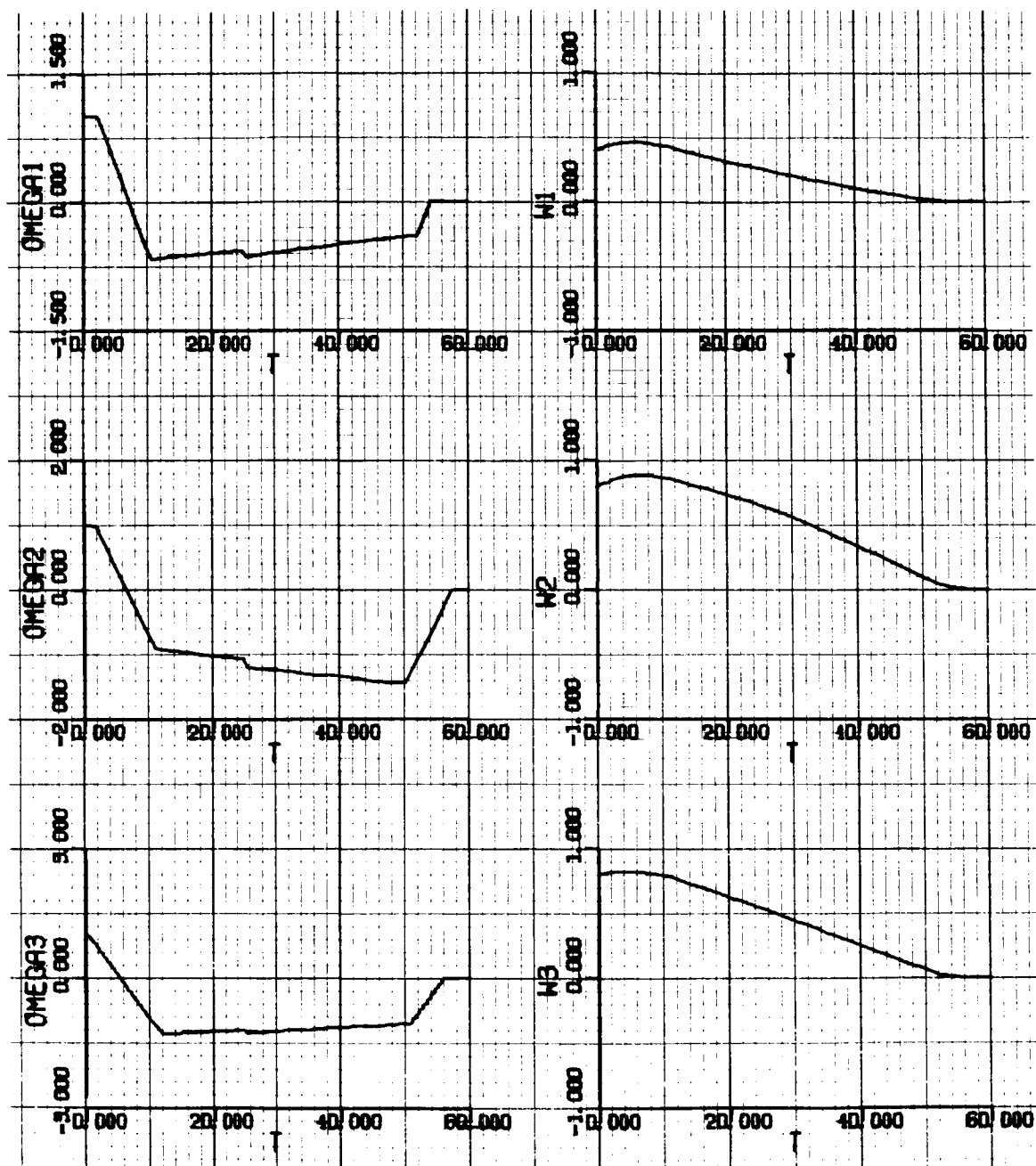
Figure 6-3b.

Figure 6-4a. Response Curves Generated by Method of Steepest-Descent for Initial Conditions of Run R-1. $|u_i| \leq .206$ deg/sec^2. $t_f = 60$ sec .
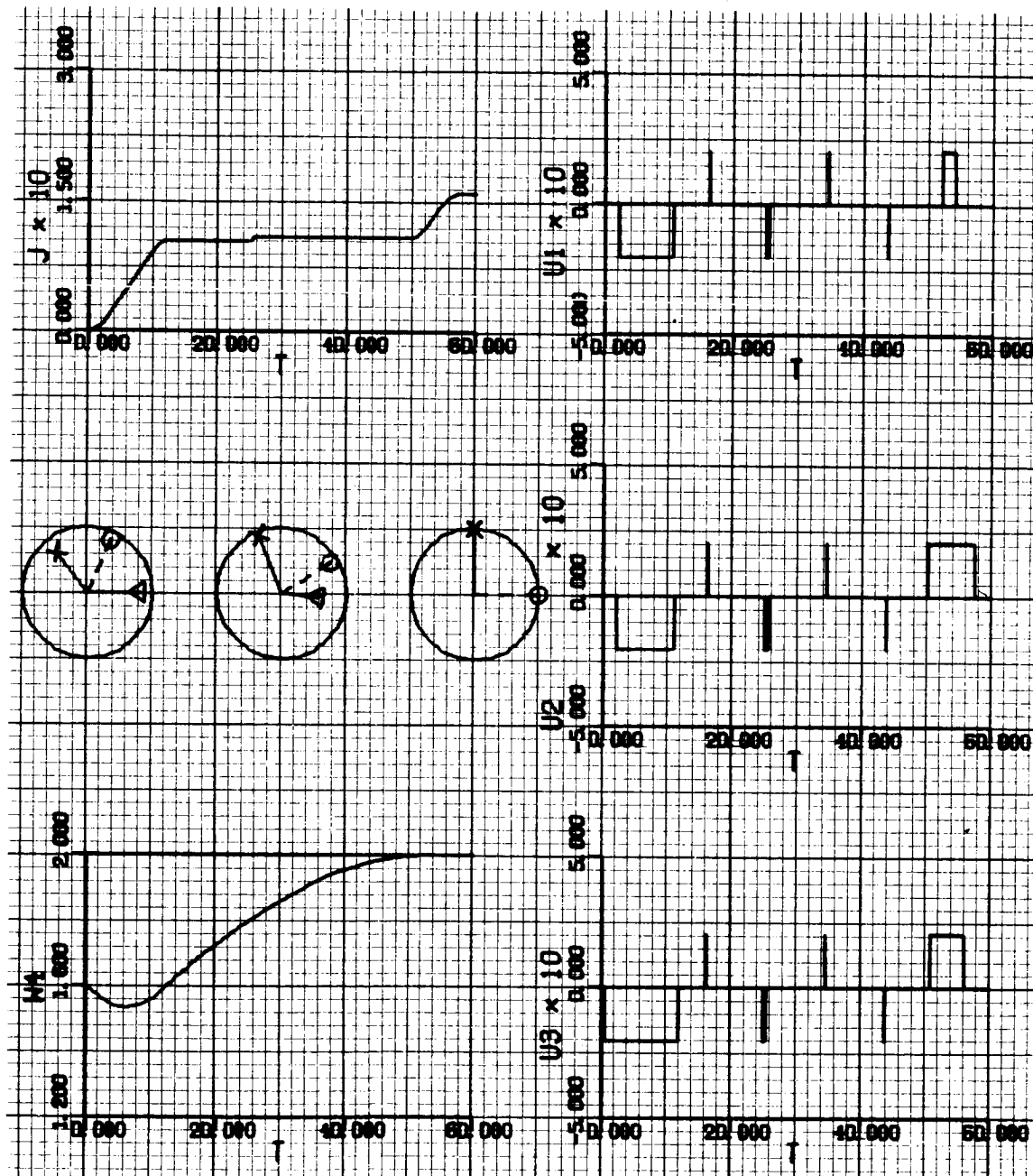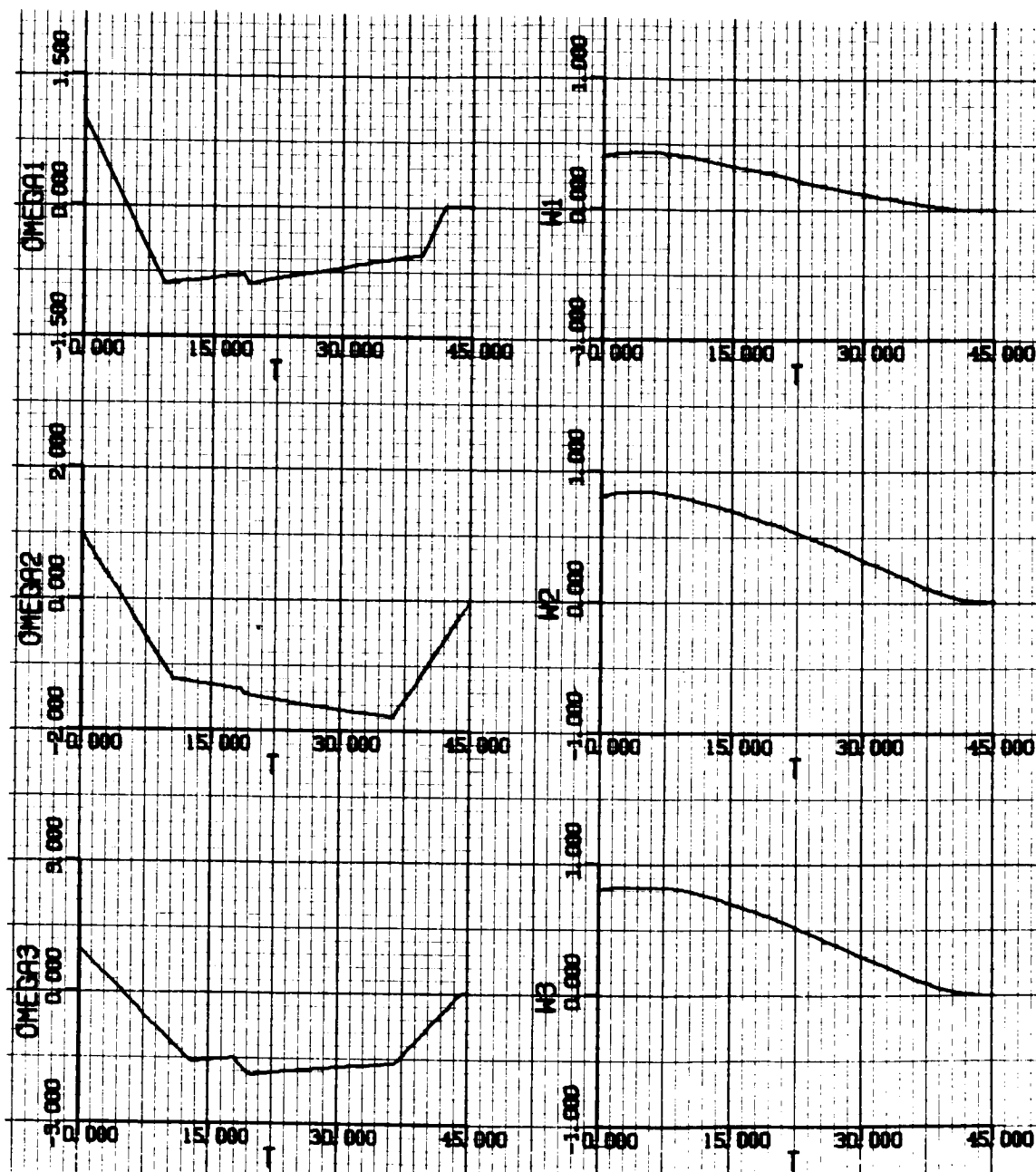
54

Figure 6-4b.

Figure 6-5a. Response Curves Generated in a Similar Fashion as Figure 6-4 with $t_f = 45$ sec . (Table V)

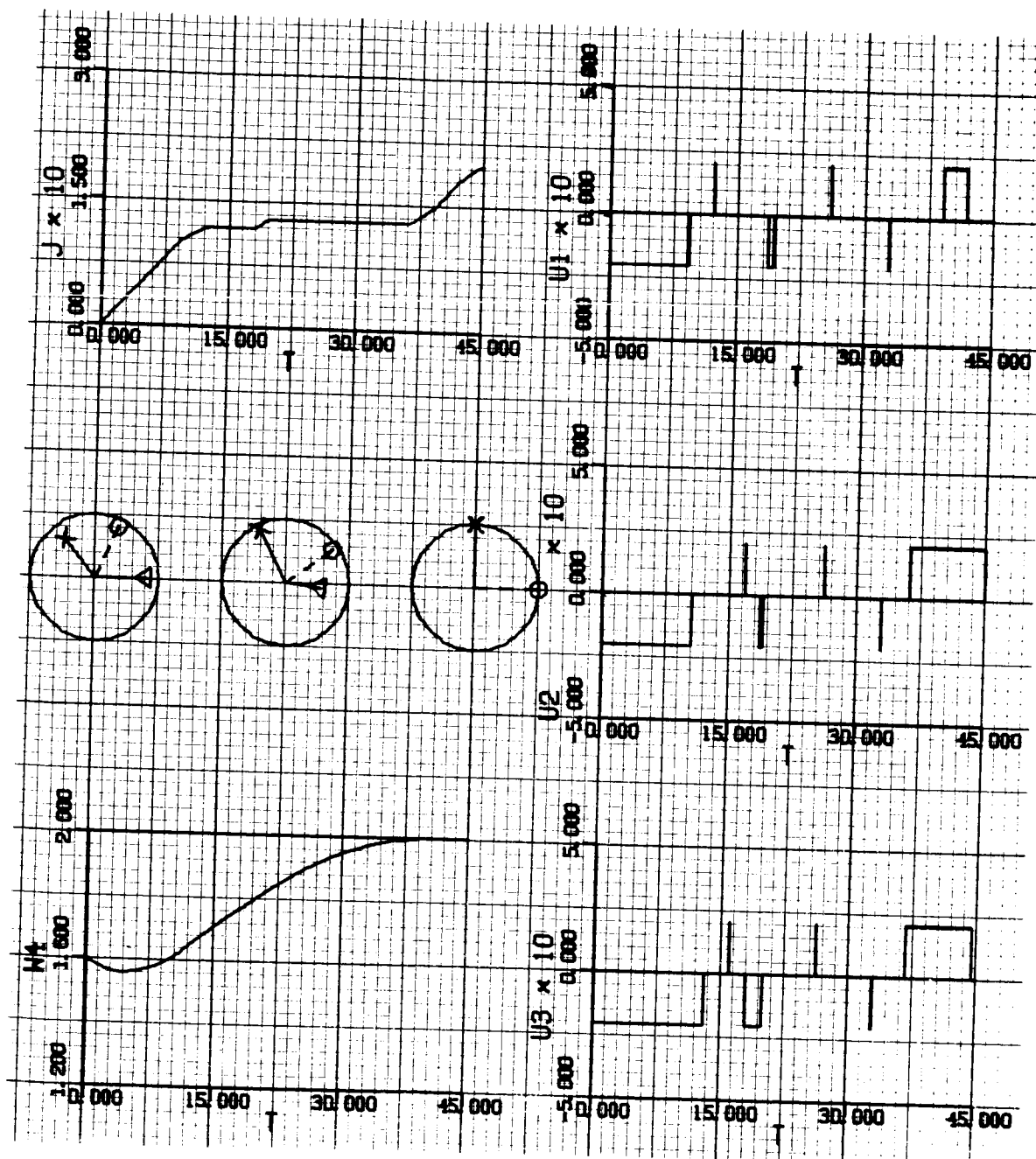Figure 6-5b.

57
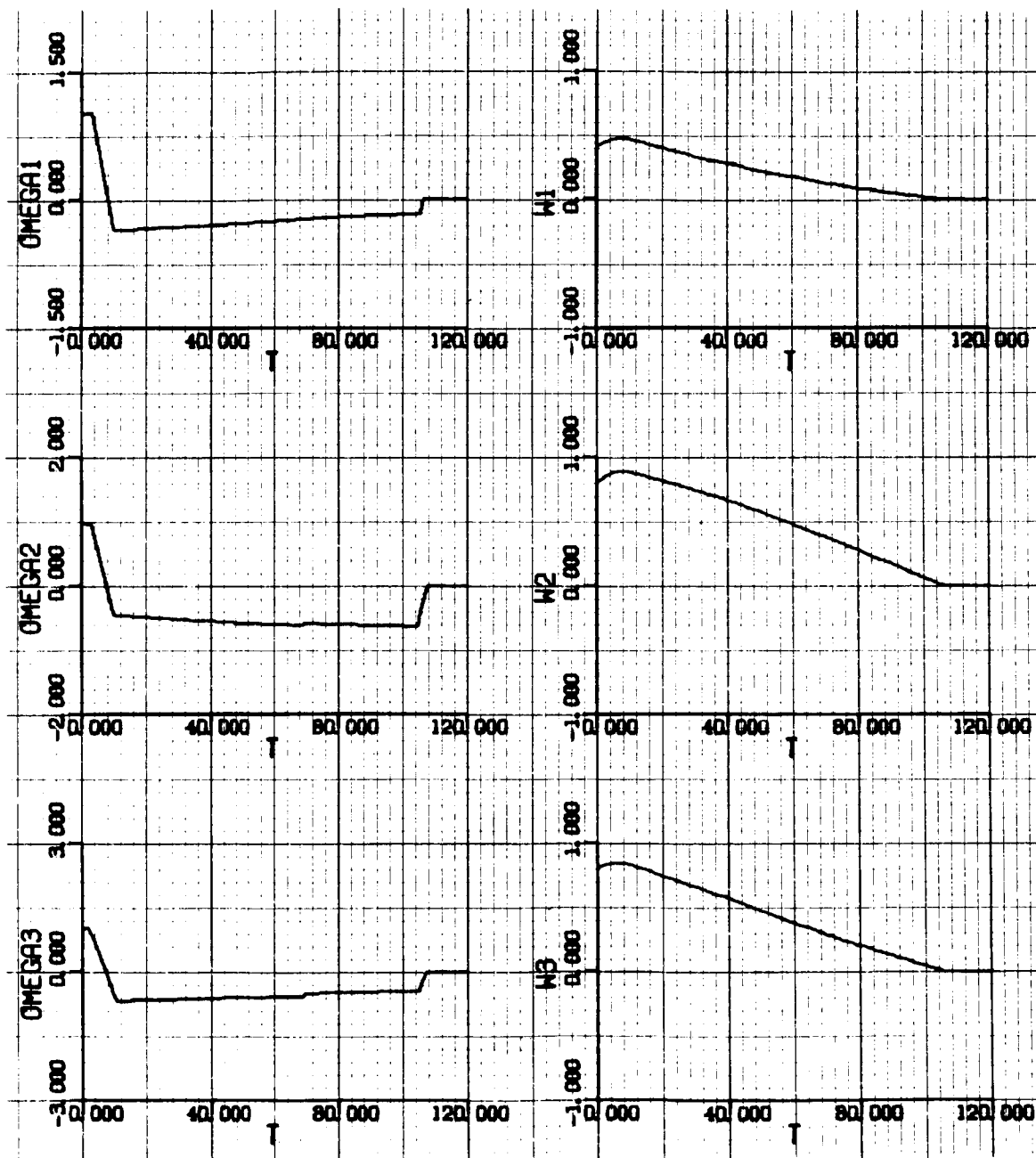
Figure 6-6a. Response Curves Generated in a Similar Fashion as Figure 6-4 with t_f = 120 sec . (Table V)
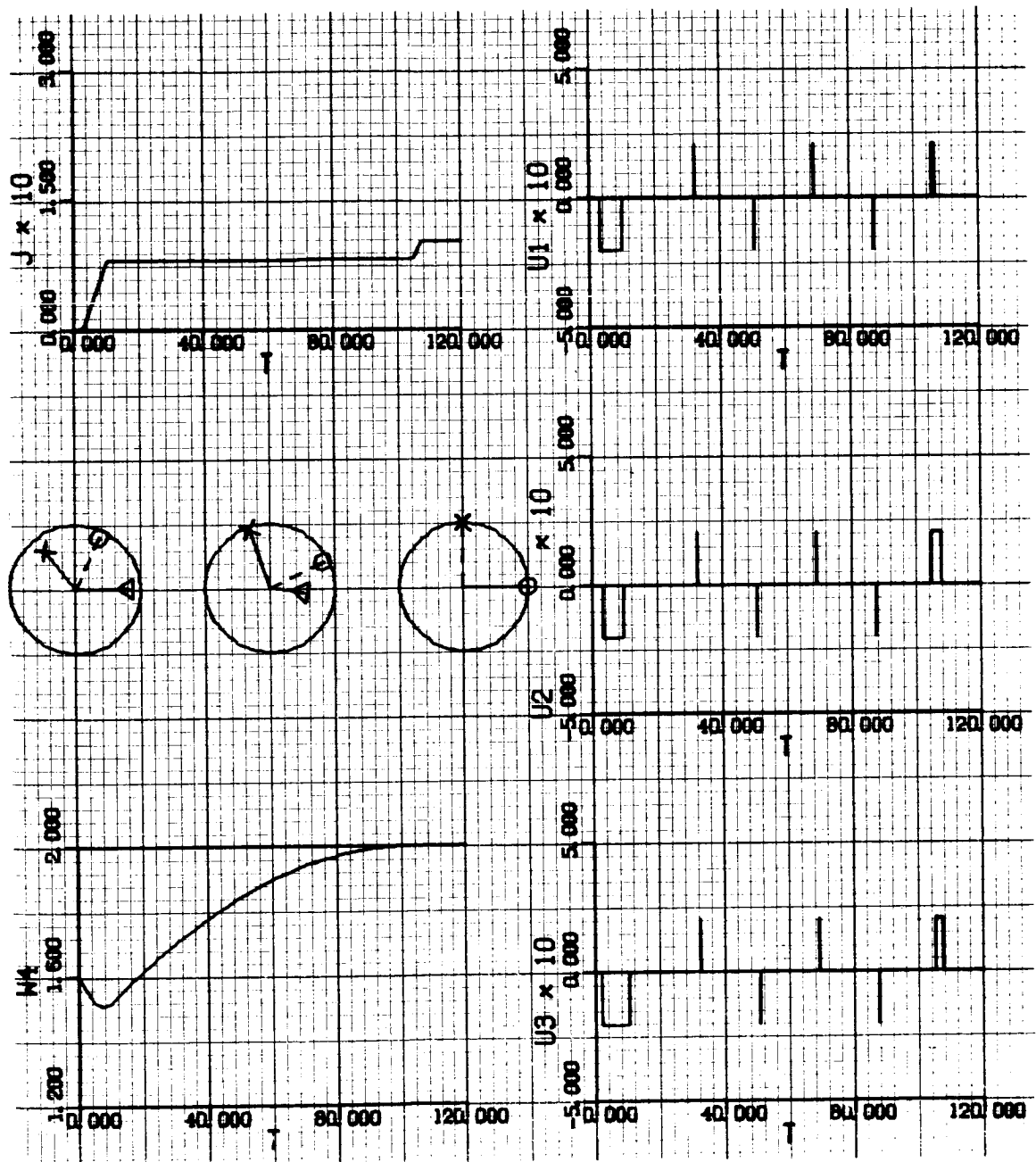
58

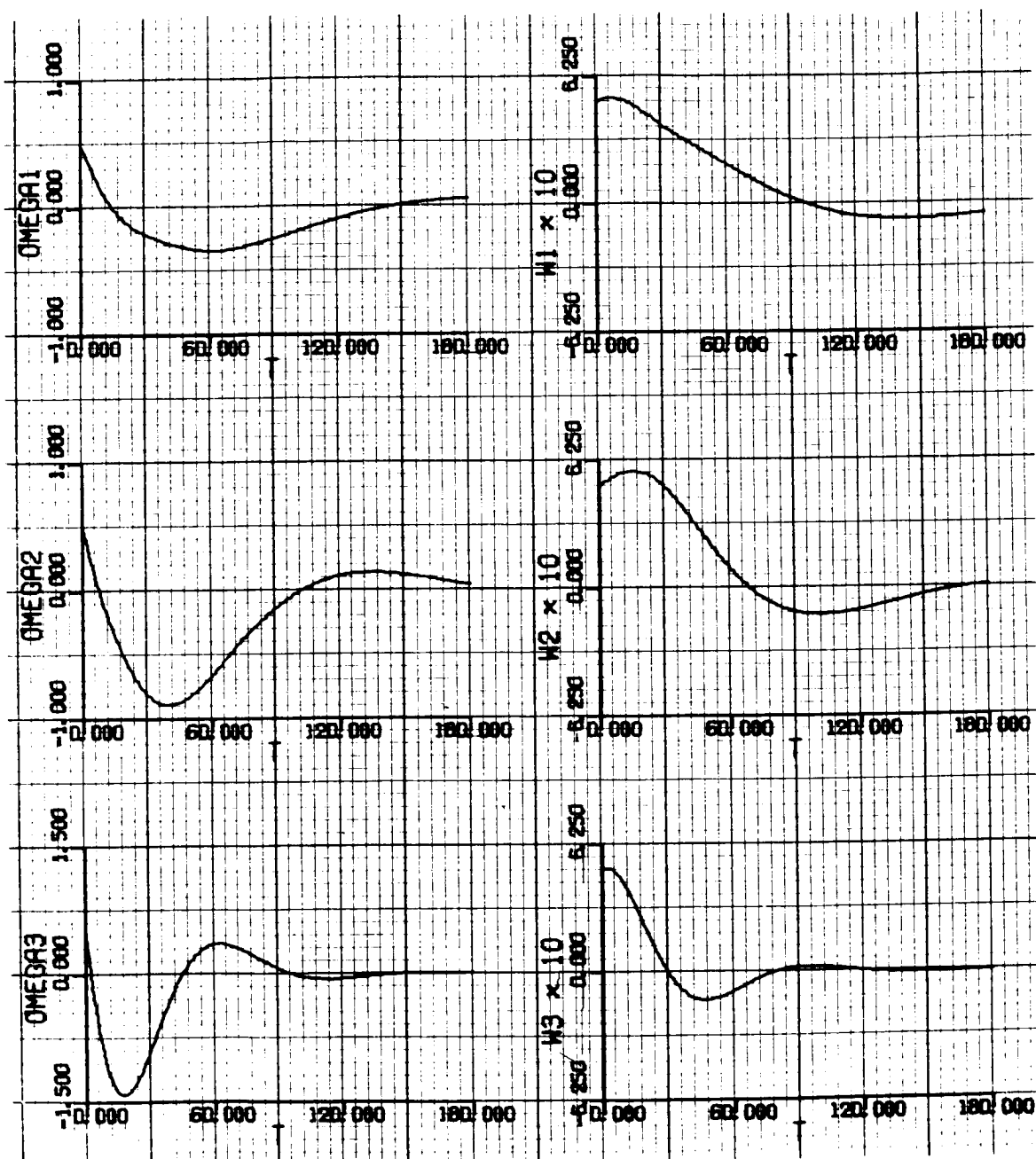Figure 6-6b.

Figure 6-7a.   Response Curves with Idealized Proportional Control for
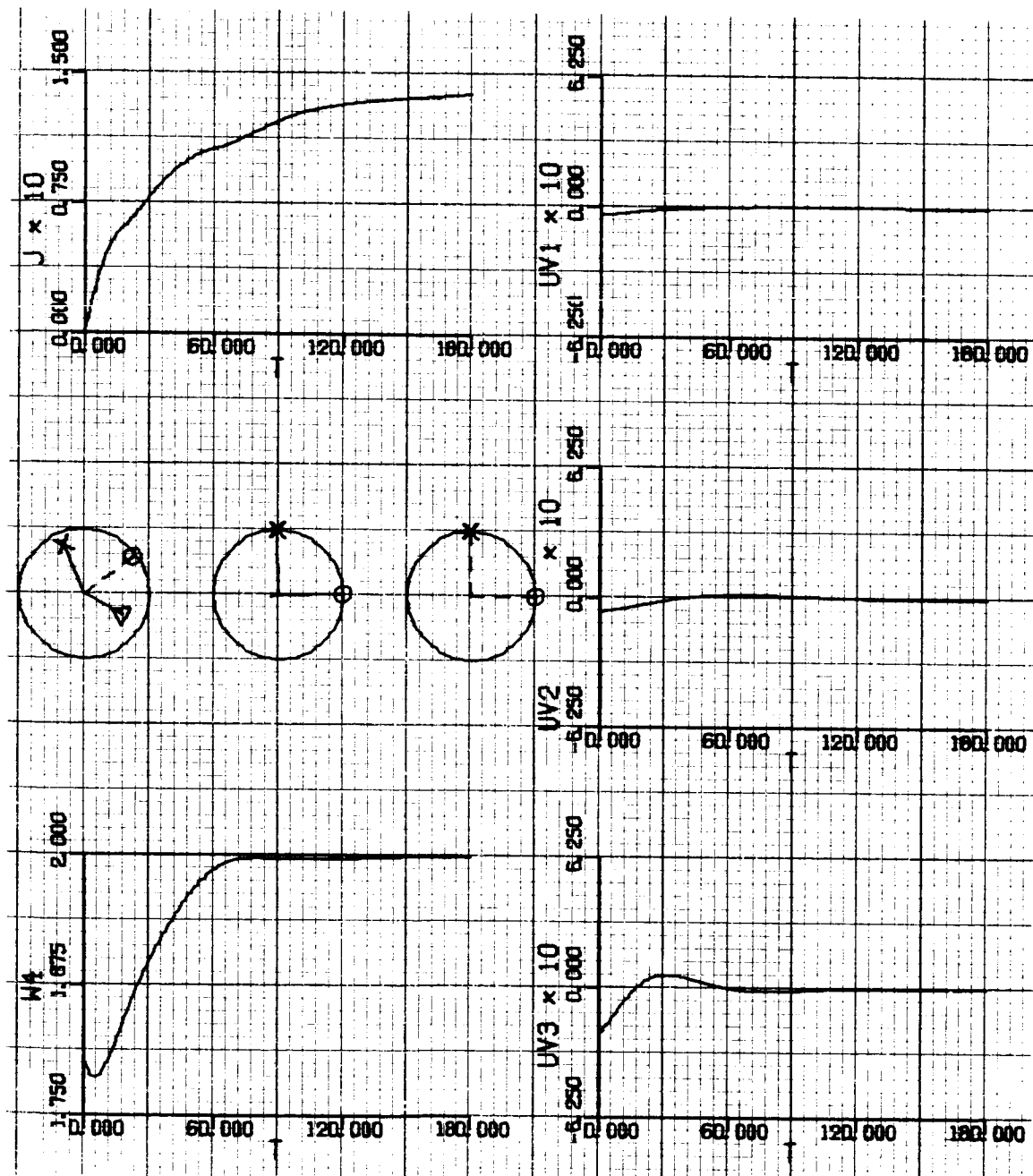Initial Conditions of Run R-2.   (Table III)

60
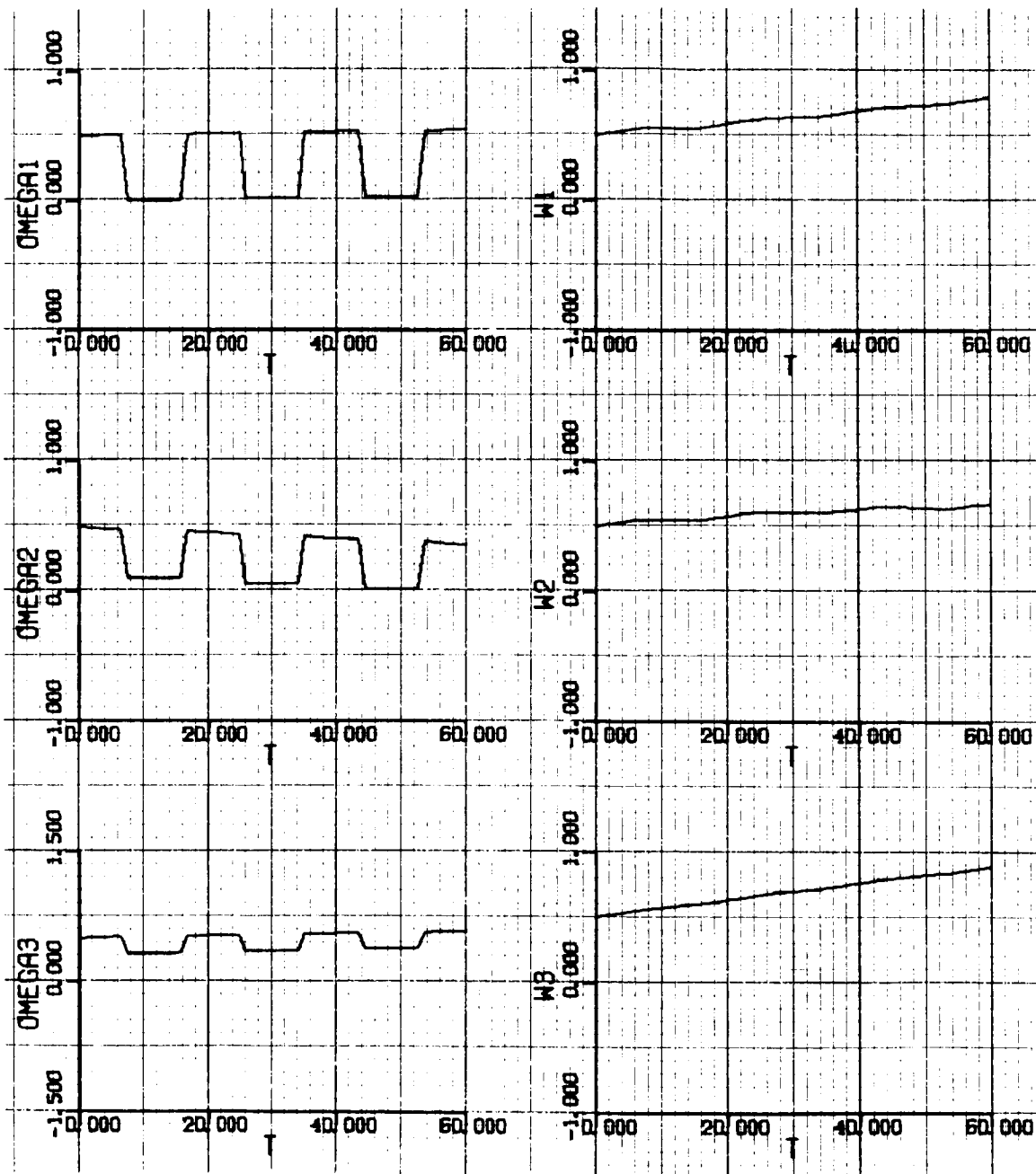
Figure 6-7b.

Figure 6-8a. Response to an Initial Guess of Control Time History.
Initial Conditions of Run R-2.

Figure 6-8b.

63
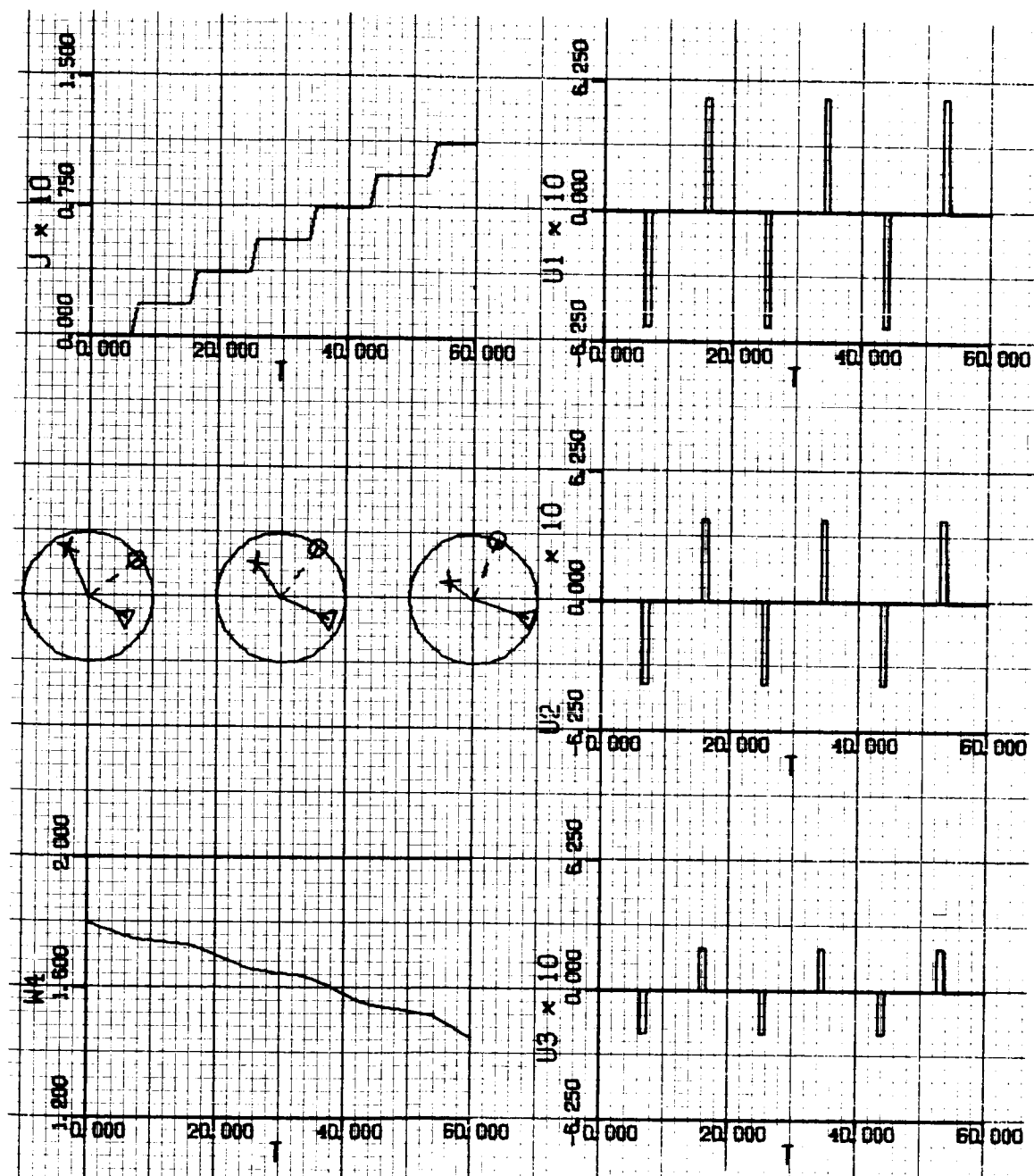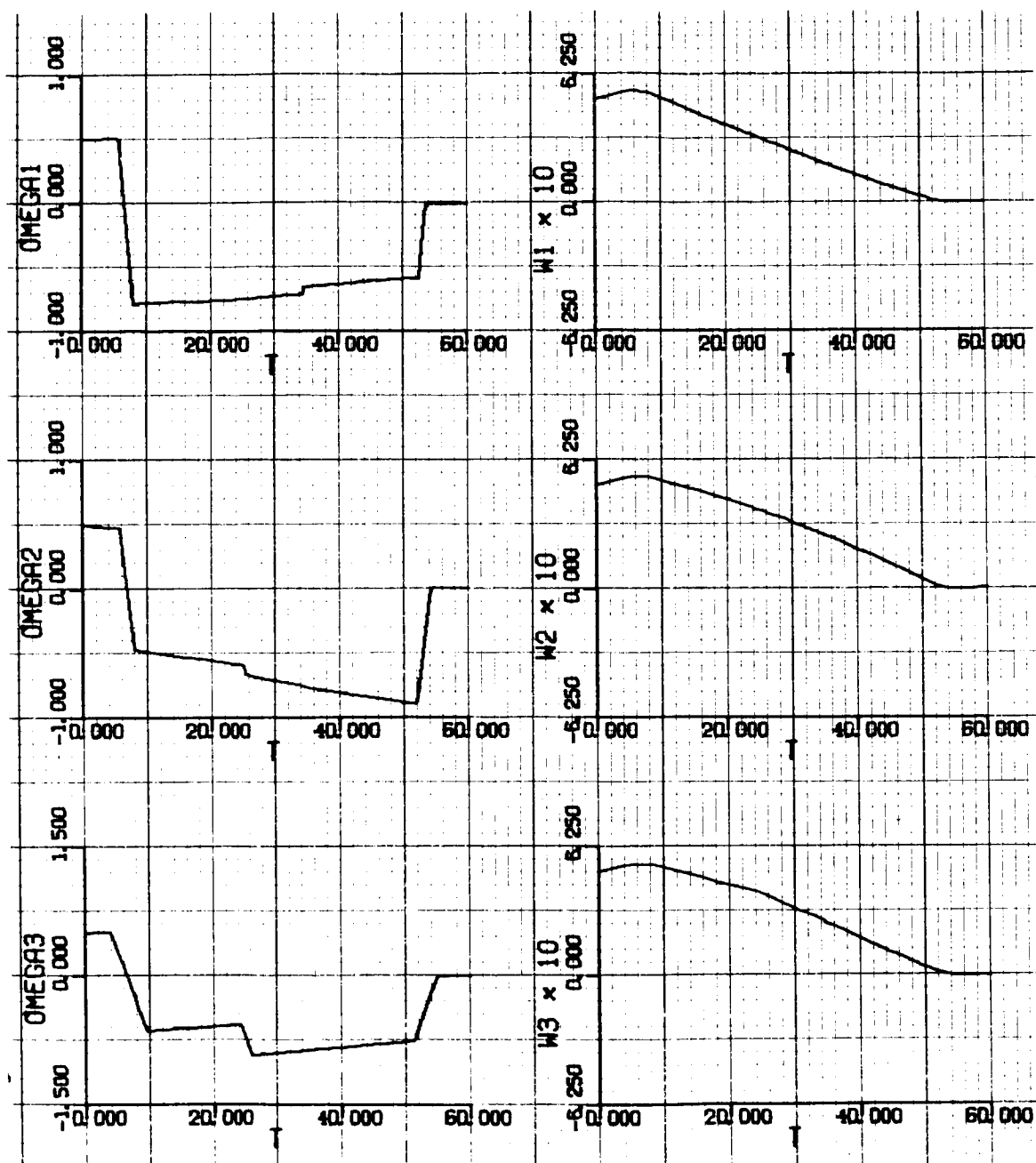
Figure 6-9a.   Response Curves Generated by Method of Steepest-Descent
from the Initial Guess Demonstrated in Figure 6-8.

Figure 6-9b.

CURVE	I.C. OF RUN	$|u_i|_{max}$, deg/sec^2		
		i=1	i=2	i=3
A	R-1	.206	.206	.206
B	R-2	.552	.403	.207

CURVE A
$J' = .142$ sec^{-1}
at $t_f = 360$ sec

CURVE B
$J' = .260$ sec^{-1}
at $t_f = 288$ sec

t_f, sec

$x_1(t_f)/J'$,
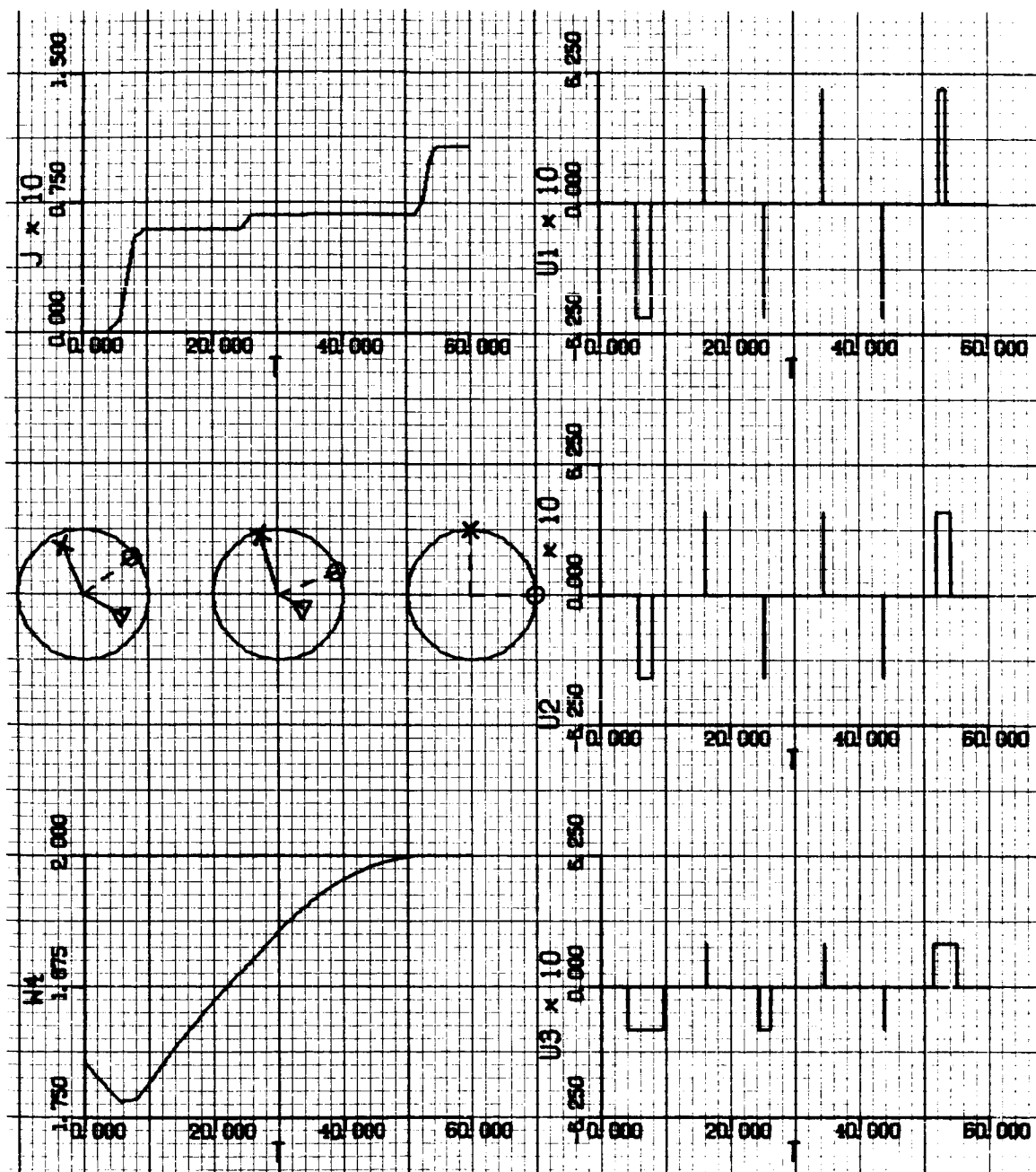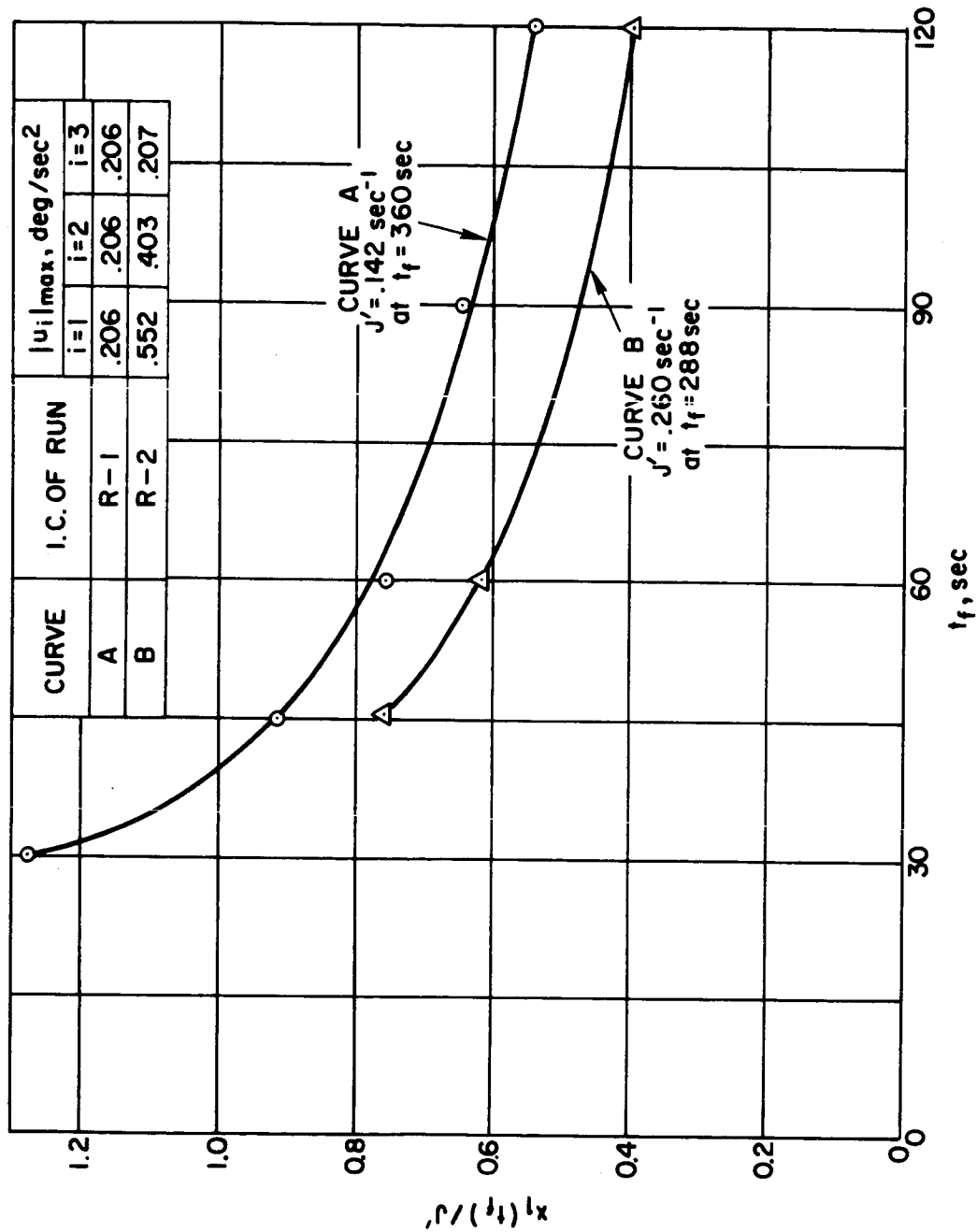
FIGURE 6-10. NORMALIZED FUEL CONSUMPTION
VS. FINAL TIME (INITIAL TIME = 0)
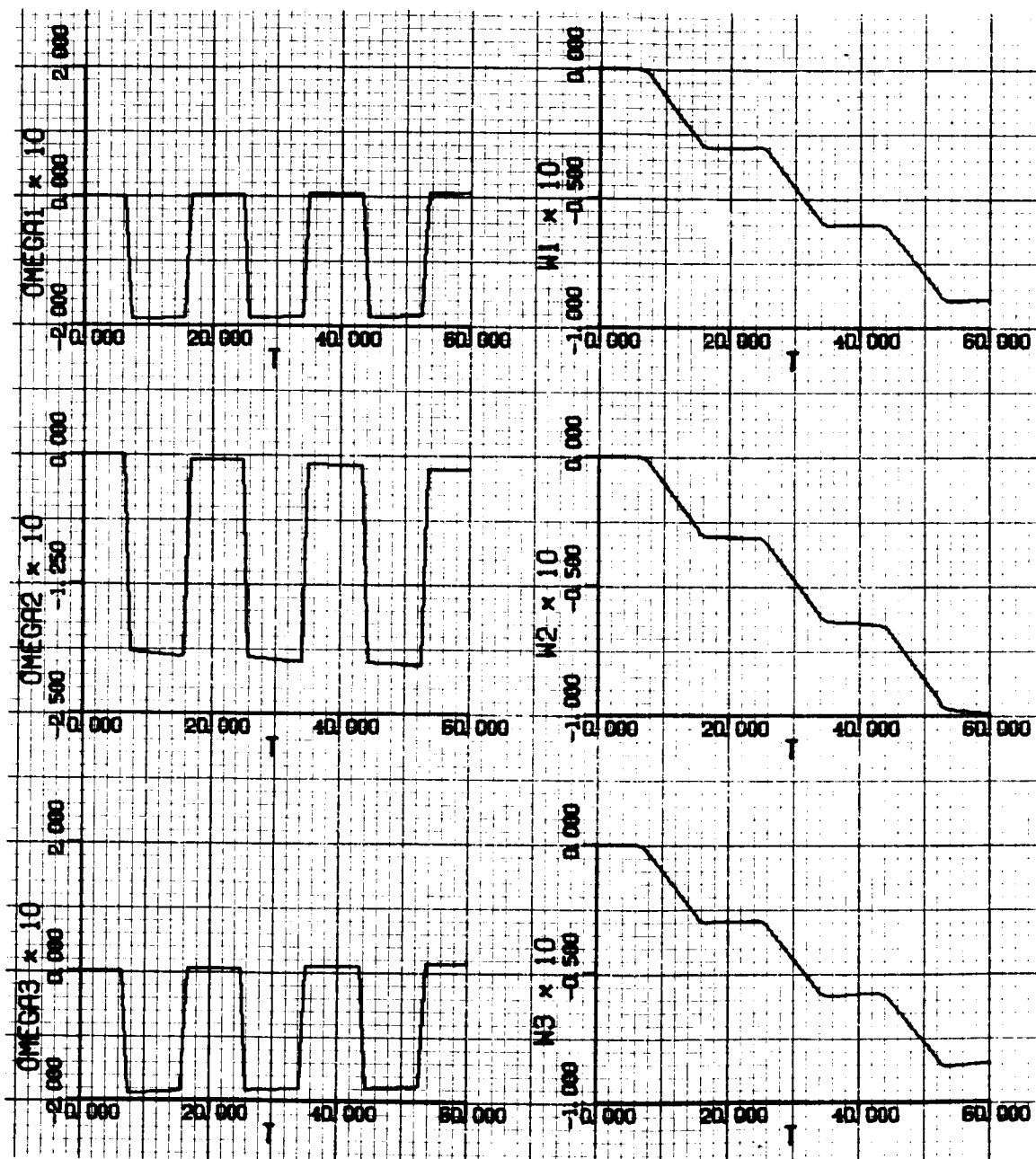
Figure 6-11a. Response to an Initial Guess of Control Time History with $x_i(t_o) = 0, i = 1,\ldots,7$.

68
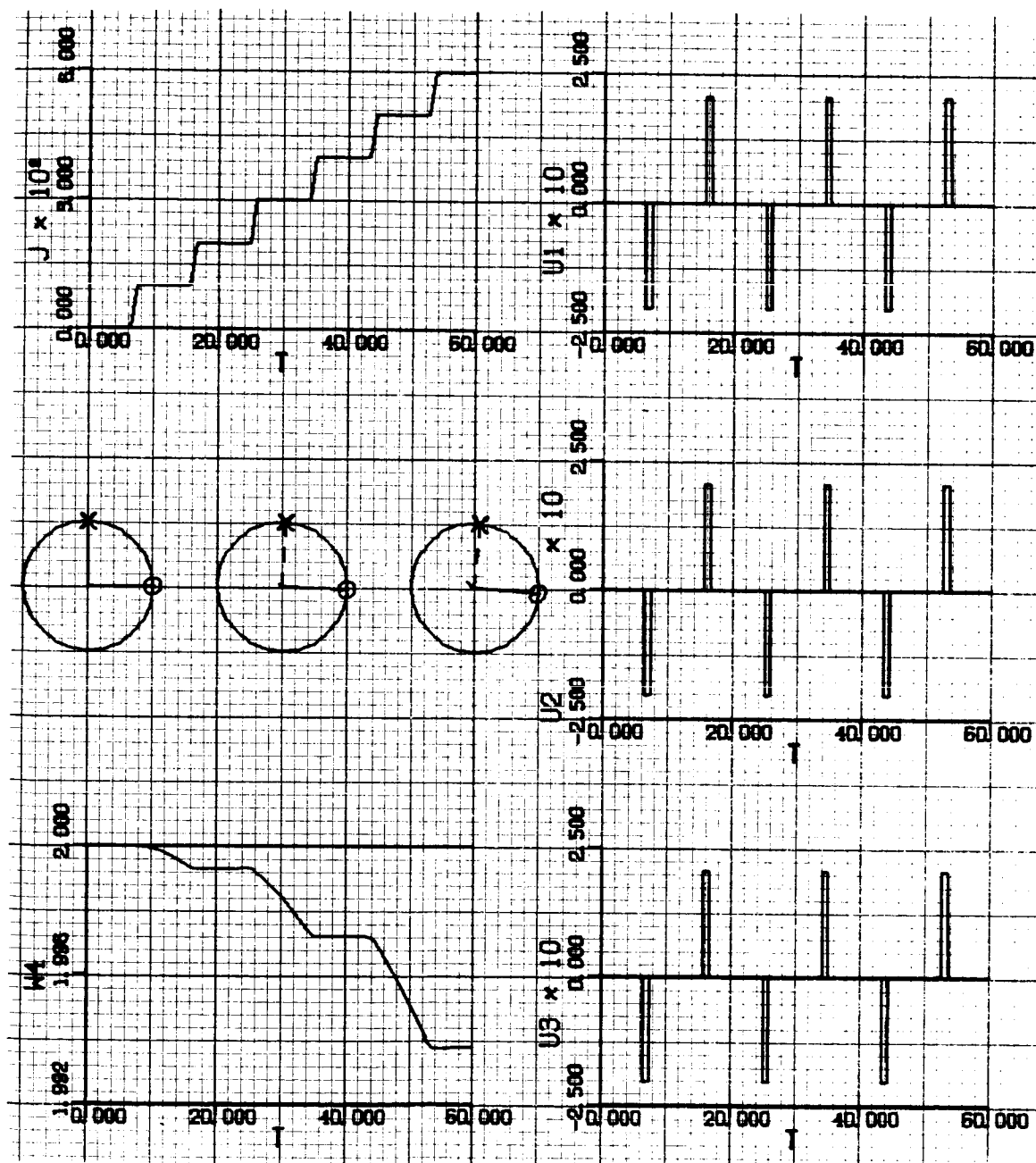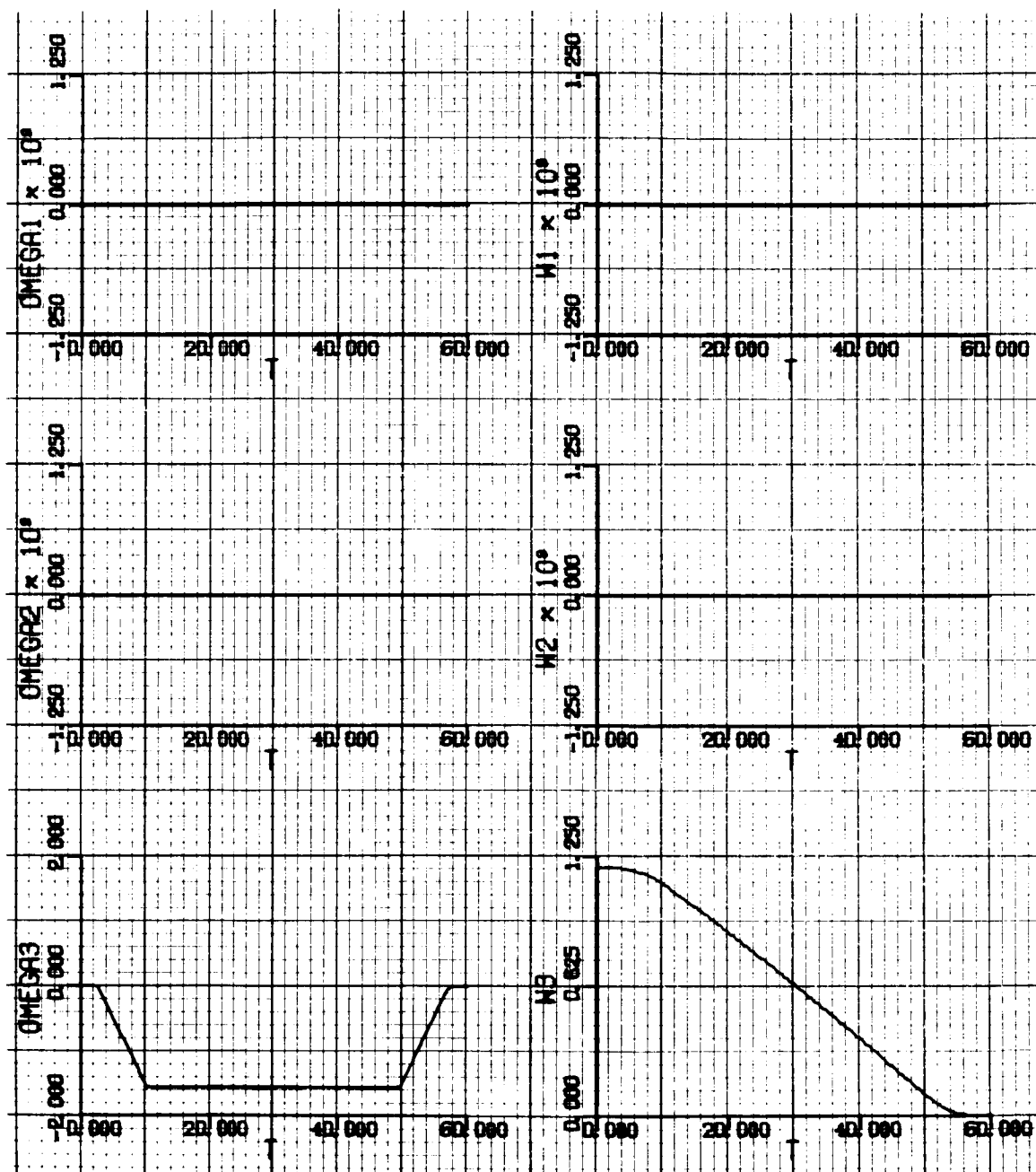
Figure 6-11b.

Figure 6-12a. Response Curves Generated by Method of Steepest-Descent
for Initial Conditions of Run R-3 (Table III).

70

Figure 6-12b.

71
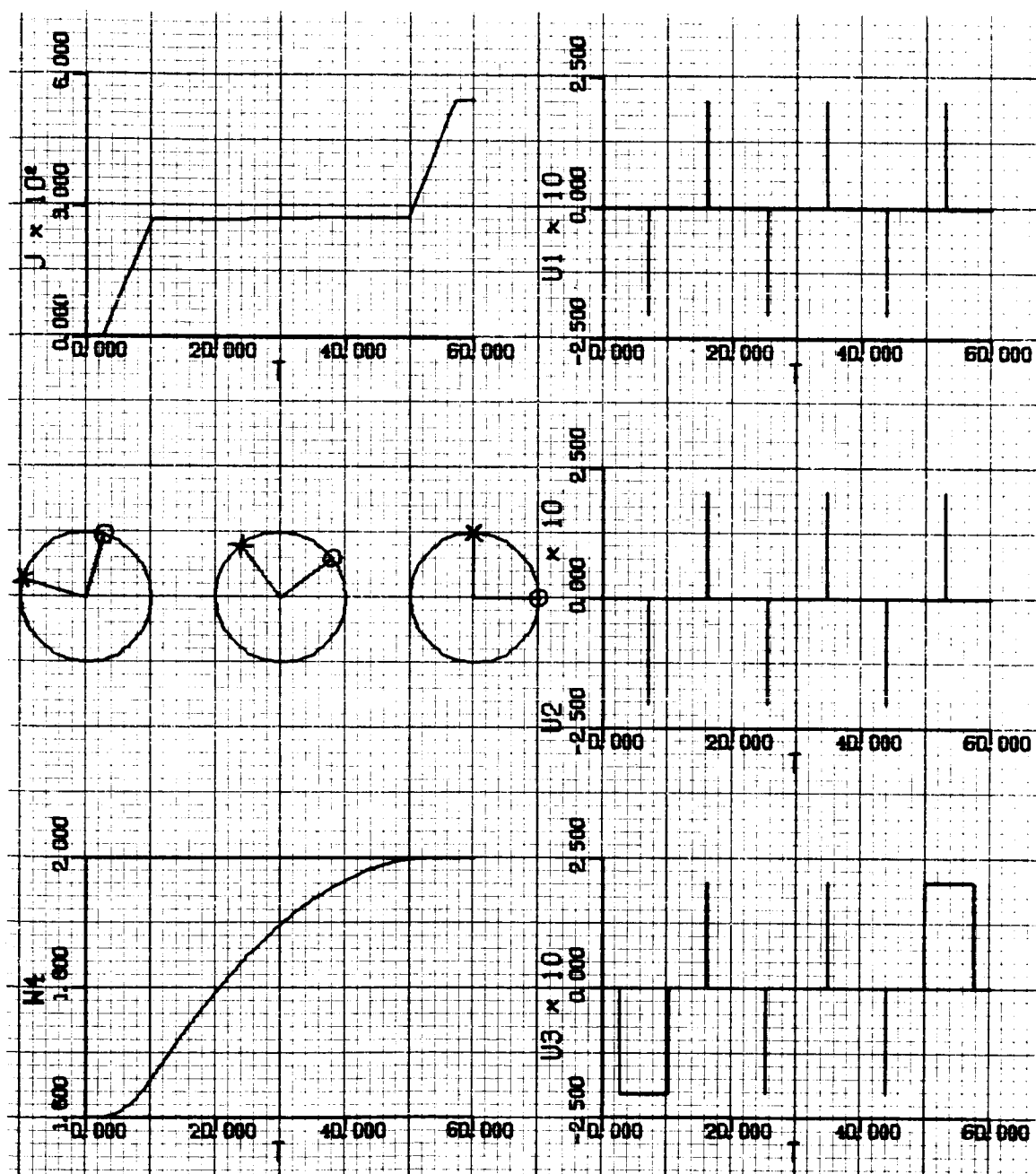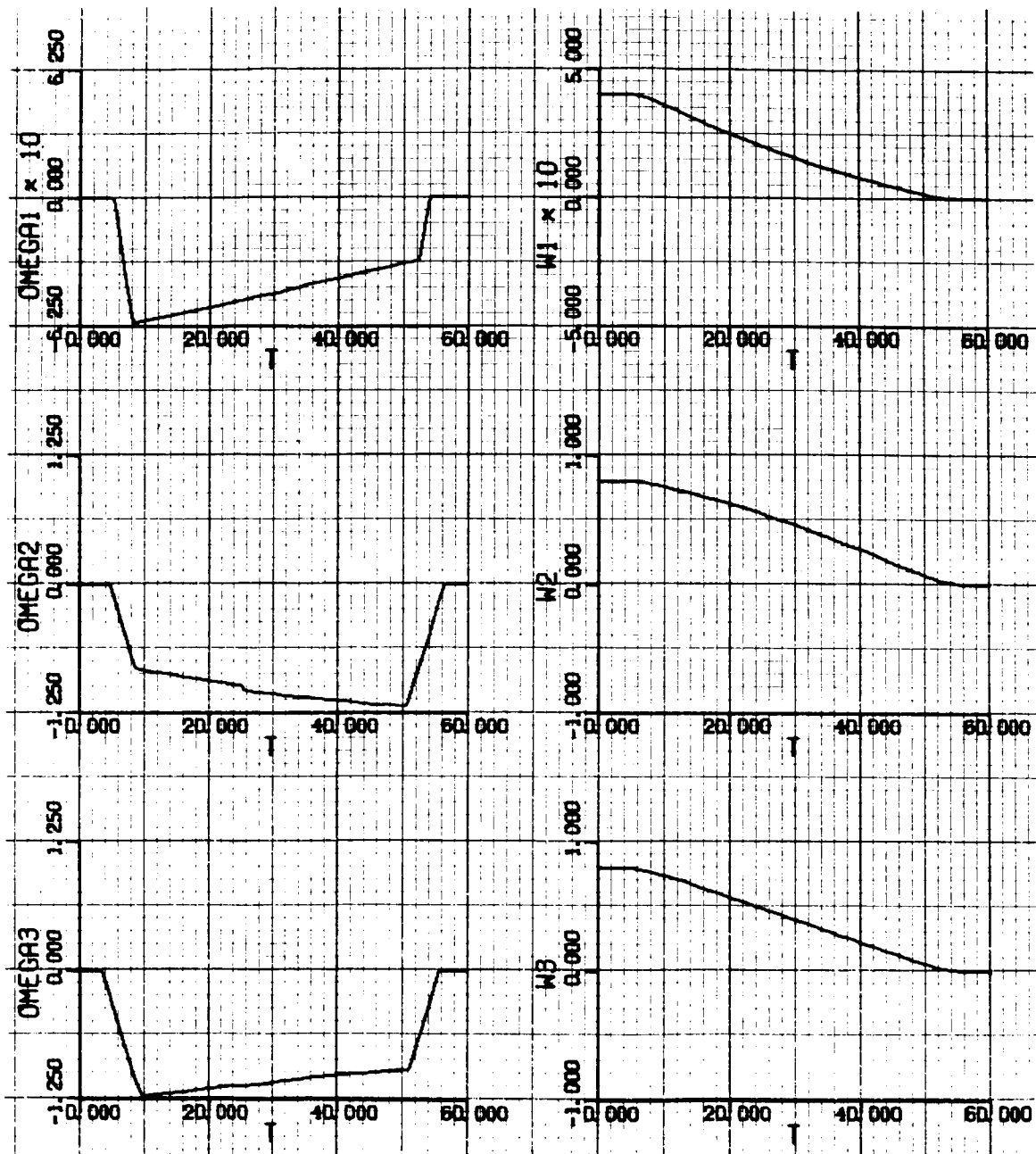
Figure 6-13a. Response Curves Generated by Method of Steepest-Descent for Initial Conditions of Run R-4 (Table III).

72

Figure 6-13b.

73
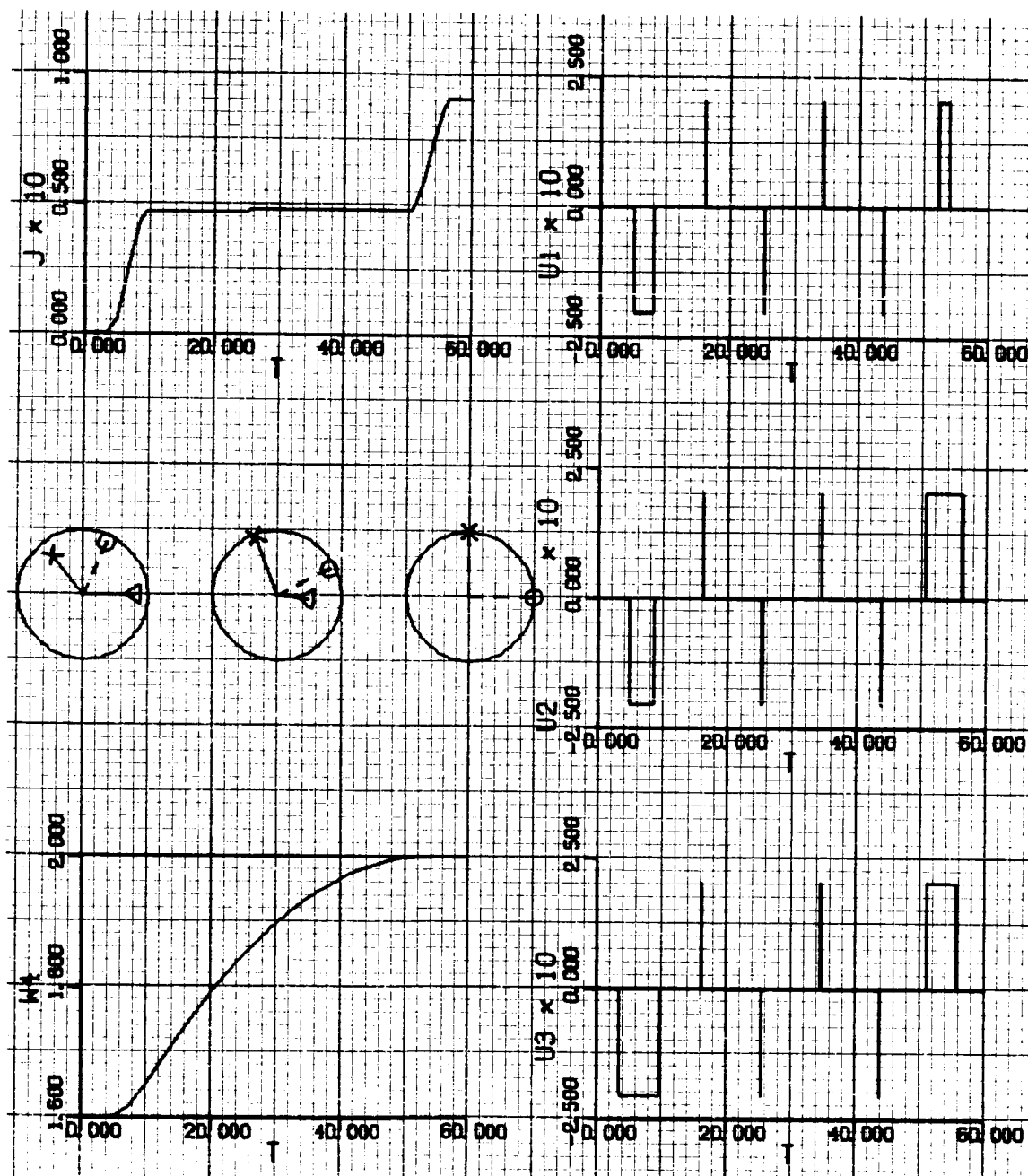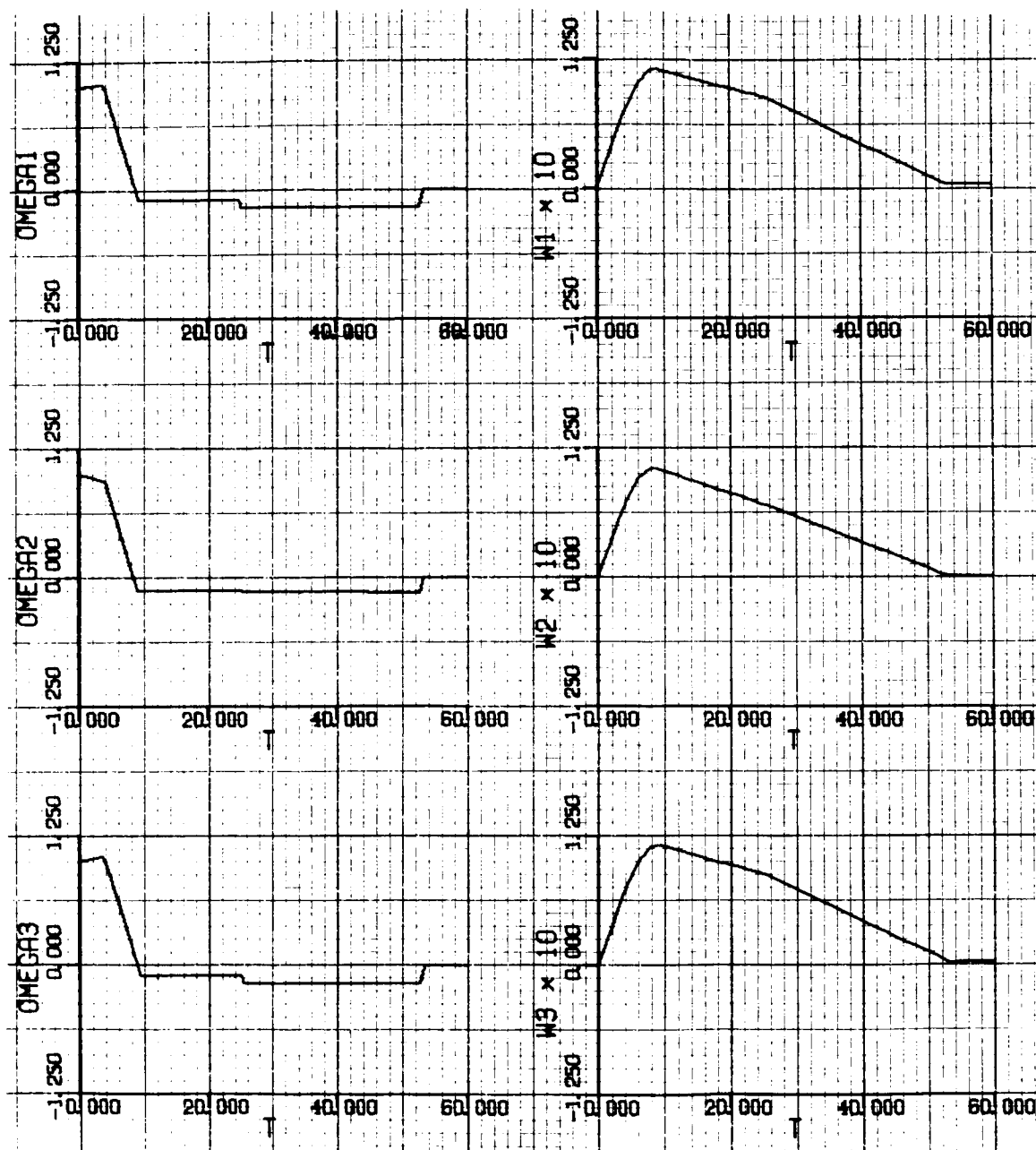
Figure 6-14a.   Response Curves Generated by Method of Steepest-Descent
for Initial Conditions of Run R-5 (Table III).

74
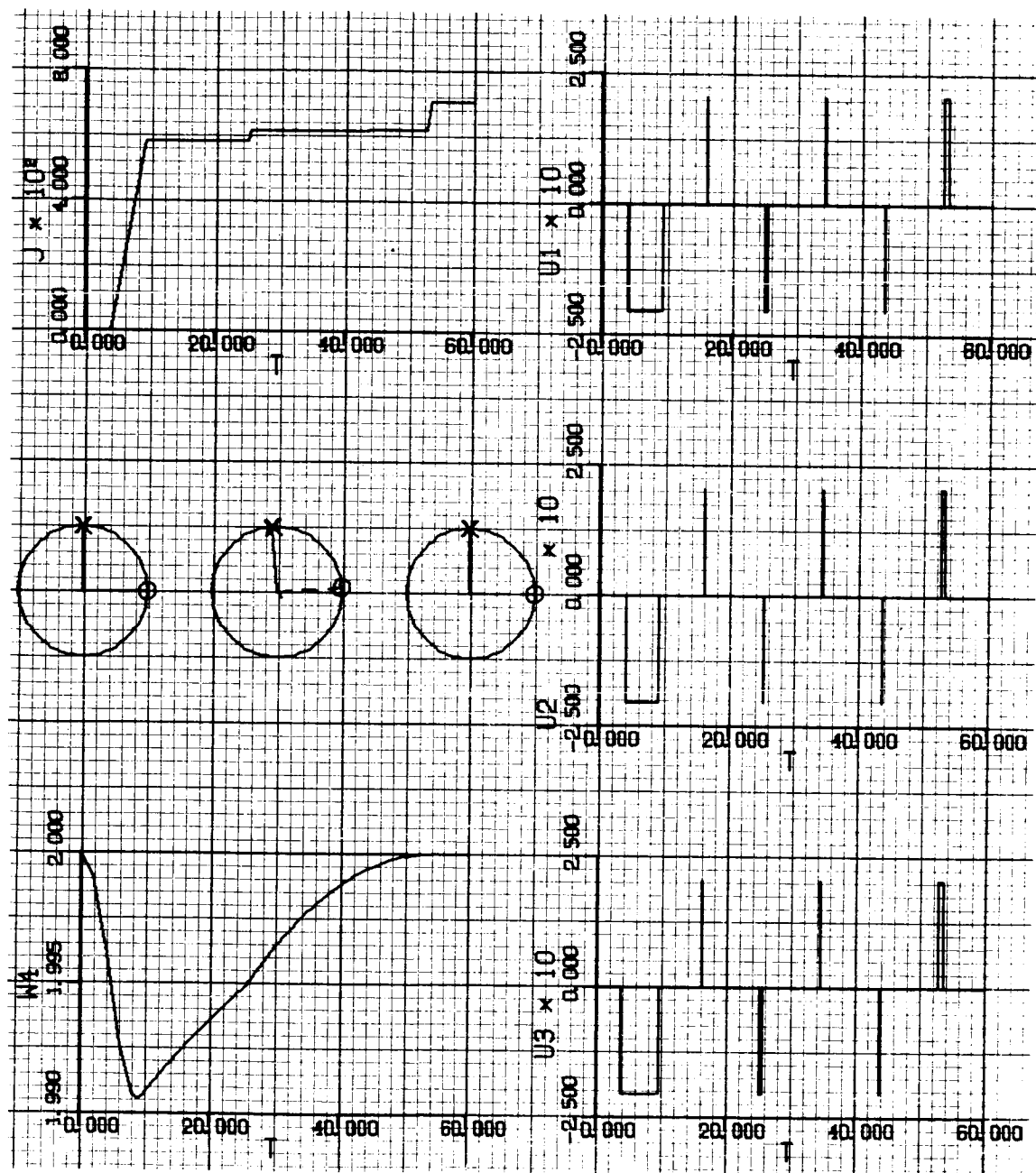
Figure 6-14b.

VII. ACQUISITION PROBLEM: LOW CONTROL TORQUE, ROTATING REFERENCE FRAME

The mathematical model of the system studied in this Chapter is found in (4-4) and (A-26). This model is much more complex than that used in the preceding chapter. In this chapter the object is to control the attitude of the satellite in a rotating reference frame while the spacecraft is being disturbed by the gravity gradient moments (A-22). The control torque levels are of the same order of magnitude as the gravity gradient disturbance torque.

A. OPTIMAL CONTROL FOR COMPARISON PURPOSES

True optimal state trajectories are generated by selecting values of the adjoint variables at $t = t_f$ and integrating the differential equations (4-4), the adjoint equation (A-25) and (A-26), and the control equations (2-9) backwards in time from $t = t_f$. The terminal constraints on the states at $t = t_f$ are employed here as well. Satellite data found in Table I is used. The parameters d_i in (4-4) are chosen to be equal to one. The bounds on the control components are selected to give equal angular acceleration in each of the three axis and to have magnitudes equal to twice the value of the maximum disturbance due to the gravity gradient. The control accelerations are therefore each:

$$|u_i|_{max} = 1.905 \times 10^{-4} \text{ deg/sec}^2 \; , \qquad (7-1)$$

for $i = 1, 2, 3$. As of June 1965, the lowest thrust level available from a cold gas propellant system was .005 lb. [Ref. 7-1]. To provide

the control acceleration level of (7-1) with the satellite moment of inertias of Table I, the lever arm for the gas jets would have to range between .53 ft and .2 ft., when using a thrust level of .005 lb. These moment arms are an order of magnitude too small for practical purposes. This design difficulty will be ignored in this study since the primary goal here is to obtain analytical insights into the present optimization problem.

Two sets of orbital parameters are used in this Chapter. Table VI contains a summary of these data. The orbit described in Set 1 is used to generate the true optimal trajectories. The two orbits appear in Figure 7-0.
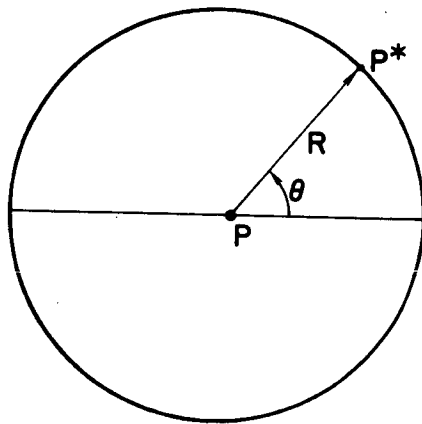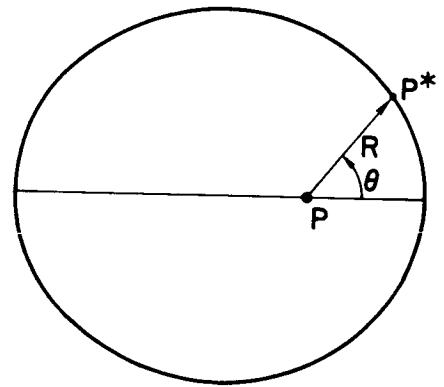
(a). $\epsilon = 0.0521$ (b). $\epsilon = 0.4$

FIGURE 7-0. TWO ELLIPTICAL ORBITS

The initial and terminal conditions and the fuel consumption are listed in Table VII for the two true optimal control runs.

A statement is found in Table VII as to whether or not the desired state at $t = t_f$ is an "instantaneous" equilibrium point. It is convenient to make the following definition:

Table VI. Orbital Parameters

Set	1	2
ϵ	.0521	.4
Appogee, mi	4651	9750
Perigee, mi	4190	4190
a, mi	4421	6970
n, $\sec^{-1}$	1.05136×10^{-3}	5.32×10^{-4}
Period of orbit, min	99	196

Radius of earth, mi	3960	
M, slug	4.11×10^{23}	
G, lb ft^2 slug^{-2}	3.42×10^{-8}	

DEFINITION I: If there exists an $n \times 1$ state vector $\overline{x}_e$ at

$t = t_f$ for the system of differential equations

such that
$$\dot{\overline{x}} = \overline{f}(\overline{x},\overline{u},t)$$

$$\theta = \overline{f}(\overline{x}_e, \theta, t_f)$$

then $\overline{x}_e = \overline{x}_e(t_f)$ is an <u>instantaneous equilibrium point</u> of the

differential equations.

By substituting the desired terminal states, $x_2 = \cdots = x_7 = 0$ and $x_8 = 2$

into the differential equations (4-4) at $t = t_f$, setting $u_1 = 0$,

and examing the eight derivatives x_1', $\ldots$, x_8' it is seen that all of

these derivatives are equal to zero except x_4' :

Table VII. Data and Results for the True Optimal Control Runs

Run	R - 6		R - 7	
t_o, sec	0		0	
t_f, sec	1196		1674	
$\theta(t_o)$, deg	-77.8		85	
$\theta(t_f)$, deg	0		180	
Orbital Parameters (Table VI)	Set 1		Set 1	
$\bar{x}(t)$:	$\bar{x}(t_o)$	$\bar{x}(t_f)$	$\bar{x}(t_o)$	$\bar{x}(t_f)$
x_1, $\sec^{-1}$	0	1.5149×10^{-3}	0	4.8029×10^{-3}
x_2, deg/sec	3.8×10^{-2}	0	-7.25×10^{-3}	0
x_3, deg/sec	-7.27×10^{-2}	0	8.8×10^{-7}	0
x_4, deg/sec	3.44×10^{-2}	0	.1263	0
x_5	.218	0	.194	0
x_6	.638	0	.664	0
x_7	.104	0	-.412	0
x_8	1.88	2	1.831	2
x_9	-5.1×10^{-2}	0	5.2×10^{-2}	0
x_{10}	.986	.9479	.993	1.0521
$\bar{\lambda}(t_f)$:				
$\lambda_1(t_f)$	-1		-1	
$\lambda_2(t_f)$	1.05		1.05	
$\lambda_3(t_f)$	-1.05		-1.10	
$\lambda_4(t_f)$	1.05		1.05	
$\lambda_5(t_f)$	-2		-2	
$\lambda_6(t_f)$	2		1	
$\lambda_7(t_f)$	-2		-2	
Control bounds, deg/sec^2	1.905×10^{-4}		1.905×10^{-4}	
Instantaneous equilibrium point at $t = t_f$	yes		yes	
ψ_R, deg	40		48	
ψ_I, deg	80		124	

$$x_4' = -\theta'' = [2(1-\epsilon^2)^{1/2} x_9]/(x_{10})^3 \qquad\qquad (7\text{-}2)$$

By requiring the above states ($x_2 = \ldots = x_7 = 0$, $x_8 = 2$) to be met at $t = t_f$, and requiring that $t = t_f$ occur at appogee or perigee where $x_9 = R' = 0$, the desired states are made to represent an "instantaneous" equilibrium point of the set of differential equations.

Table VII contains reference to two sets of angles, ψ_R and ψ_I . ψ_R represents the total equivalent rotation between the initial and the final states, measured with respect to the rotating reference frame (x_r, y_r, z_r) ; whereas, ψ_I denotes the total equivalent rotation between the initial and final states*, measured with respect to the inertial reference frame (x_e, y_e, z_e) . The latter quantity is more meaningful for this study, since the total rotation in inertial space accounts for the primary expenditure of fuel.

Time responses depicting the two optimal state trajectories are found in Figures 7-1 and 7-3. For the figures to be perfectly correct, the control should not have been turned off at $t = t_f$. The symbols and units for the figures in Chapter VII are described in Table IV.

---

*Several ways exist to compute the total rotation in inertial space. Perhaps the most direct is to express the transformations between the various reference frames in terms of direction cosine matrices and then multiply these together to obtain a single transformation matrix. As discussed in Ref. A-2 the total equivalent rotation, $\psi(t)$, for this single transformation at a fixed time t is found by equating the trace of its matrix with the expression $1 + 2\cos\psi(t)$, and then solving for $\psi(t)$. The trace of a matrix is equal to the sum of the elements on the main diagonal.

B. STEEPEST-DESCENT SOLUTIONS

The extended method of steepest-descent was used to generate solutions to the optimization problem for a number of sets of initial conditions and orbital parameters. The same computational techniques were used to generate the solutions in this Chapter as in the prior one. Two runs were made starting from the sets of initial conditions of Run R-6 and Run R-7 above. Table VIII summarizes the steepest-descent solutions, and compares them with the true optimal solutions. As seen from a comparison of the relevent figures the true optimal trajectories are quite similar to the trajectories generated by the method of steepest-descent. The control pulses are placed in different positions, thereby contributing to the higher cost of the latter trajectories. All of the trajectories generated for this chapter come to within the acceptable distance (6-2) of the desired terminal state. As discussed in the literature on the method of steepest-descent, this method is useful in computing a state trajectory which is nearly optimal; however to come closer to the optimal solution another technique such as the method based on the second variation. must be resorted to. In the case where the control is continuous the matrix $C(t_o)$ in (B-12) becomes singular as the optimal control is reached; however, when the control is bounded and the switching times are treated as control parameters the matrix $D(t_o)$ will usually not become singular when the optimal is approached.

It was decided to generate a steepest-descent solution to an acquisition problem with control acceleration bounds set at 25% of those in (7-1) (50% of the maximum value of the gravity gradient disturbance). The data for this problem is found in Table IX, Run R-8. The resulting

Table VIII. Comparison of True Optimal Solutions with Solutions by
Method of Steepest-Descent.

Initial Conditions of Run:	R-6	R-7
$x_1(t_f)$, sec^{-1}(optimal):	1.5149×10^{-3}	4.8029×10^{-3}
$x_1(t_f)$, sec^{-1}(steepest-descent):	1.7012×10^{-3}	5.5577×10^{-3}
% that steepest-descent is higher than optimal:	12.3	15.7
Number of iterations* for steepest-descent solution:	15	34
Optimal solution found in Figure:	7-1	7-3
Steepest-descent solution found in Figure:	7-2	7-4

*An iteration takes approximately 36 seconds for the mathematical model considered in this chapter.

state trajectories are found in Figure 7-5. Even with the low control

acceleration levels acquisition is possible. No comparison was made

between this solution and a true optimal one.

Another problem which was solved by the method of steepest-descent

is described in Run R-9 of Table IX. The data are the same as in Run R-6

except that some arbitrary set of nonzero terminal constraints is spec-

ified. After 25 iterations the solution is found in Figure 7-6. Since

the equivalent rotation in Run R-9 is greater than in Run R-6 the cost

should be, and is, higher.

The influence of the orbital parameters is demonstrated by the five

runs summarized in Table X, and Figures 7-7 through 7-11. Each run has

82

Table IX. Data and Results for Runs R-8 and R-9

Run	R-8		R-9	
t_o, sec	0		0	
t_f, sec	2869		1196	
$\theta(t_o)$, deg	-92.4		-77.8	
$\theta(t_f)$, deg	92.4		0	
Orbital Parameters (Table VI)	Set 1		Set 1	
$\bar{x}(t)$:	$\bar{x}(t_o)$	$\bar{x}(t_f)$	$\bar{x}(t_o)$	$\bar{x}(t_f)$
x_1, sec^{-1}	0	3.5755×10^{-3}	0	4.2533×10^{-3}
x_2, deg/sec	-5.45×10^{-2}	0	Same	0
x_3, deg/sec	.1104	0	as	0
x_4, deg/sec	9.3×10^{-2}	0	in	0
x_5	-7.3×10^{-2}	0	Run	0
x_6	-1.053	0	R-6	-.5
x_7	-.452	0		.6
x_8	1.64	2		1.84
x_9	-5.2×10^{-2}	5.2×10^{-2}		0
x_{10}	.999	.999		.9479
No. of iterations	29		25	
Control bounds, deg/sec^2	$.476 \times 10^{-4}$		1.905×10^{-4}	
Instantaneous equilibrium point at $t = t_f$	no		no	
ψ_R, deg	70		74	
ψ_I, deg	210		121	
Results in Figure:	7-5		7-6	

Table X. Effect of Varying Orbital Parameters

Run	R-10	R-11	R-12	R-13	R-14
$\theta(t_o)$, deg	0	180	0	90	180
$\theta(t_f)$, deg	147	320	119	150	218
Orbital Parameters (Table VI):	Set 1	Set 1	Set 2	Set 2	Set 2
$x_1(t_f) \times 10^3$, sec^{-1}	5.4543	4.9618	4.5515	3.5046	2.921
No. of iterations	26	13	20	21	13
Control bounds, deg/sec^2	← 1.905 × 10^{-4} →			← 1.955 × 10^{-4} →	
ψ_I, deg	104	100	82	54	54
Results in Figure:	7-7	7-8	7-9	7-10	7-11

Common Data:

t_o : 0 ,

t_f : 2400 sec

Initial Conditions: $x_1 = 0$, $x_2 = x_3 = x_4 = .01$ deg/sec, $x_5 = .4$, $x_6 = x_7 = .8$, $x_8 = 1.6$

Terminal Conditions: $x_2 = \cdots = x_7 = 0$, $x_8 = 2$

Instantaneous equilibrium pt., $t = t_f$: No

common initial and terminal constraints and a common time period. The amount of fuel consumed, $x_1(t_f)$, is plotted in Figure 7-12 against the total equivalent rotation in inertial space, ψ_I . A good correlation exists between the two quantities as is expected.

The extended method of steepest-descent makes it possible to compute approximations to extremal trajectories in each of the above cases in spite of the fact that the control torque is low, that the terminal constraints do not represent an instantaneous equilibrium point, or that the orbital eccentricity is high. Several more runs were made to investigate more fully the capabilities and limitations of this method:

i. An initial guess of a nominal control time history was made which closely approximated the optimal shown in Figure 7-1. After 29 iterations convergence to the set of terminal constraints was not achieved. This result supports the conclusion, discussed in Chapter VI, that many more switchings than the optimal number are needed for efficient usage of the extended method of steepest-descent.

ii. One pulse was removed from the above initial nominal control time history and the extended method of steepest-descent used. It was found that the D matrix (B-17) became singular, since not enough pulses existed to control the satellite to the desired terminal constraint.

iii. The exact switching times were used as an initial guess of a nominal trajectory. Even though a true optimal trajectory was present the D matrix did not become singular. The reason that this did not occur is due to the way in which the optimal control has been simulated in the method of steepest-descent. The true optimal control should not be switched off at $t = t_o$ and $t = t_f$ in most cases. There exists no way to leave the control on at t_o or t_f in the present version of

the extended method of steepest-descent; therefore, the control as seen by this technique is not the same as the true optimal, even though the state trajectories are identical. The true optimal control and the control that is simulated in the method of steepest-descent are found in Figure 7-13a and Figure 7-13b, respectively.

Figure 7-1a. True Optimal Response Curves. Run R-6 (Table VII).
Compare with Figure 7-2.

88

Figure 7-1b.

89

Figure 7-2a.   Response Curves Generated by Method of Steepest-Descent for Initial Conditions of Run R-6 (Table VII). Compare with Figure 7-1.
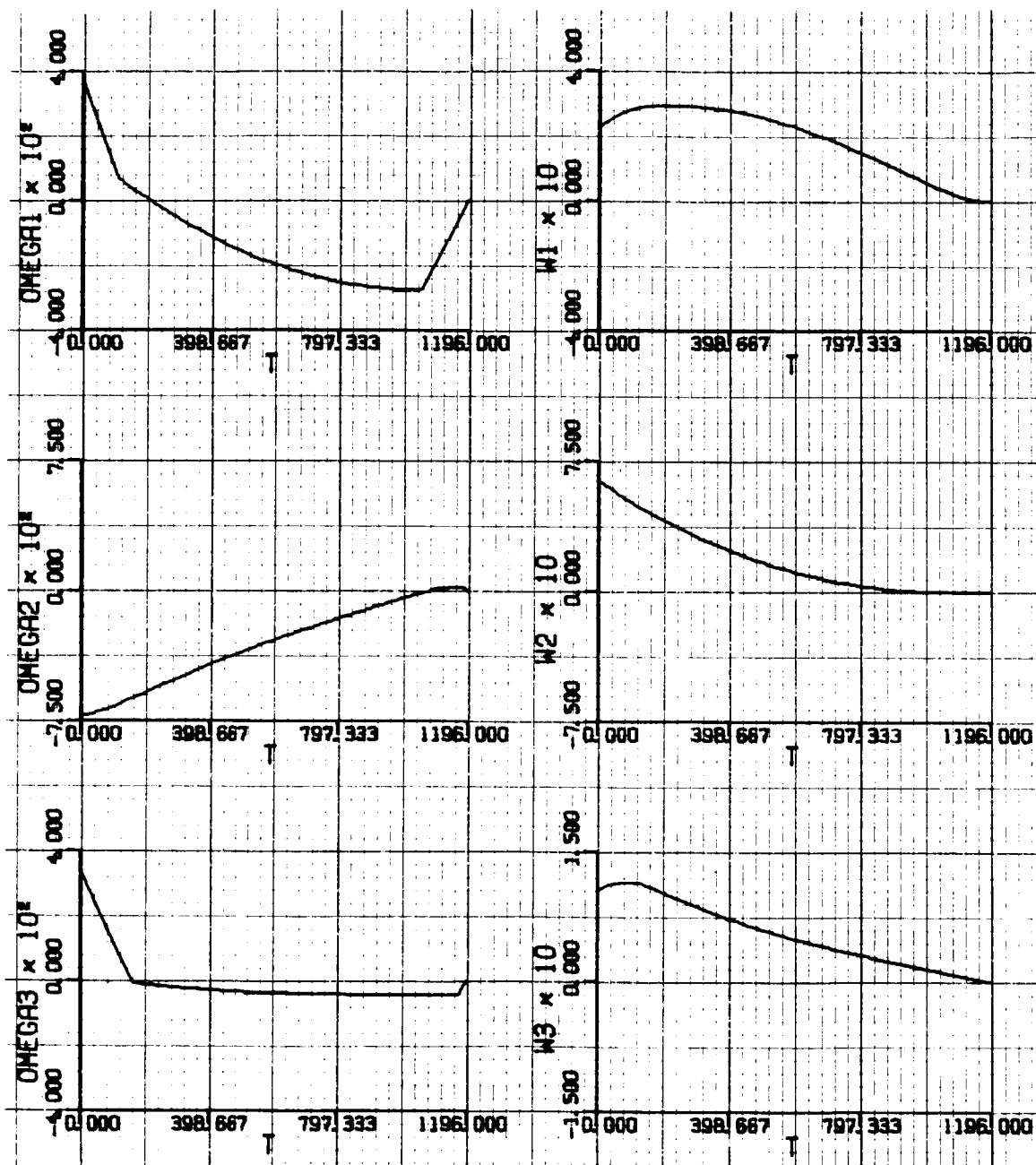
90

Figure 7-2b.

91
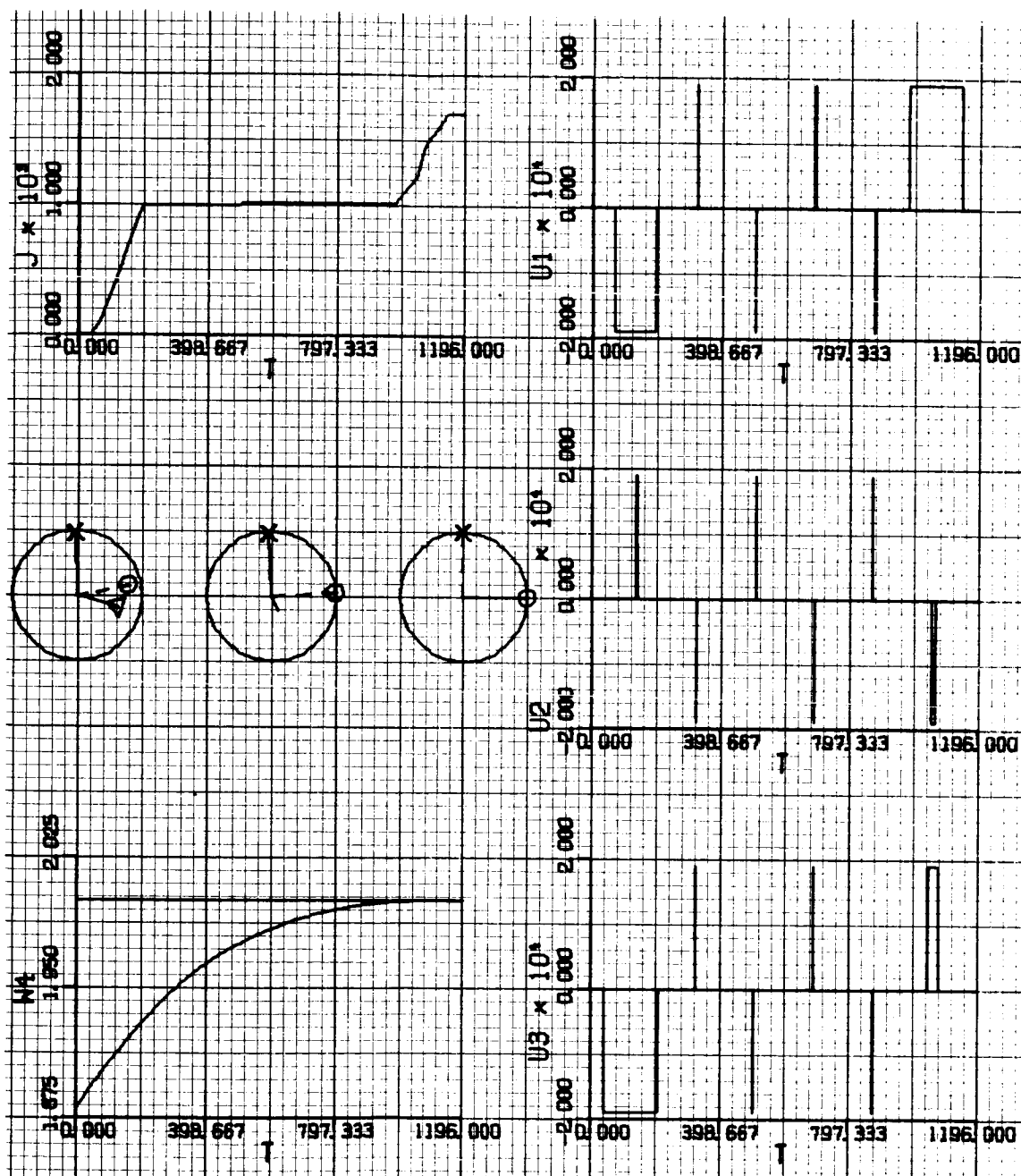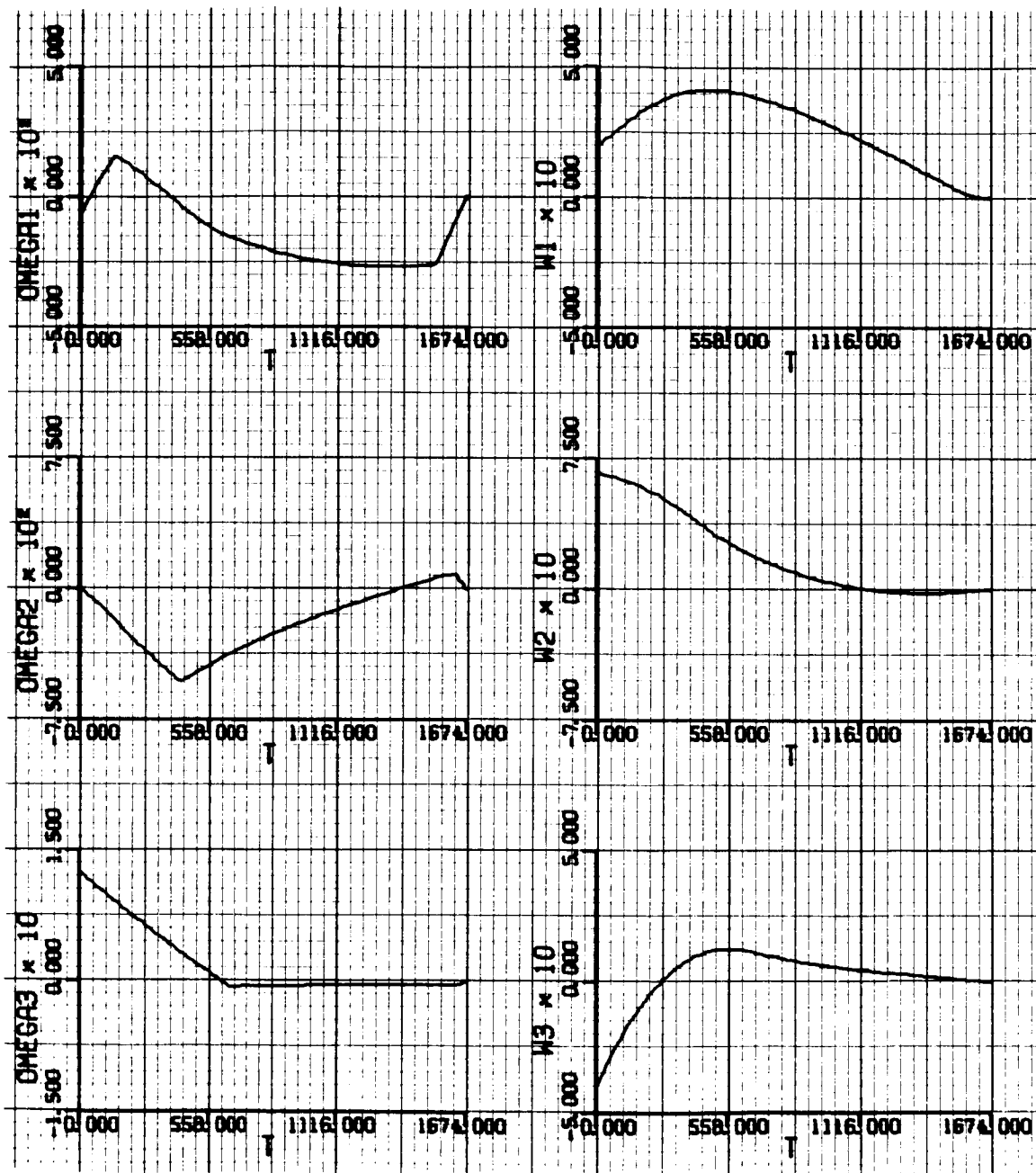
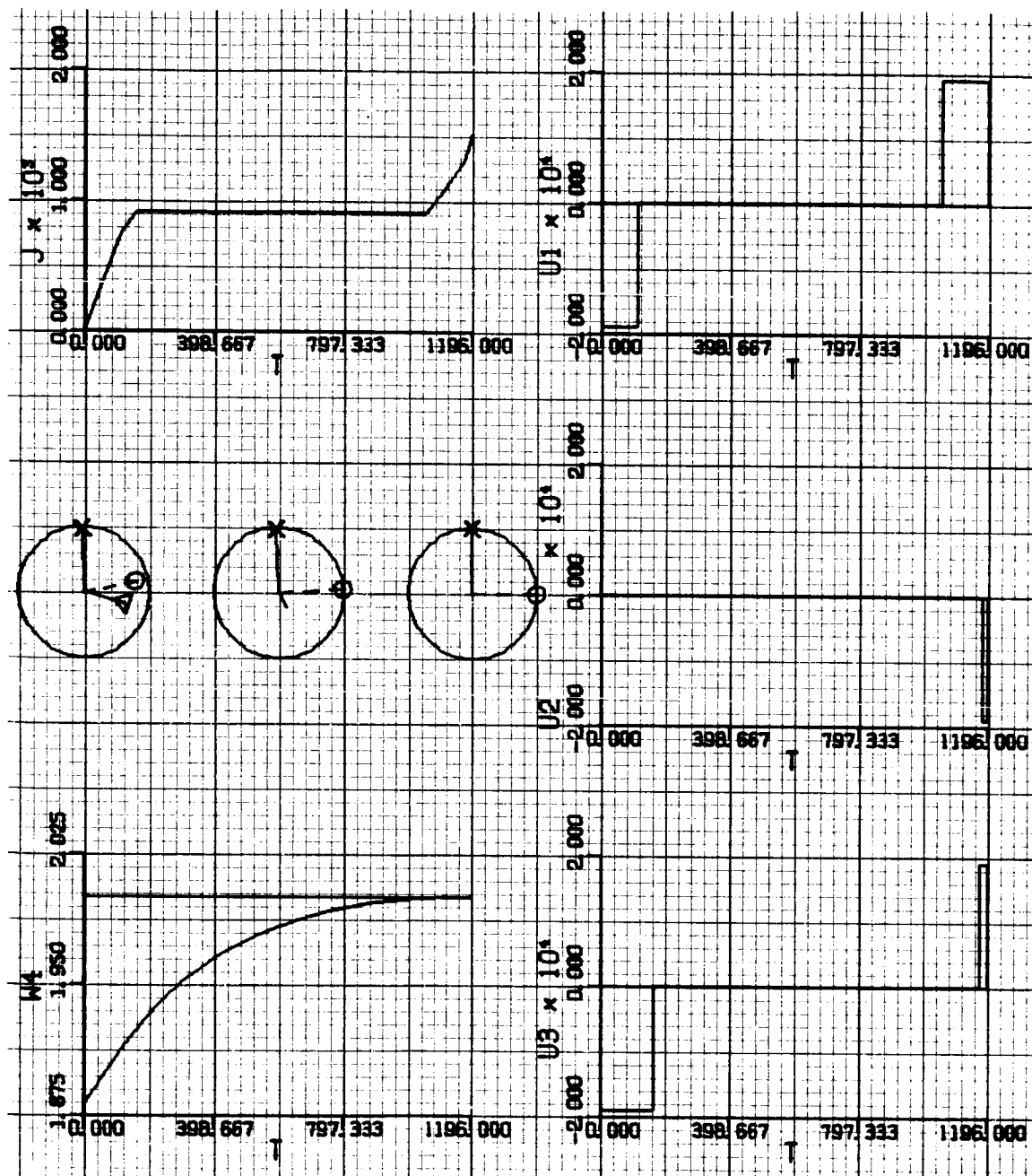Figure 7-3a. True Optimal Response Curves. Run R-7 (Table VII). Compare with Figure 7-4.

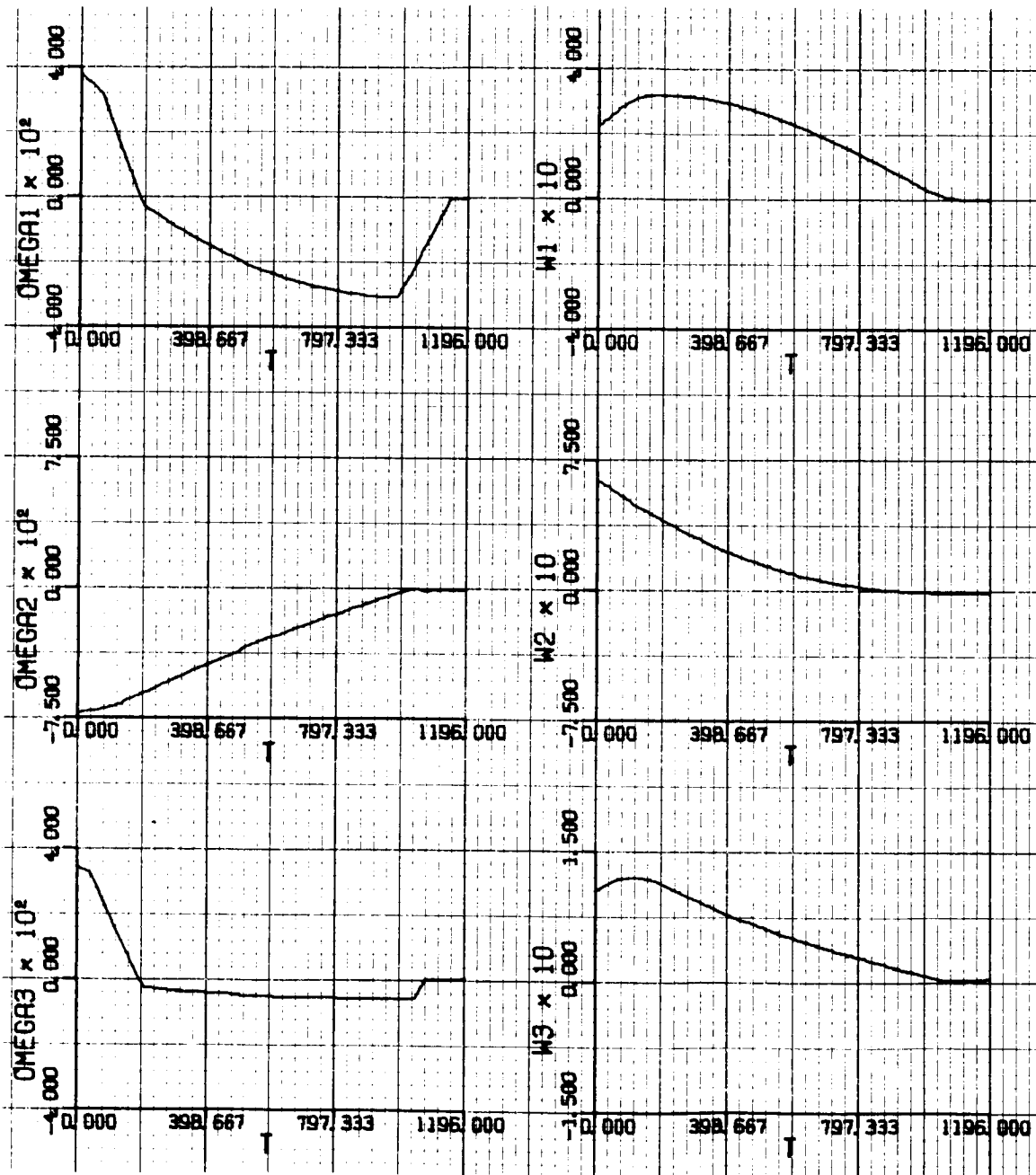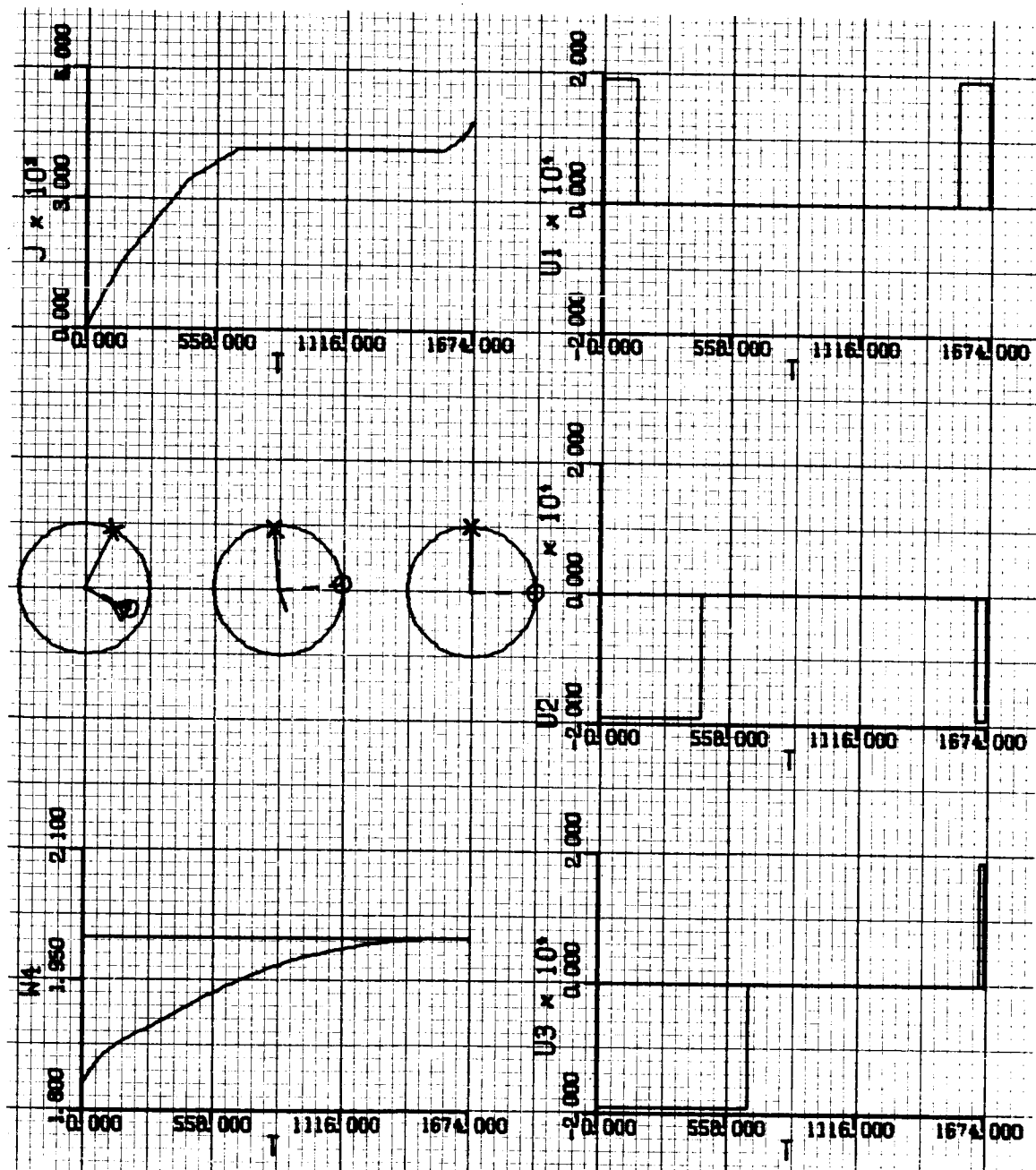Figure 7-3b.
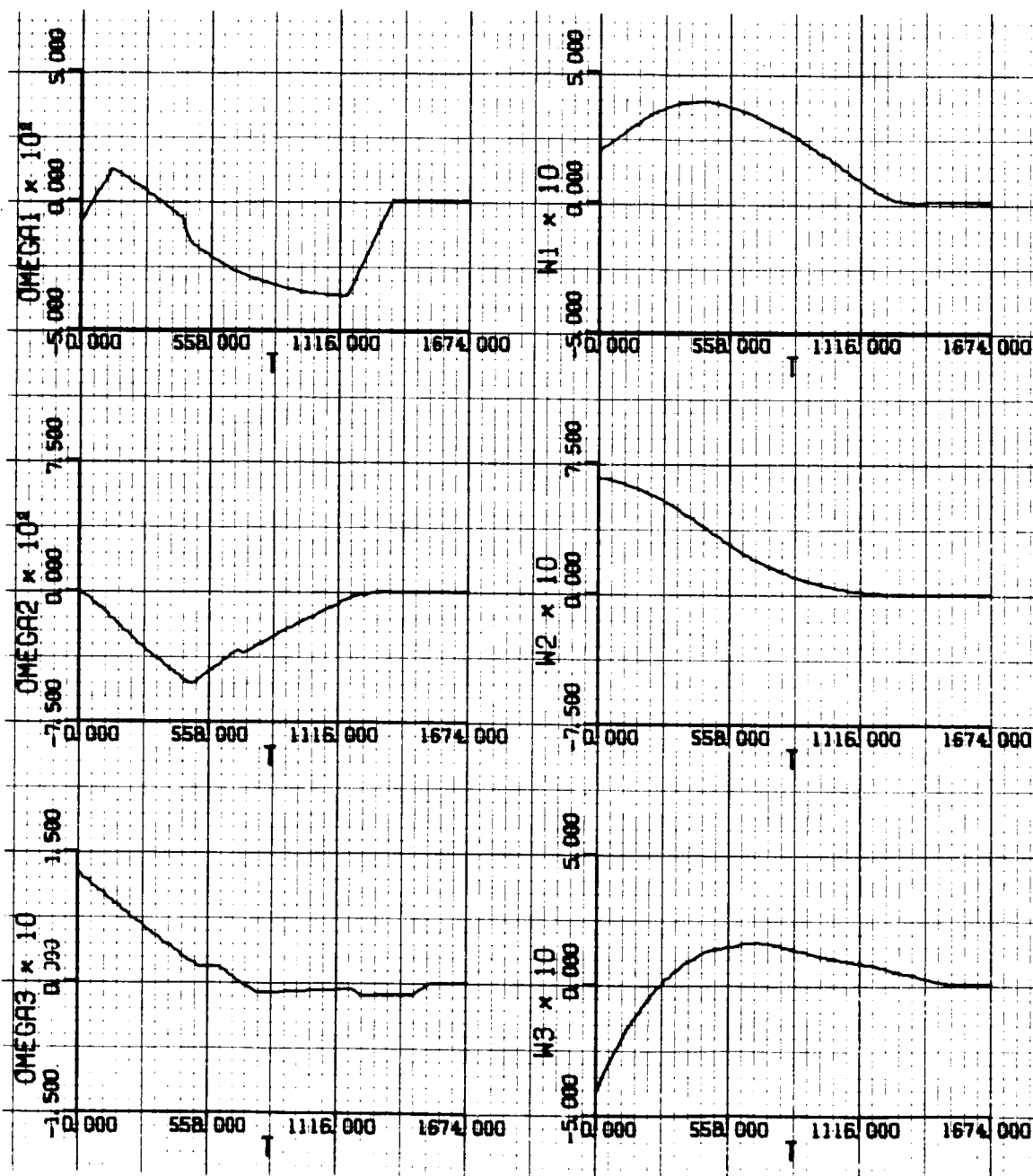
Figure 7-4a.   Response Curves Generated by Method of Steepest-Descent
for Initial Conditions of Run R-7 (Table VII).   Compare
with Figure 7-3.

Figure 7-4b.

95
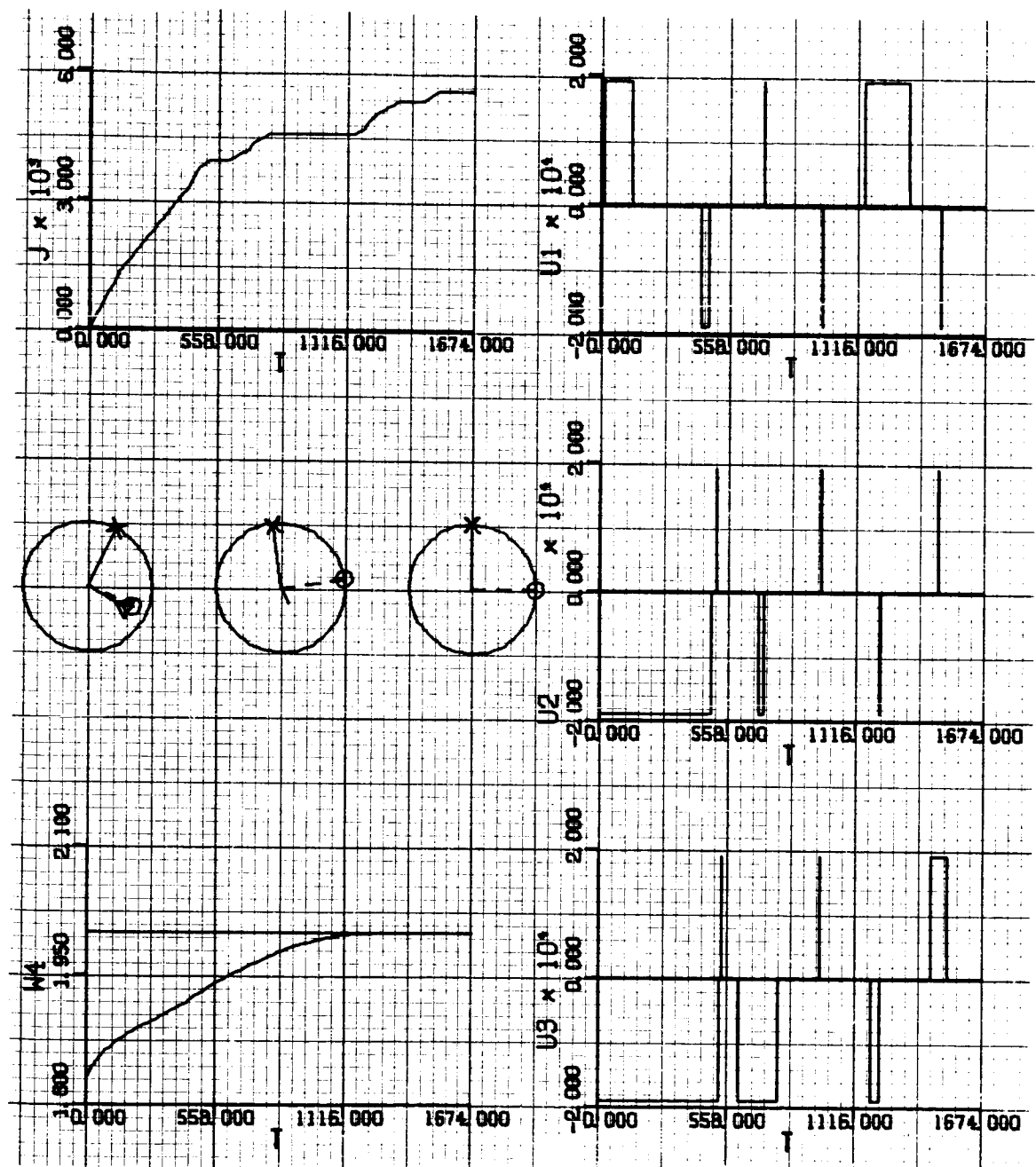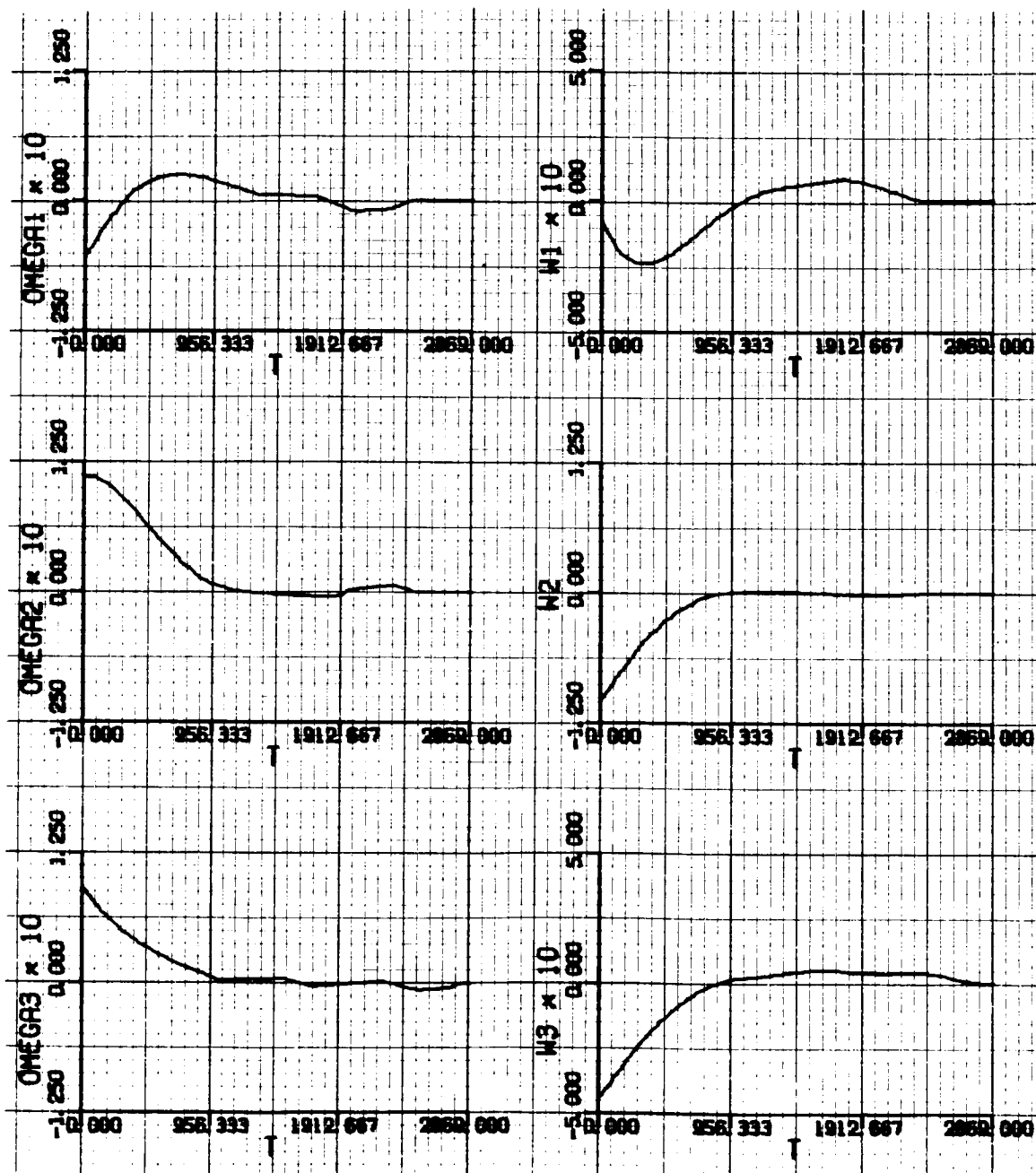
Figure 7-5a. Response Curves with Low Control Torque. Run R-8
              (Table IX).

96
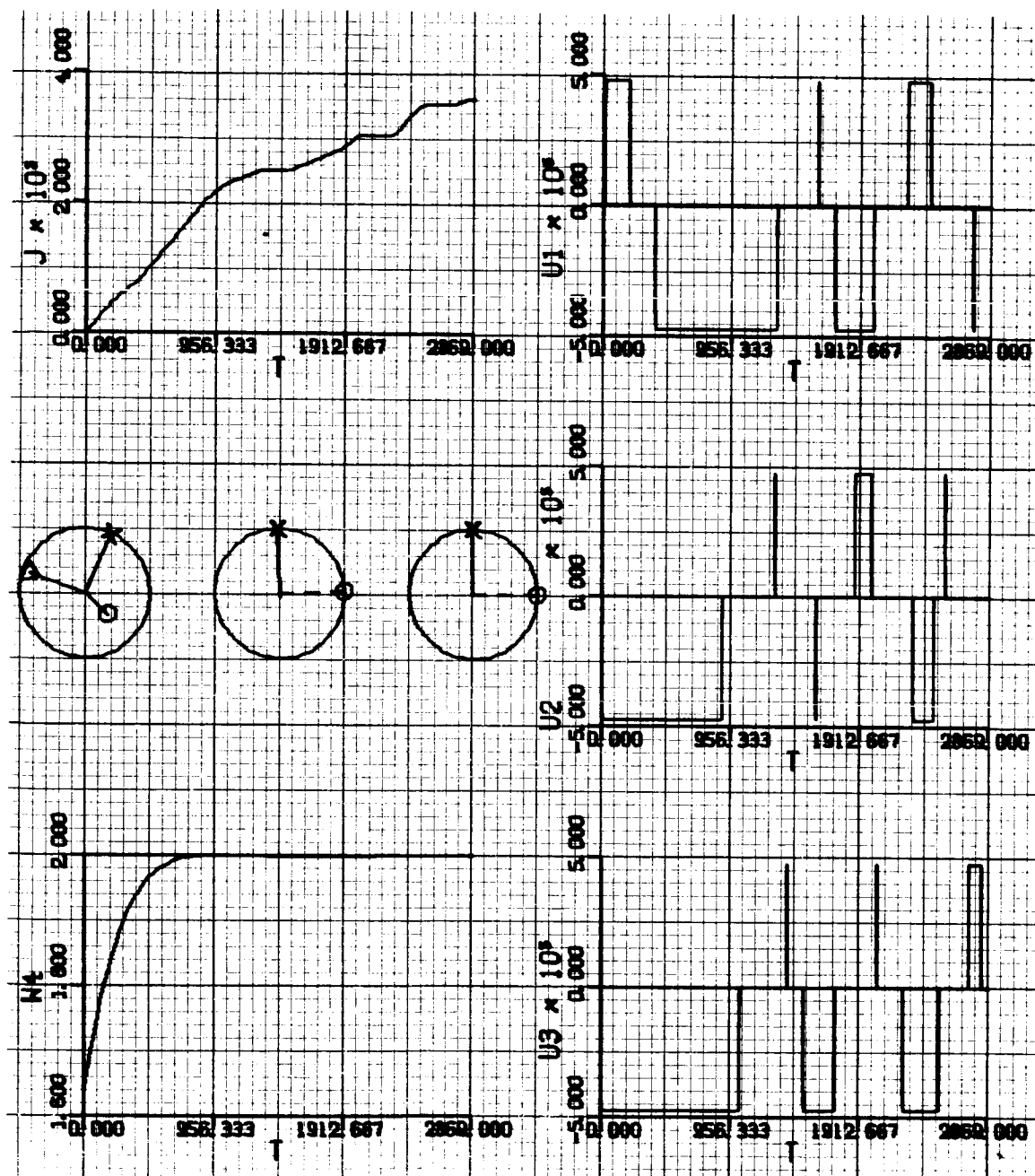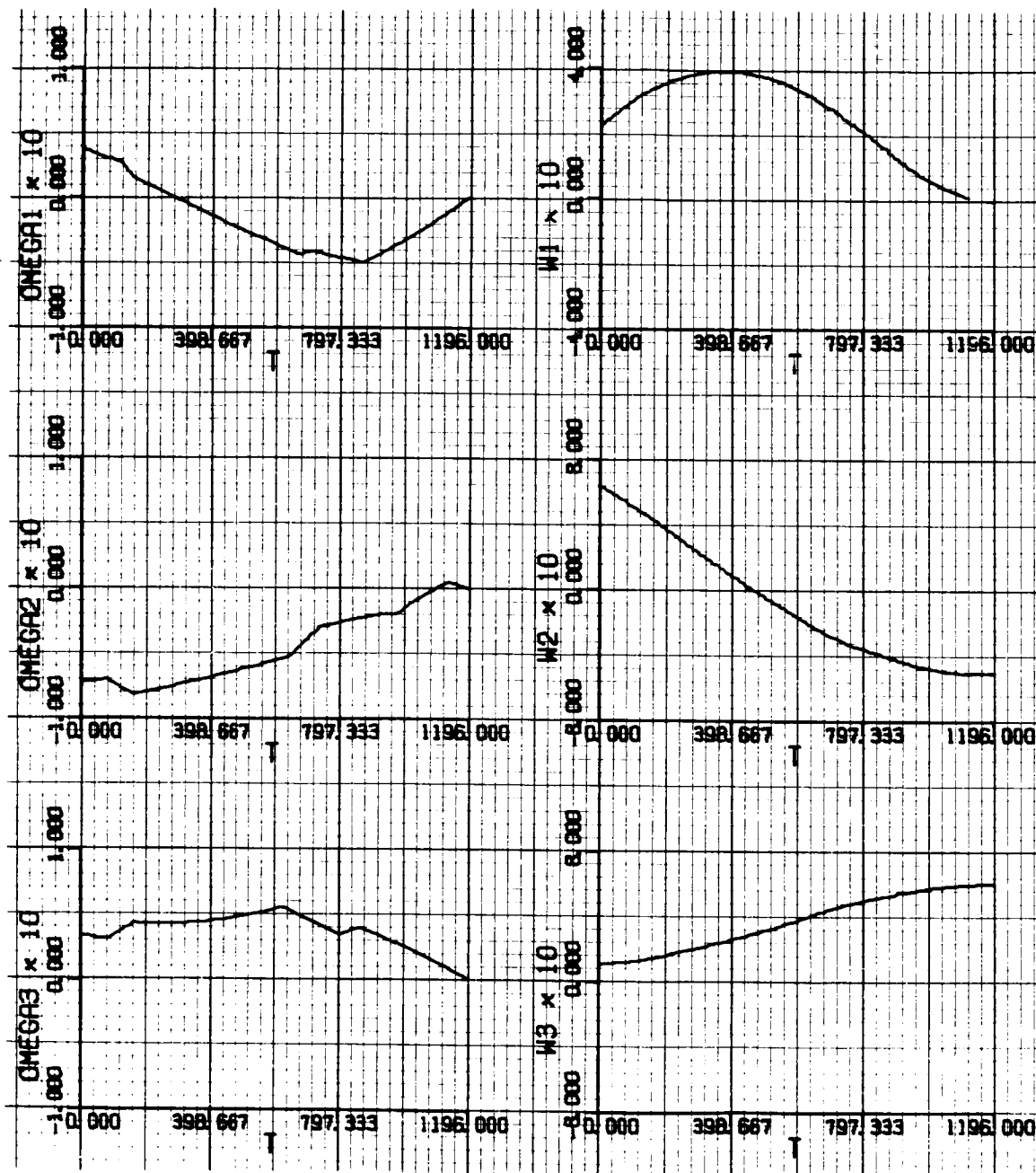
Figure 7-5b.

Figure 7-6a.   Response Curves with a Set of Nonzero Terminal Constraints.
Run R-9 (Table IX).

98
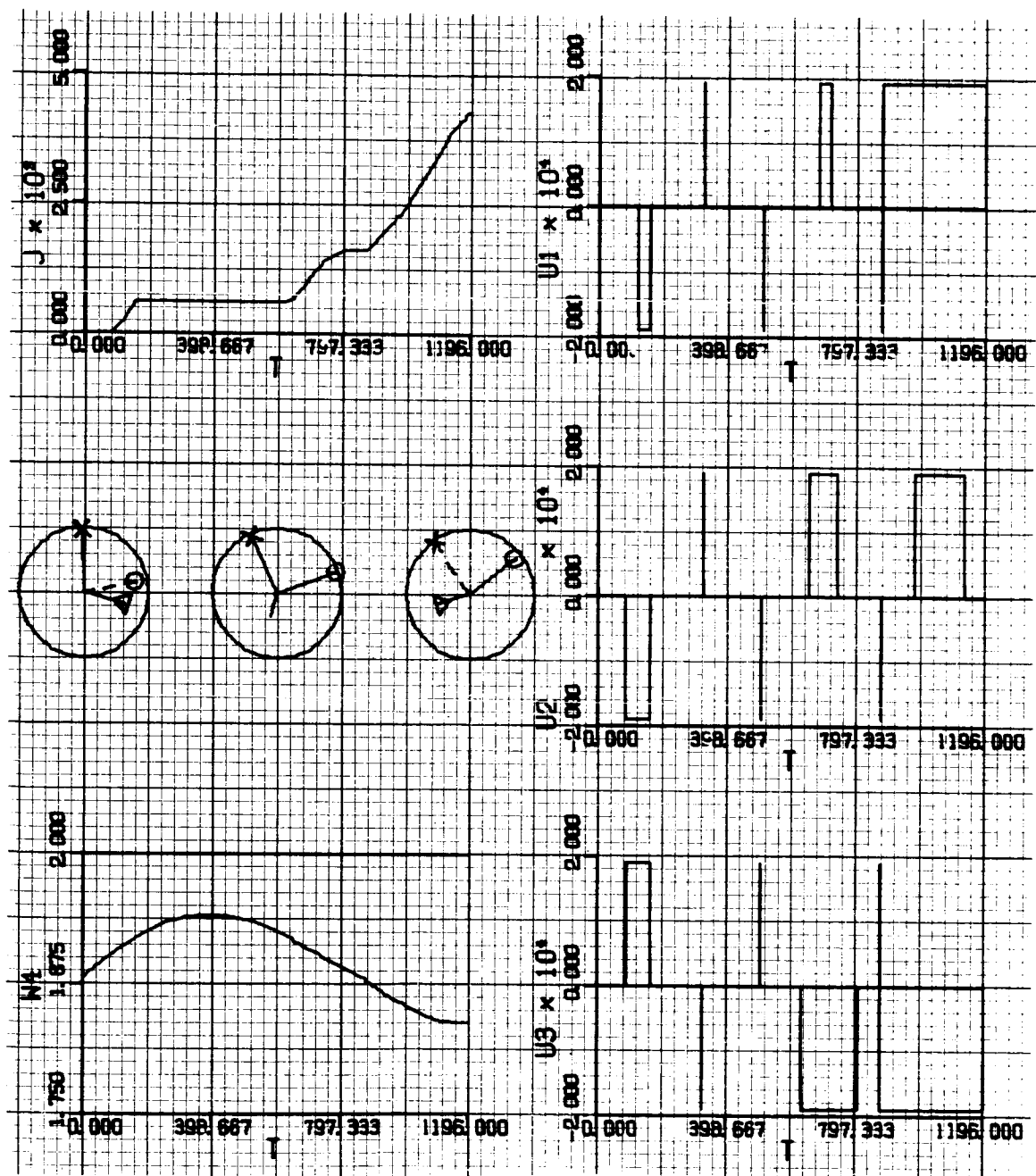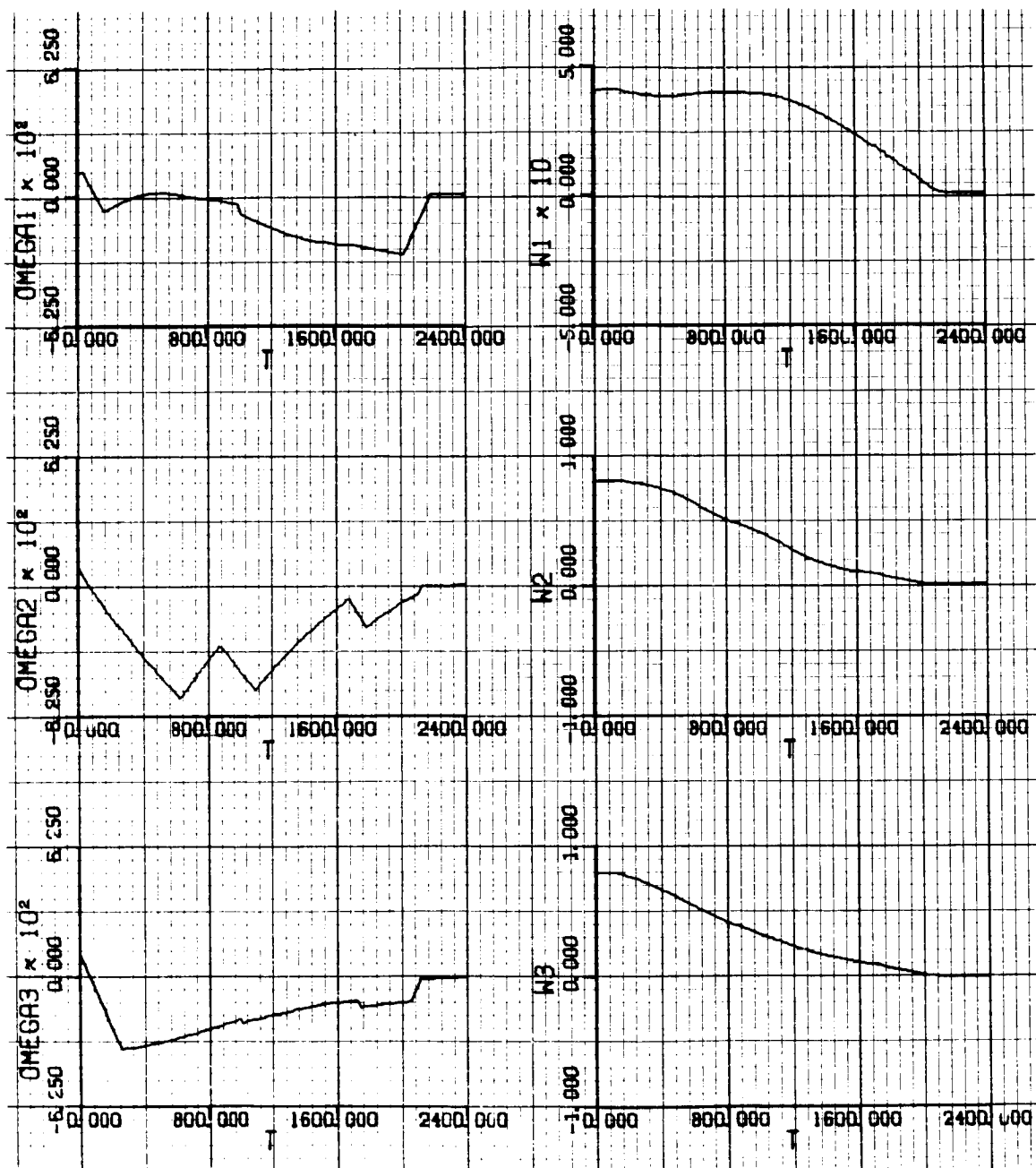
Figure 7-6b.

Figure 7-7a.   Response Curves with Orbital Parameters Specified in
Run R-10 (Table X).

Figure 7-7b.

101

Figure 7-8a.   Response Curves with Orbital Parameters Specified in Run
R-11 (Table X).

102
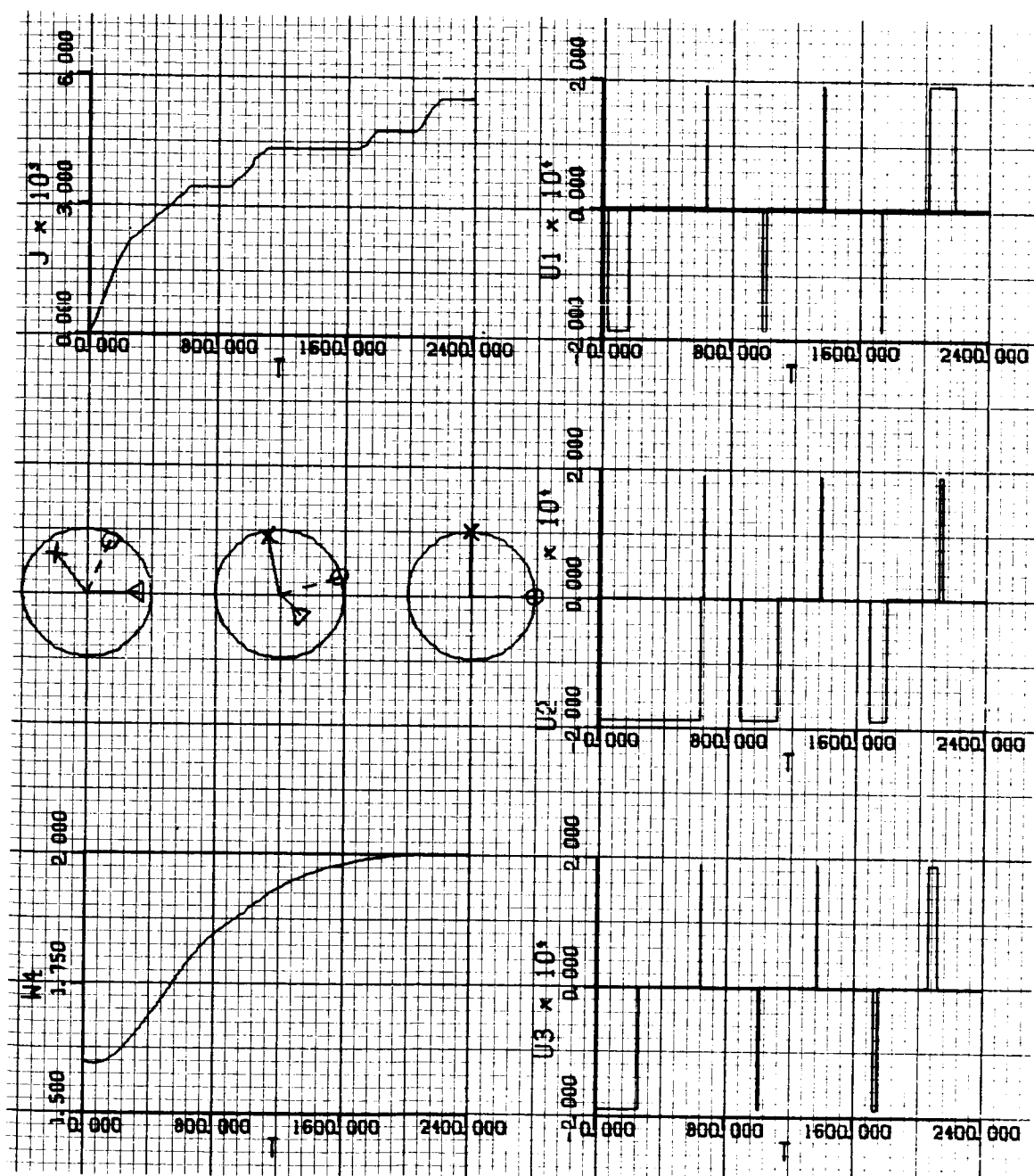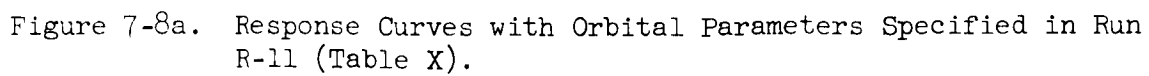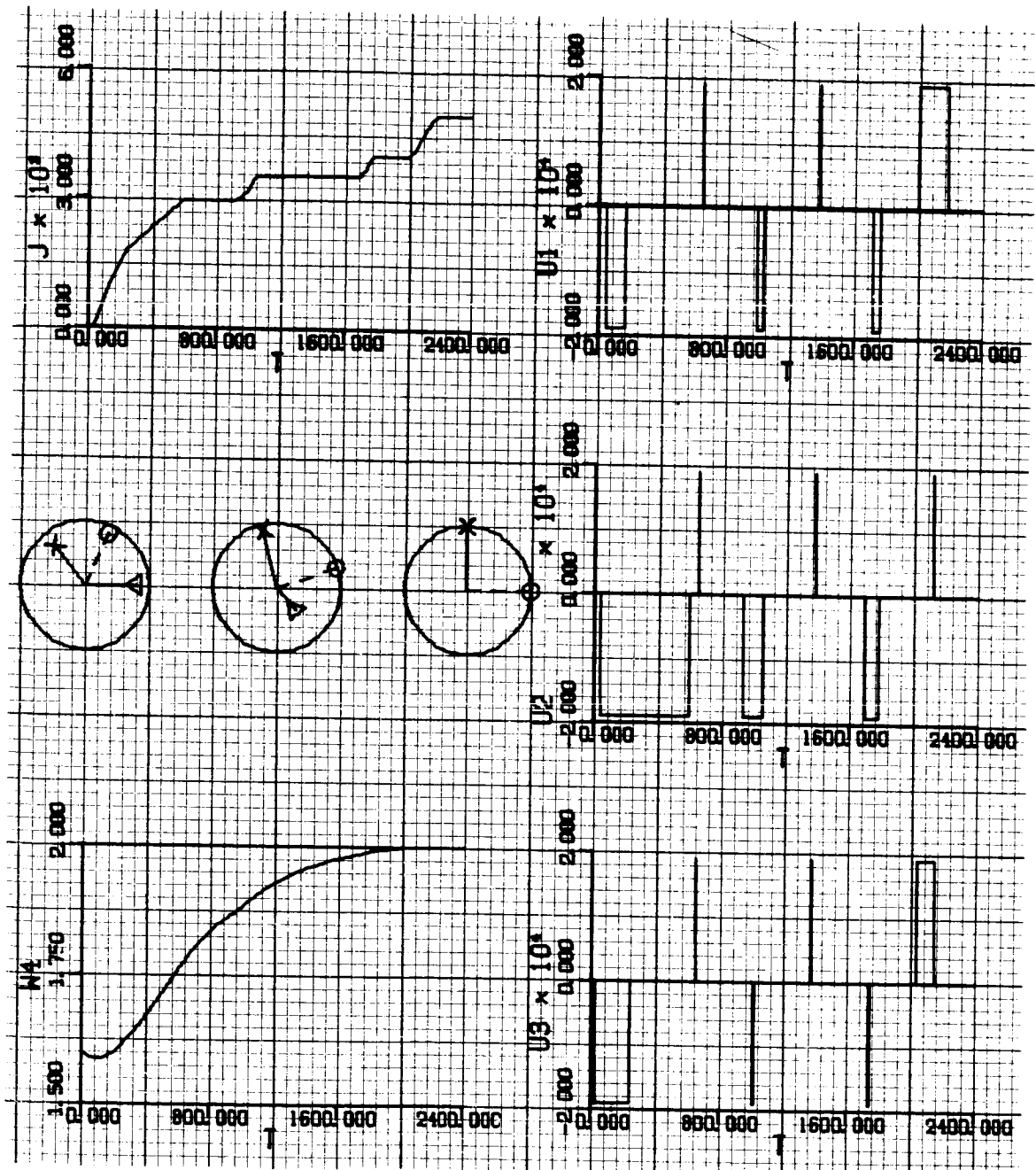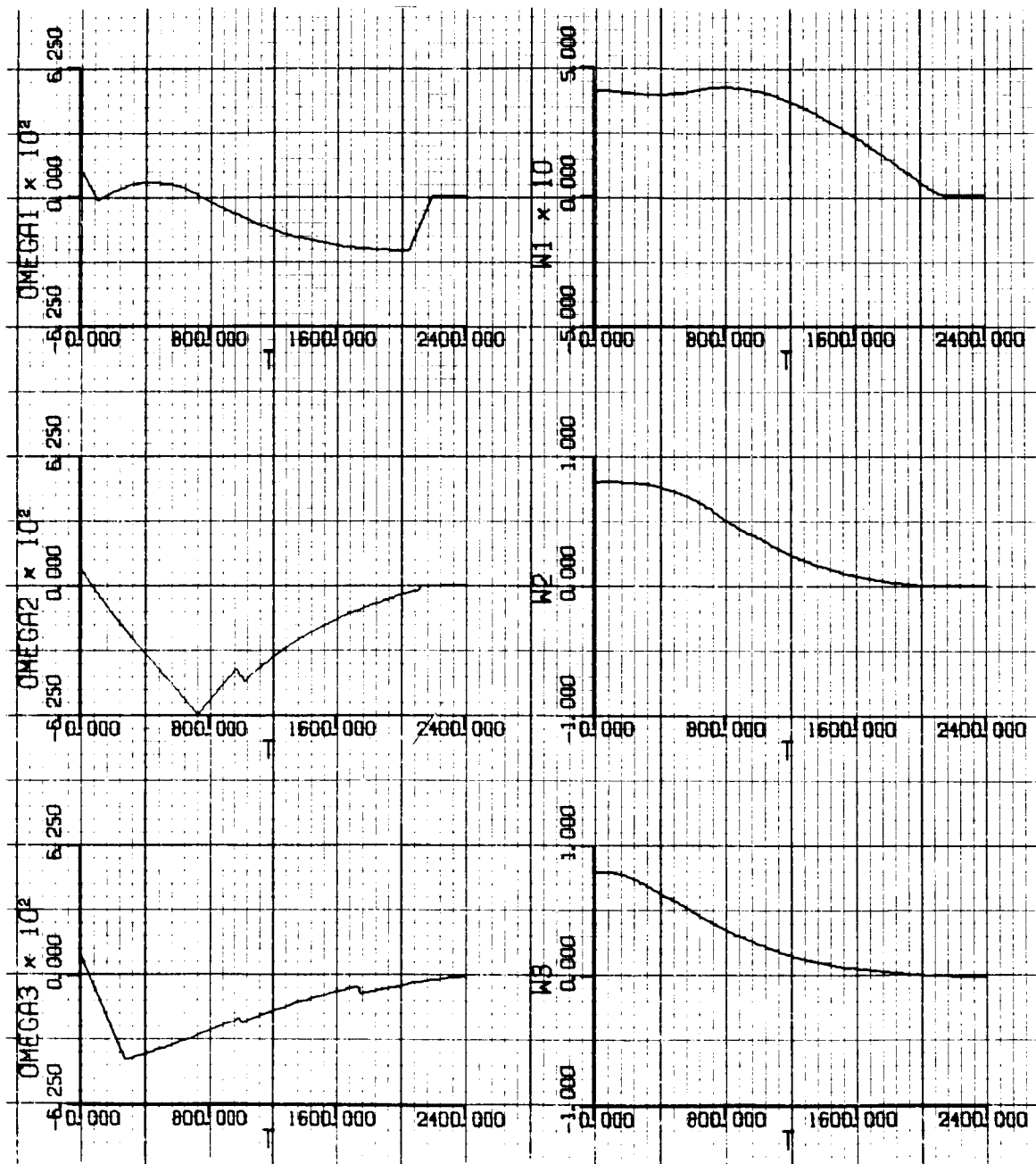
Figure 7-8b.

Figure 7-9a. Response Curves with Orbital Parameters Specified in
Run R-12 (Table X).
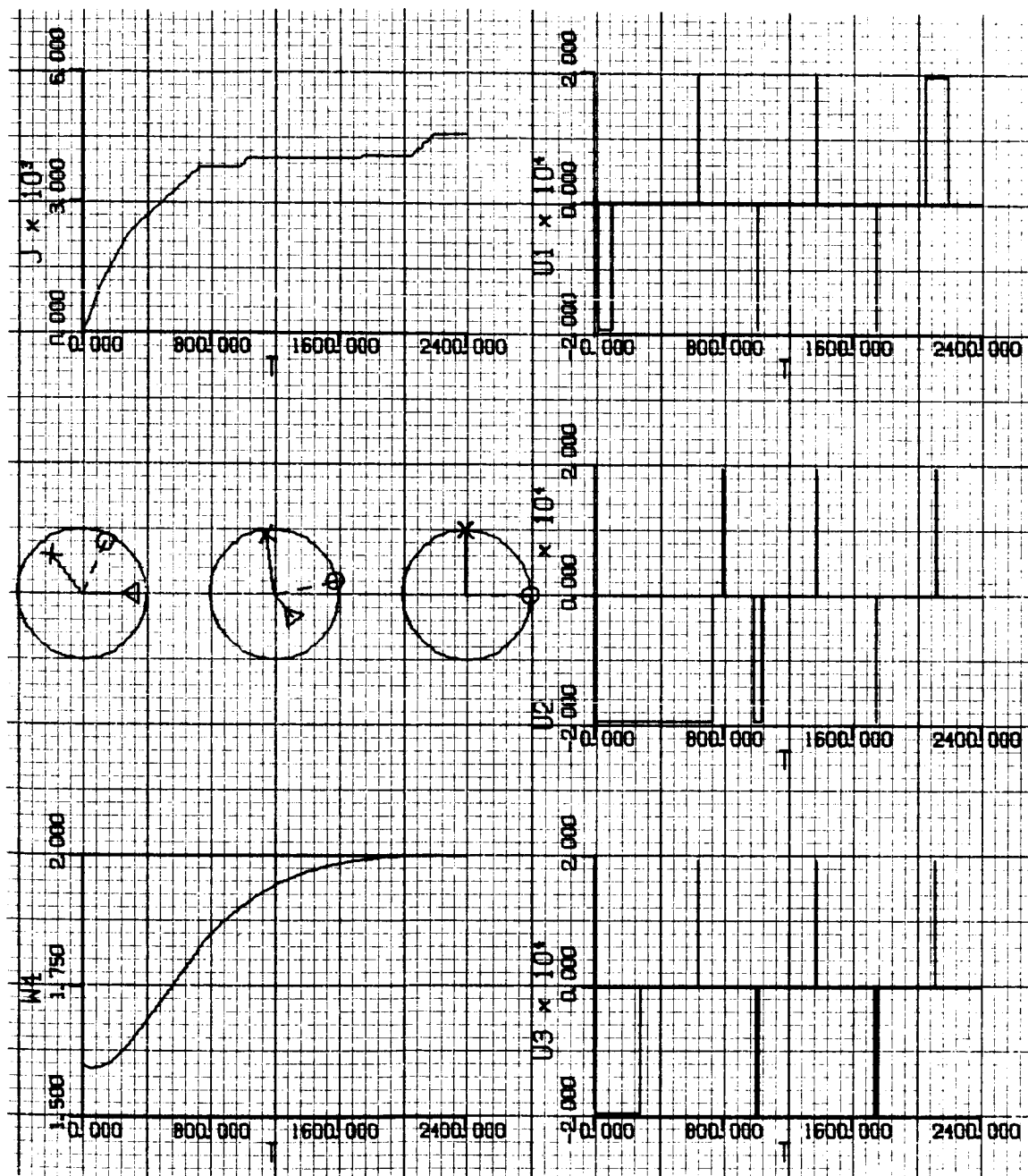
Figure 7-9b.
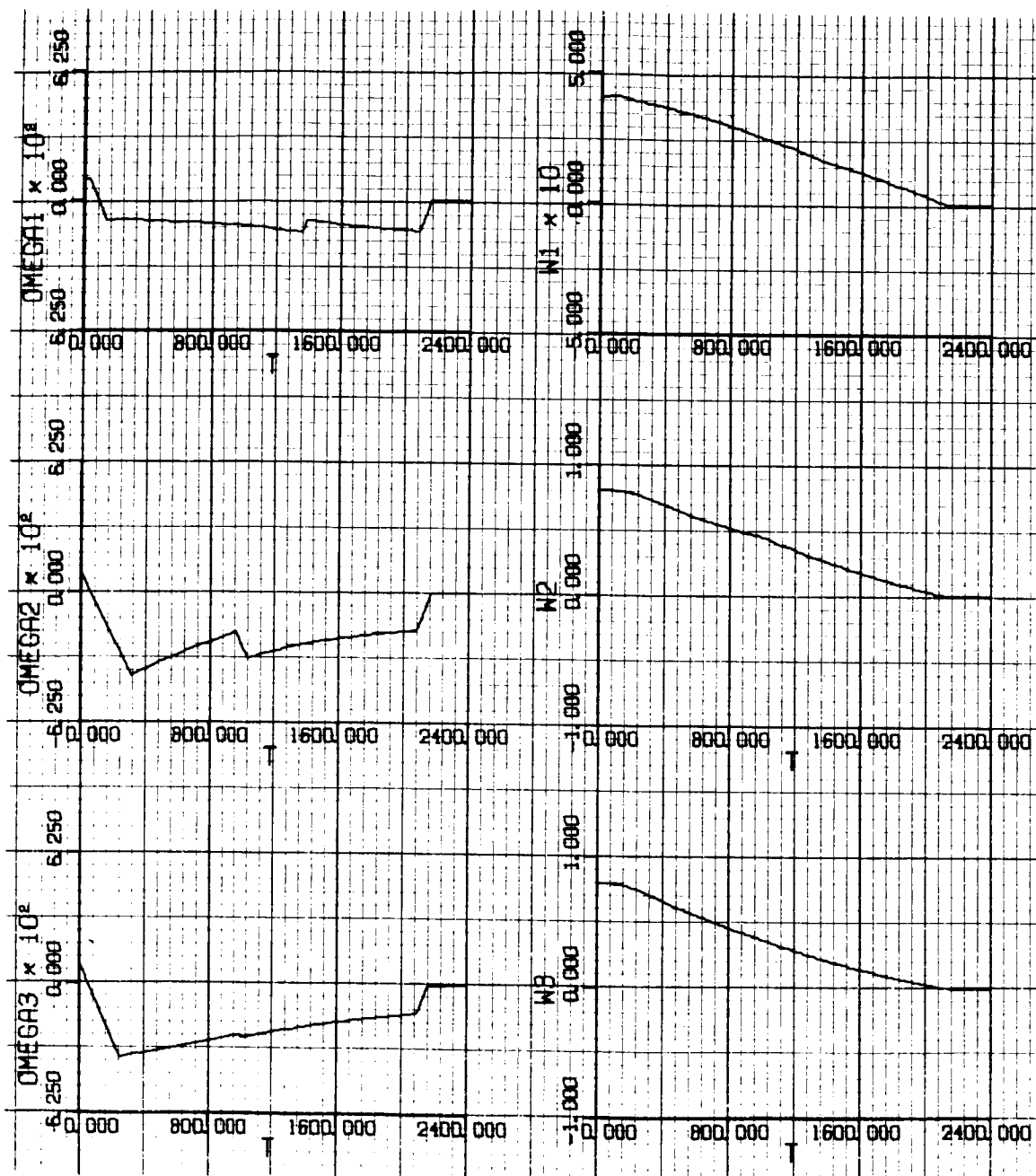
Figure 7-10a.   Response Curves with Orbital Parameters Specified in
Run R-13 (Table X).
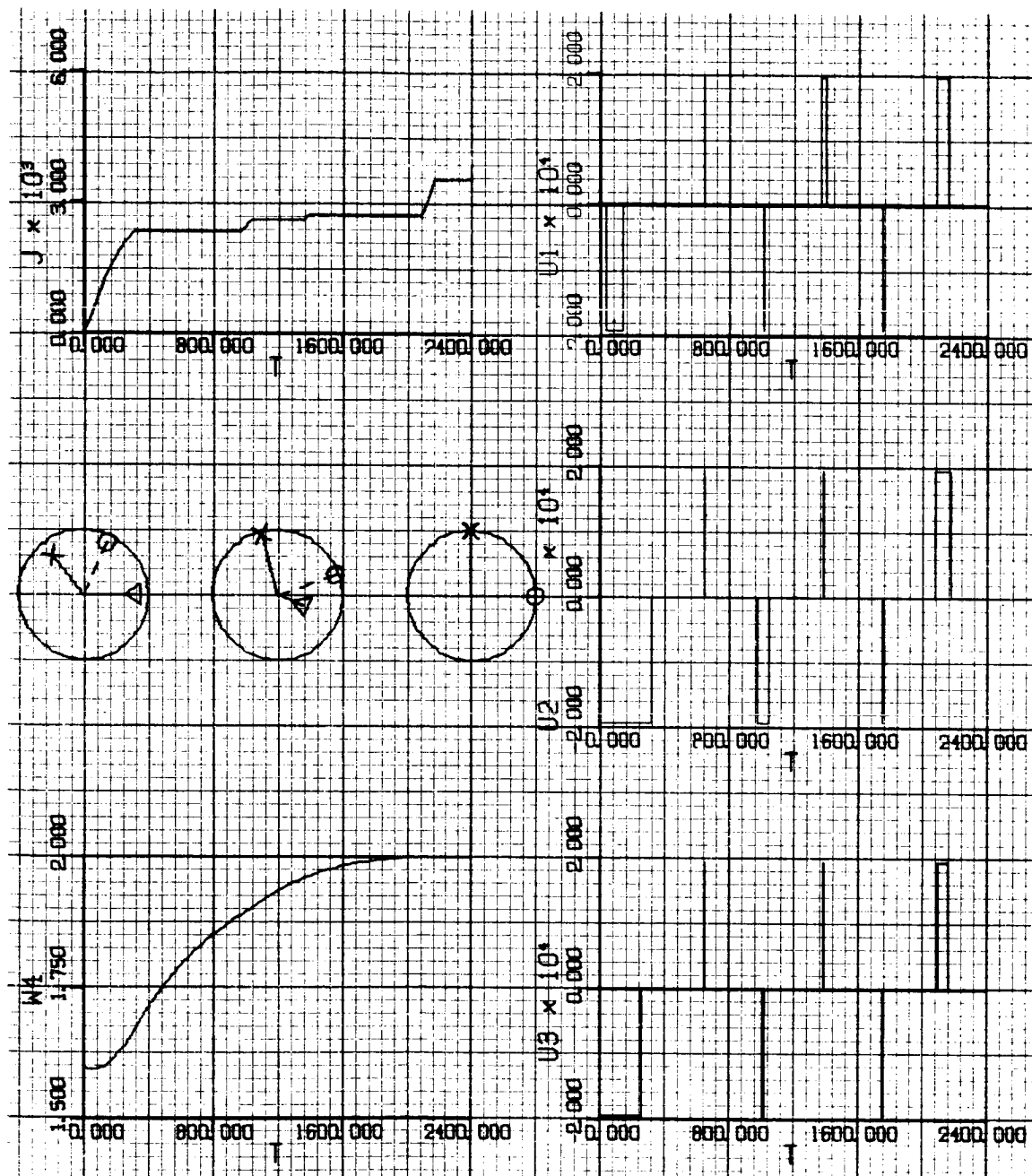
Figure 7-10b.
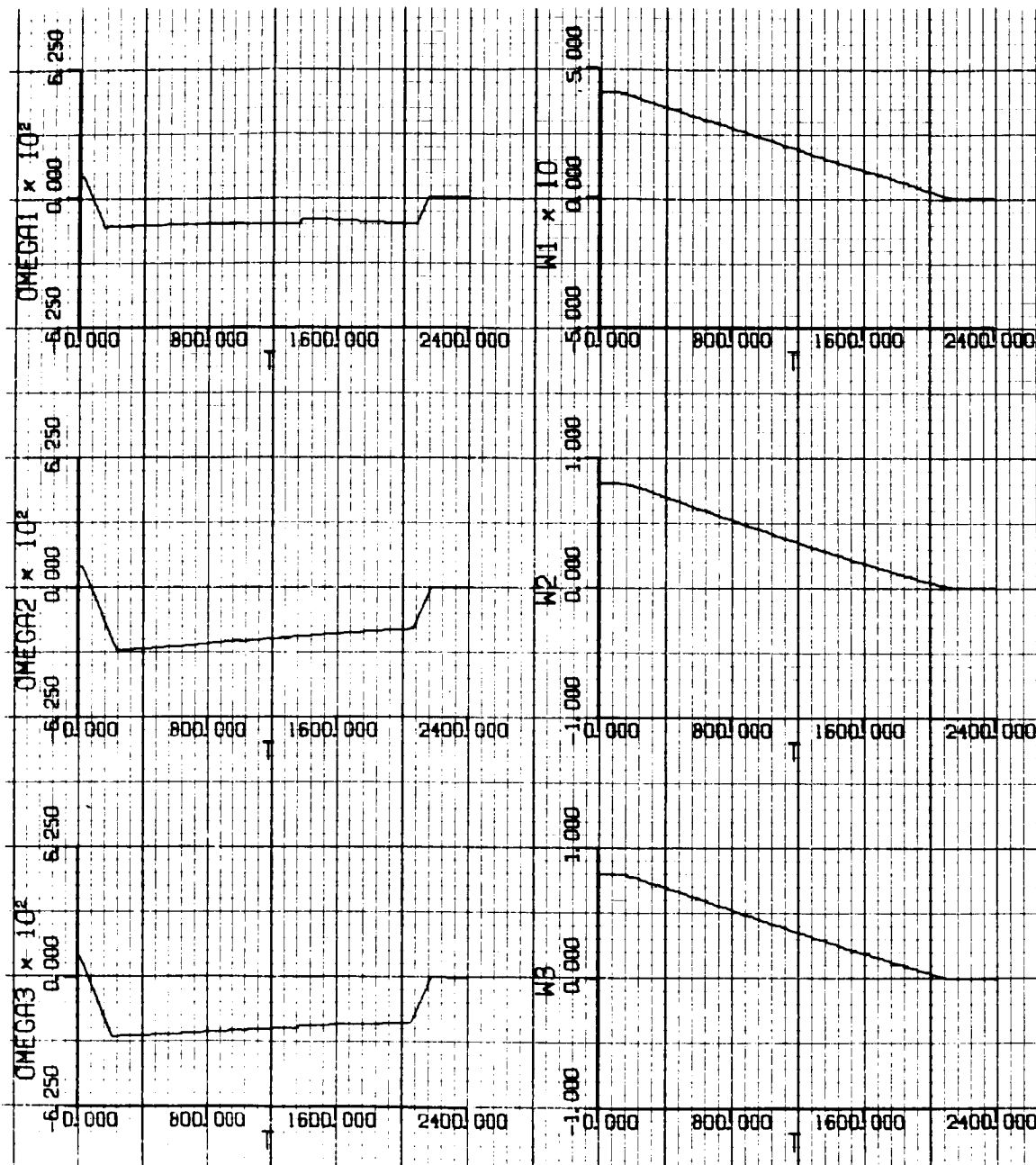
Figure 7-11a. Response Curves with Orbital Parameters Specified in Run R-14 (Table X).
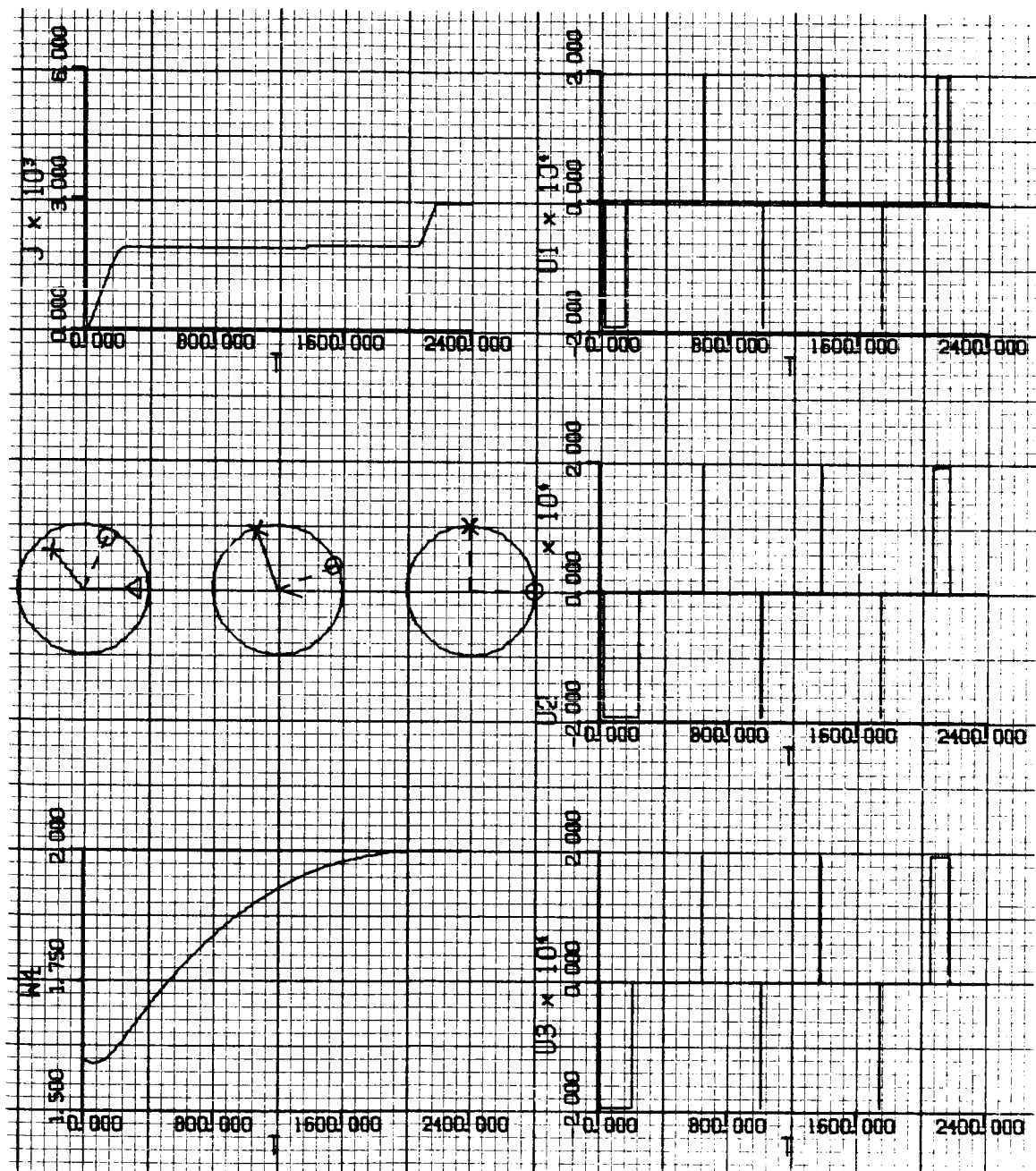
Figure 7-11b.
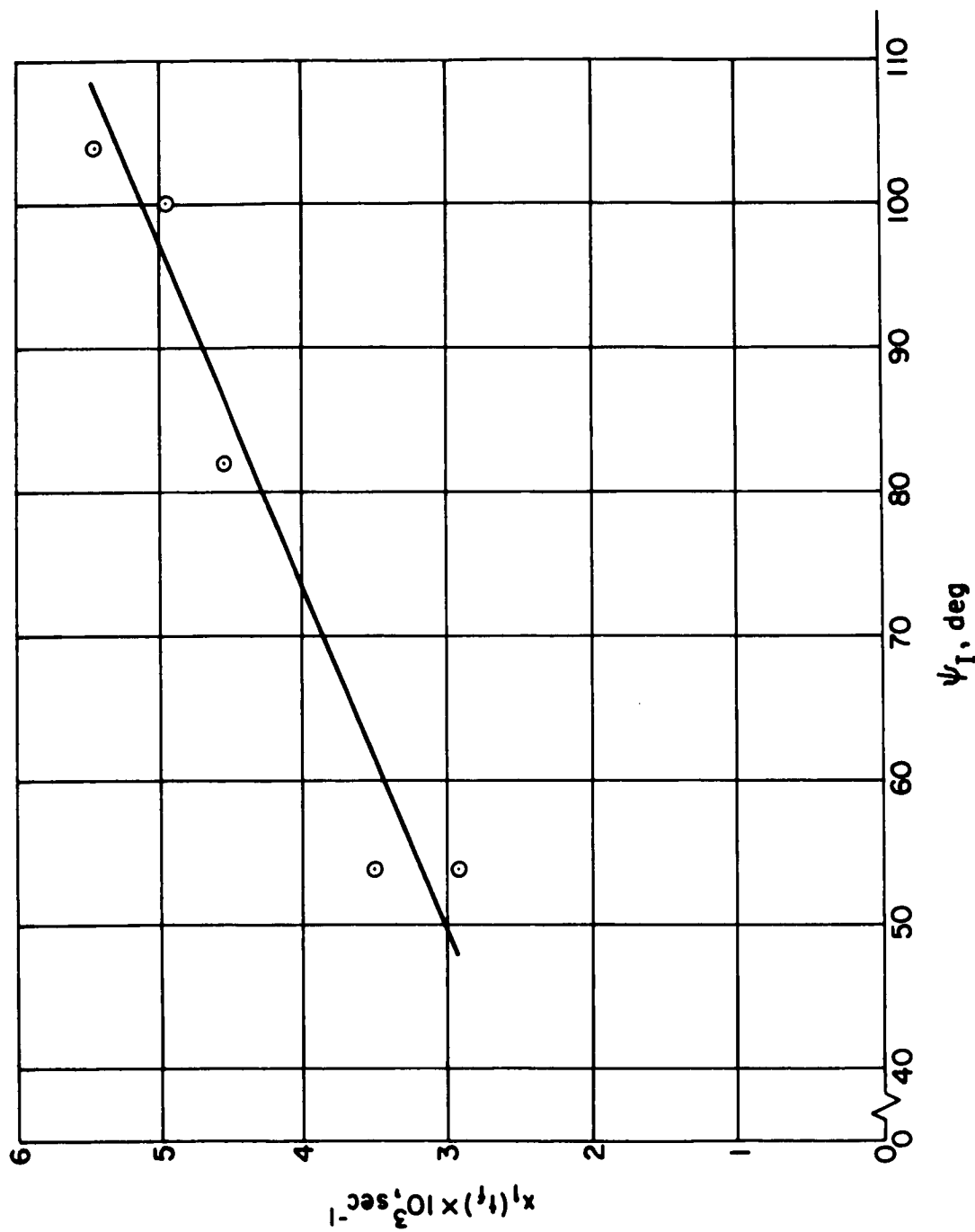
FIGURE 7-12. RELATIONSHIP BETWEEN FUEL CONSUMPTION AND EQUIVALENT ROTATION IN INERTIAL SPACE

110
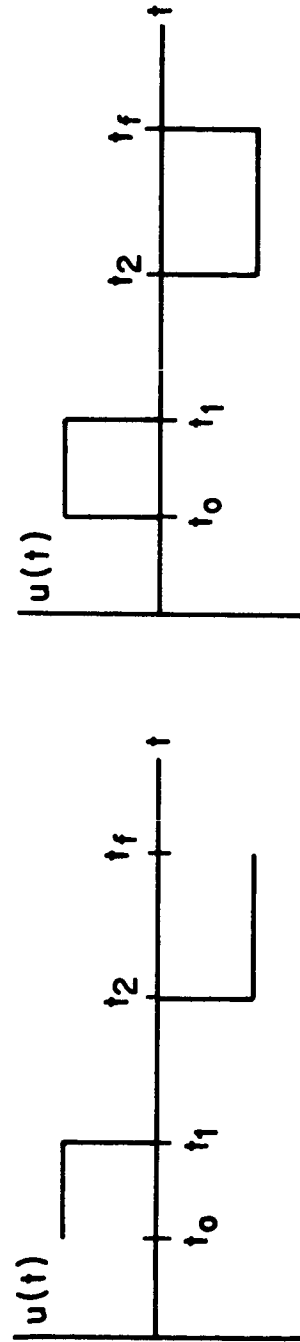
(a) TRUE OPTIMAL CONTROL   (b) SIMULATED CONTROL

FIGURE 7-13. TRUE OPTIMAL CONTROL AND
SIMULATED CONTROL

111

VIII. CONCLUSIONS

A. SUMMARY OF RESULTS

1. Development of an Extended Method of Steepest-Descent

By extending the method of steepest-descent to solve problems which contain bounds on the control components, by moving the switching times about, a new computational tool has been developed. This extended method of steepest-descent was used to solve the minimum-fuel optimization problem for two nonlinear, sixth-order mathematical models. Insights were gained during the solution of these optimization problems which led to a number of recommendations concerning computational procedures. It was found that an initial guess of the control time history should contain many more switching times than the optimal number. In addition convergence to the optimal solution was improved by selecting the sign of the first control pulse in each axis to be of opposite sign to that of the initial rate about that body axis. It was also found that even if the initial nominal control time history resulted in a state trajectory which badly missed the terminal constraints, subsequent iterations rapidly improved the initial guess. The derivation of the extended method and a list of computational procedures or considerations is found in Chapters V, VI and in Appendix B.

2. Computation of Optimal Trajectories for the Spacecraft Attitude Acquisition Problem

The extended method of steepest-descent was used to generate approximately optimal trajectories for the spacecraft attitude acquisition problem. In Chapter VI the state trajectories generated by

112

this method are compared with those generated by an idealized 3 axis proportional state feedback control system. It was found that trajectories generated by the former technique consumed less fuel, acquired the desired orientation more quickly and used lower control torque magnitudes than those required by the feedback scheme.

In Chapter VII a comparison is found between trajectories generated by steepest-descent and true optimal trajectories. The extended method of steepest-descent provides similar trajectories which satisfy the terminal constraints while using as much as 15% more fuel than optimal. This method may be computing trajectories which are only relative extremals and not absolute extremals. This computational technique repeatedly has produced control time histories which contain periods of no control about each body axis near $t = t_o$ and $t = t_f$. This characteristic has in all probability contributed to the 10 to 15% higher cost of these trajectories. The extended method of steepest-descent usually does not experience the difficulty of inverting a D matrix which has become singular when an extremal trajectory is approached.

It is not practical to generate an optimal control time history on board a spacecraft with present state-of-the-art computers since it takes as much as 15 minutes to compute a local extremal by the extended method of steepest-descent. However, a primary contribution of this report is the conclusion that the extended method of steepest-descent can be used to generate a set of nearly optimal state trajectories, starting from a finite set of arbitrary initial conditions, which may be used as design goals or standards for sub-optimal acquisition control schemes.

Chapters VI and VII contain many variations of the orbital parameters, initial conditions, terminal constraints, reference frames and control parameters. It is found that as long as the initial state trajectory or the optimal state trajectory does not pass through the singularity which occurs when the total equivalent rotation with respect to the desired orbital reference frame, ψ_R, equals 180 degrees, then convergence to an approximately optimal trajectory is possible.

B. RECOMMENDATIONS FOR FUTURE STUDIES

In this study the method of steepest-descent has been sucessfully extended and near-optimal trajectories generated for the spacecraft attitude acquisition problem; however, there are still some open questions of real importance:

i. Can convergence to an optimal solution be improved? It might be helpful if a computational method based on the second variation be derived to handle problems which contain bounds on the control components, and which contain pulses as the basic form of the control time history.[*] Convergence to an extremal trajectory would then most likely be improved for this class of problem.

ii. Can a useful general purpose digital computer program be written based on the extended method of steepest-descent? By being able to rapidly incorporate a specific system model into a general digital program one could readily obtain near optimal trajectories.

iii. What modifications are required to the digital simulation so that minimum time problems can be studied?

---

[*]A computational method such as this has recently been developed [Ref. 8-1]. This new method has been used to devise feedback control schemes.

At present the stopping condition for the forward numerical integration is difficult to express for time optimal problems.

iv. What feedback control laws provide good approximations to the optimal control?

It would be of interest to experiment with feedback control schemes for the satellite acquisition problem which might closely approximate the nearly optimal trajectories that are generated by the extended method of steepest-descent.

APPENDIX A: DERIVATION OF SYSTEM EQUATIONS

In this appendix coordinate systems are introduced and the equations of motion of a satellite are derived. The cost functional for optimal control is discussed and the adjoint equations are developed.

1. Coordinate Systems

In discussing the motion of a satellite in an orbit about an attracting body such as the earth certain coordinate frames are important. The three most important reference frames will be described in this section.

Figures A-1 and A-2 indicate the coordinate systems chosen in the development of the equations of motion. It is assumed that the attracting body is an inertially fixed point mass located at P, and that the center of mass of the satellite at P* moves in either a circular or an elliptical orbit about the point of attraction. Figure A-1 shows two of the right handed cartesian coordinate systems in addition to the geometry of the ellipse. The origin of the (x_e, y_e, z_e) axes is located at the point P with $z_e \perp$ to the plane of the orbit and the x_e, y_e pair oriented arbitrarily in the orbit plane. The (x_r, y_r, z_r) coordinate frame is centered at P* with $z_r \parallel$ to z_e . The (x_r, y_r, z_r) frame will be referred to as the orbital reference frame and may have one of two possible orientations for the purpose of this study: it may remain parallel to the inertial reference frame or it may change its orientation such that x_r always remains parallel to the local vertical, which is equivalent to saying x_r remains in the direction of the radius vector $\bar{r}$ from P to P* .
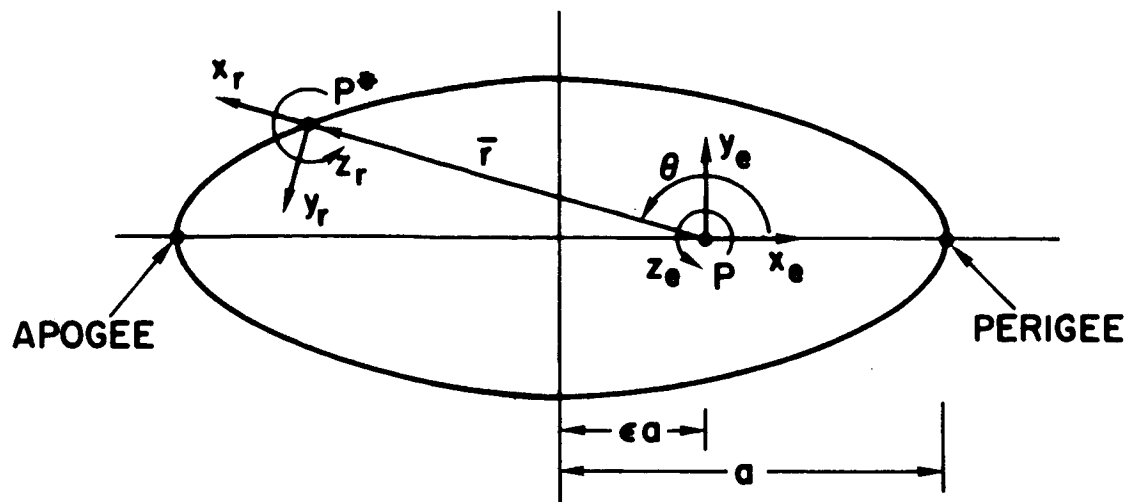
FIGURE A-1. ORBITAL AND INERTIAL
REFERENCE FRAMES
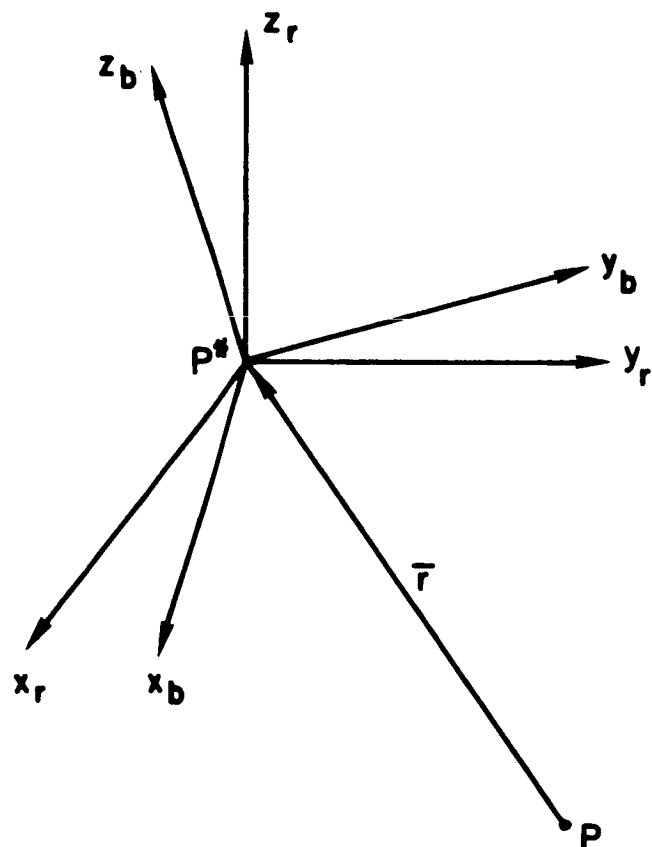
FIGURE A-2. ORBITAL AND BODY FIXED
REFERENCE FRAMES

117

A final reference frame of interest, shown in Figure A-2 and called the body fixed reference frame, is the (x_b, y_b, z_b) set, which is centered at P* and fixed to the satellite's centroidal principal axes of inertia.

Unit vectors parallel to each of the axes above will be denoted by the vector $\bar{n}$ with appropriate subscripts. For example, $\bar{n}_{xr}$ denotes the unit vector parallel to the x_r axis.

2. Equations of Motion

a. Orbital Equations

Equations describing the motion of the center of mass of the satellite at P* in an elliptical orbit about the point mass P are presented here [Ref. A-1]. By introducing the change of dependent variable

$$\boxed{R = r/a} \qquad (A-1)$$

where a = the major semidiameter

r = the distance from P to P*

and the change of independent variable

$$\boxed{\tau = nt}$$

where

$$n = (GM/a^3)^{1/2}$$

G = the universal gravitational constant

M = the mass of P

the desired form of the differential equations is written:

118

$$R' = V$$

$$V' = [(1-\epsilon^2)/R^3]-R^{-2}$$

(A-2)

where

ϵ = the eccentricity

$$(\quad)' = \frac{d(\quad)}{d\tau}$$

The two equations (A-2) may then be integrated on the digital computer at the same time as the dynamical equations that describe the attitude motion of the satellite. The initial conditions for (A-2) are conveniently expressed in terms of $\theta_o = \theta(\tau_o)$ and ϵ :

$$R(\tau_o) = (1-\epsilon^2)/(1 + \epsilon \cos \theta_o)$$

$$V(\tau_o) = \epsilon \sin \theta_o/(1-\epsilon^2)^{1/2}$$

(A-3)

Ref. A-1 provides two additional algebraic relationships for the first and second derivations of θ :

$$\theta' = (1-\epsilon^2)^{1/2} R^{-2}$$

$$\theta'' = -2(1-\epsilon^2)^{1/2} VR^{-3}$$

(A-4)

θ is the angle between x_e and x_r as shown in Figure A-1.

Differential equations (A-2) with initial conditions (A-3) and relations (A-4) provide the necessary equations to specify the orbital characteristics as required by the dynamical equations of motion.

b. Dynamical Equations

Euler's dynamical equations [Ref. A-2] may be written as:

119

$$I_x \dot{\omega}_x^B - (I_y - I_z)\omega_y^B \omega_z^B = N_x$$

$$I_y \dot{\omega}_y^B - (I_z - I_x)\omega_z^B \omega_x^B = N_y \qquad\qquad (A-5)$$

$$I_z \dot{\omega}_z^B - (I_x - I_y)\omega_x^B \omega_y^B = N_z$$

where I_x, I_y, I_z are the centroidal principal moments of inertia of the body, N_x, N_y, N_z are the components of external torque, and $\omega_x^B, \omega_y^B, \omega_z^B$ are the components of the total inertial angular velocity of the body.

The total inertial angular velocity of the body, resolved in the (x_b, y_b, z_b) frame, can be expressed as

$$\bar{\omega}^B = \omega_x^B \bar{n}_{xb} + \omega_y^B \bar{n}_{yb} + \omega_z^B \bar{n}_{zb} \quad . \qquad\qquad (A-6)$$

When the orbital reference frame is rotating as discussed in Section A-1, the angular velocity of this reference frame, $\bar{\omega}^R$, becomes

$$\bar{\omega}^R = \dot{\theta}\bar{n}_{zr} \quad . \qquad\qquad (A-7)$$

A third angular velocity is of interest, the angular velocity, $\bar{\omega}^{B/R}$, of the body with respect to the orbital reference frame. This is related to the above angular velocities by the vector equation:

$$\bar{\omega}^{B/R} = \bar{\omega}^B - \bar{\omega}^R \quad . \qquad\qquad (A-8)$$

When this angular velocity is resolved in the (x_b, y_b, z_b) reference frame it may be written as*:

$$\bar{\omega}^{B/R} = x_2 \bar{n}_{xb} + x_3 \bar{n}_{yb} + x_4 \bar{n}_{zb} \quad . \qquad\qquad (A-9)$$

---

*Use is made here of state space notation for simplicity of presentation.

It is necessary to consider the transformation to the body fixed coordinate frame from the orbital reference frame which may be expressed as:

$$
\begin{bmatrix} \bar{n}_{xb} \\ \bar{n}_{yb} \\ \bar{n}_{zb} \end{bmatrix} = \begin{bmatrix} a_{11} & a_{12} & a_{13} \\ a_{21} & a_{22} & a_{23} \\ a_{31} & a_{32} & a_{33} \end{bmatrix} \begin{bmatrix} \bar{n}_{xr} \\ \bar{n}_{yr} \\ \bar{n}_{zr} \end{bmatrix} = A \begin{bmatrix} \bar{n}_{xr} \\ \bar{n}_{yr} \\ \bar{n}_{zr} \end{bmatrix} , \quad (A\text{-}10)
$$

where the a_{ij} components of the matrix A are direction cosines. The operation implied by the orthogonal matrix of transformation A describing the physical motion of the rigid body is a rotation.

After these preparations the dynamical equations (A-5) can be expressed in terms of the relative angular velocity components of (A-9) and the direction cosines in (A-10). By using equations (A-6) through (A-10), the three components of total inertial angular velocity may be written as

$$
\omega_x^B = x_2 + \dot{\theta} a_{13}
$$

$$
\omega_y^B = x_3 + \dot{\theta} a_{23} \qquad (A\text{-}11)
$$

$$
\omega_z^B = x_4 + \dot{\theta} a_{33} .
$$

As may be seen from (A-5), the time derivatives of the expressions in (A-11) are required. These are

$$
\dot{\omega}_x^B = \dot{x}_2 + \ddot{\theta} a_{13} + \dot{\theta} \dot{a}_{13}
$$

$$
\dot{\omega}_y^B = \dot{x}_3 + \ddot{\theta} a_{23} + \dot{\theta} \dot{a}_{23} \qquad (A\text{-}12)
$$

$$
\dot{\omega}_z^B = \dot{x}_4 + \ddot{\theta} a_{33} + \dot{\theta} \dot{a}_{33}
$$

By combining (A-5), (A-11) and (A-12) and making use of the definitions of the inertia parameters:

$$K_x = \frac{I_z - I_y}{I_x} \;,\quad K_y = \frac{I_x - I_z}{I_y} \;,\quad K_z = \frac{I_y - I_x}{I_z} \;,\qquad (A\text{-}13)$$

three differential equations for the relative angular velocity components may be written:

$$\dot{x}_2 = N_x/I_x - \ddot{\theta}a_{13} - \dot{\theta}\dot{a}_{13} - K_z(x_3 + \dot{\theta}a_{23})(x_4 + \dot{\theta}a_{33})$$

$$\dot{x}_3 = N_y/I_y - \ddot{\theta}a_{23} - \dot{\theta}\dot{a}_{23} - K_y(x_4 + \dot{\theta}a_{33})(x_2 + \dot{\theta}a_{13}) \qquad (A\text{-}14)$$

$$\dot{x}_4 = N_z/I_z - \ddot{\theta}a_{33} - \dot{\theta}\dot{a}_{33} - K_z(x_2 + \dot{\theta}a_{13})(x_3 + \dot{\theta}a_{23})$$

Before these equations may be solved, the external torques must be defined, initial conditions must be specified, and equations for the direction cosines and their derivatives have to be written in terms of kinematical representations such as direction cosines, Euler angles or Euler parameters.

c. Kinematical Equations

Extensive study has been made in the recent literature [Ref. 3-1, A-3] of the relative merits of various schemes to describe and to compute the spacial rotations of a rigid body. These references state that for the present problem of determing the large angle maneuvers of an unsymmetrical rigid body and controlling the three body-fixed axes (x_b, y_b, z_b) to a specific orientation in space, Euler parameters provide the most useful characteristics for analysis and for simulation. One of the reasons for this recommendation is that the classical and the non-classical Euler angles create singularities in the equations at 0

and at 90 degrees of rotation respectively; whereas, when integrating the equations of motion and their adjoint equations using Euler parameters, the singularity does not appear until the total rotation as described by the transformation A approaches 180 degrees. For the present analysis rotations up to 180 degrees are to be considered and a scheme which avoids a singularity in numerical integration for smaller rotations is essential. A further reason for using Euler parameters is that only algebraic relations appear in the expressions for the derivatives in contrast to the appearance of trigonometric functions when Euler angles are used.

One disadvantage of Euler parameters is that they bear little relation to the physical situation. One cannot readily measure Euler parameters as would be required in a practical feedback scheme which would use them to provide attitude information. The direction cosines or Euler angles are easily measured from sensor outputs and, of course, a transformation to Euler parameters could be made; however, this transformation would cause additional complexity in the feedback system. In spite of this limitation of the Euler parameters they will still be used in this primarily analytical study.

The next step, then, is to express the matrix of transformation A of (A-10) in terms of the Euler parameters and to obtain suitable differential equations for them. Except for the case when $A = I$, the identity matrix, or when the rotation implied by A is through an angle which is an exact integral multiple of π , the matrix A has three distinct eigenvalues. One of the eigenvalues is always $+1$. Now denote by $\bar{e}$ the eigenvector of A corresponding to the eigenvalues $+1$ and define its magnitude

123

to be 1 . This unit vector has the same components in either the (x_b, y_b, z_b) or the (x_r, y_r, z_r) coordinate frames, viz. e_x, e_y, e_z [Ref. A-2]. This vector corresponds to the direction in space about which a single rotation through an angle ψ could be made which would yield the rotation implied by A . The four Euler parameters are defined as (see Ref. A-4):

$$W_1 = 2 \cos(\psi/2) e_x$$

$$W_2 = 2 \cos(\psi/2) e_y \qquad \text{(A-15)}$$

$$W_3 = 2 \cos(\psi/2) e_z$$

$$W_4 = 2 \sin(\psi/2)$$

These four parameters are not independent, for a quick calculation reveals that

$$\boxed{\sum_{i=1}^{4} W_i^2 = 4 \quad ;} \qquad \text{(A-16)}$$

therefore, there exists but three independent Euler parameters corresponding to the three degrees of freedom of rotation. The direction cosines may be expressed in terms of the Euler parameters [Ref. A-3]:

$$a_{11} = 1/2(W_1^2 + W_4^2) - 1$$

$$= 1/4(W_1^2 + W_4^2 - W_2^2 - W_3^2)$$

$$a_{12} = 1/2(W_2 W_1 + W_3 W_4)$$

$$a_{13} = 1/2(W_3 W_1 - W_2 W_4)$$

$$a_{21} = 1/2(W_1 W_2 - W_3 W_4)$$

$$a_{22} = 1/2(W_2^2 + W_4^2) - 1$$

$$= 1/4(W_2^2 + W_4^2 - W_1^2 - W_3^2) \qquad \text{(A-17)}$$

$$a_{23} = 1/2(W_3 W_2 + W_1 W_4)$$

$$a_{31} = 1/2(W_1 W_3 + W_2 W_4)$$

$$a_{32} = 1/2(W_2 W_3 - W_1 W_4)$$

$$a_{33} = 1/2(W_3^2 + W_4^2) - 1$$

$$= 1/4(W_3^2 + W_4^2 - W_1^2 - W_2^2)$$

Four differential equations for the Euler parameters are given below [Ref. A-3]:

$$\dot{W}_1 = 1/2(x_2 W_4 - x_3 W_3 + x_4 W_2)$$

$$\dot{W}_2 = 1/2(x_2 W_3 + x_3 W_4 - x_4 W_1) \qquad \text{(A-18)}$$

$$\dot{W}_3 = 1/2(-x_2 W_2 + x_3 W_1 + x_4 W_4)$$

$$\dot{W}_4 = 1/2(-x_2 W_1 - x_3 W_2 - x_4 W_3) \quad .$$

Examination of the dynamical equations (A-14) shows that three more relationships are required, viz. the expressions for $\dot{a}_{i3}$ $(i = 1,2,3)$.

By differentiating (A-17) and by making use of (A-17) and (A-18) the following expressions are obtained:

$$\dot{a}_{13} = x_4 a_{23} - x_3 a_{33}$$

$$\dot{a}_{23} = x_2 a_{33} - x_4 a_{13} \qquad\qquad (A-19)$$

$$\dot{a}_{33} = x_3 a_{13} - x_2 a_{23}$$

Once the torque and the initial conditions are known, the seven equations, when (A-14) and (A-18) have been combined, may be integrated after use has been made of the relationships (A-17) and (A-19). An alternative now exists: the seven differential equations may be integrated to obtain the three components of the relative angular velocity, x_2, x_3 and x_4 , and the four Euler parameters, the algebraic relation (A-16) being used to check the accuracy of integration; or one of the Euler parameters may be eliminated from the differential equations, and the resulting six first-order differential equations integrated. The former method has been chosen, as the relative ease of integrating an additional equation far outweighs the need for repetitve use of the square-root function on the digital computer which would be the case if (A-16) were solved for one of the Euler parameters and this parameter eliminated from the differential equations.

> d. External and Control Torques

Expressions are required for the components of external and control torque N_x, N_y, N_z , in body coordinates. The three components of the control vector $\bar{u}$, which will be specified as a function of the states or as a function of time, are assumed to act about the three

principal axes. The magnitude of each of the components will be bounded in some of the considered cases. It is assumed that there exist no dynamics associated with the production of this control torque and that the magnitudes of the bounds on the torque components may be arbitrarily small.

A further term in the expressions for N_x, N_y, N_z is the external disturbance torques due to the gravity gradient. The disturbance torque will be considered when its magnitude and that of the control torque are of the same order. The expressions for the torque components may then be written as:

$$N_x = I_x u_x + N_{xg}$$

$$N_y = I_y u_y + N_{yg} \tag{A-20}$$

$$N_z = I_z u_z + N_{zg}$$

where u_x, u_y, u_z are the components of the control vector, and N_{xg}, N_{yg}, N_{zy} are the components of the gravity gradient torque. These components are given in Ref. A-5 as:

$$N_{xg} = 3(GM/r^3)(I_z - I_y)(\bar{n}_{xr} \cdot \bar{n}_{yb})(\bar{n}_{xr} \cdot \bar{n}_{zb})$$

$$N_{yg} = 3(GM/r^3)(I_x - I_z)(\bar{n}_{xr} \cdot \bar{n}_{xb})(\bar{n}_{xr} \cdot \bar{n}_{zb}) \tag{A-21}$$

$$N_{zg} = 3(GM/r^3)(I_y - I_x)(\bar{n}_{xr} \cdot \bar{n}_{xb})(\bar{n}_{xr} \cdot \bar{n}_{yb})$$

where the $\bar{n}_{xr}$ vector, in the rotating orbital reference frame, is parallel to the local vertical. By using the transformation A in (A-10) and the definitions (A-13) and equations (A-20) the following expressions for the ratio of torques to moments of inertia are written:

$$N_x/I_x = u_x + 3(GM/r^3)K_x a_{21} a_{31}$$

$$N_y/I_y = u_y + 3(GM/r^3)K_y a_{11} a_{31} \qquad \text{(A-22)}$$

$$N_z/I_z = u_z + 3(GM/r^3)K_z a_{11} a_{21}$$

These expressions are now ready for substitution in (A-14).

3. Minimum-Fuel Cost Functional

The cost functional J , which is to be minimized is an integral (over a fixed time period) of the weighted sums of the amount of fuel used for control,

$$J(\bar{u}) = \int_{t_o}^{t_f} (d_1|u_x| + d_2|u_y| + d_3|u_z|)dt \qquad \text{(A-23)}$$

where the weights $d_i(i = 1,2,3)$ are for the most part assumed to be equal, and the initial and final times, t_o and t_f , are parameters which are fixed for each specific case.

4. Summary of Differential Equations

The differential equations describing the orbital dynamics, the attitude motion of the satellite and the minimum-fuel cost functional are summarized in Chapter IV.

5. Adjoint Equations

The expressions for the elements of the matrix M found in the adjoint differential equation $\bar{\lambda}' = -M^T(\tau)\bar{\lambda}$ for the two sets of differential equations (4-4) and (4-6) are found below. The above form of the adjoint equation is only valid when the variational problem possesses no subsidiary conditions on the states when τ satisfies

$\tau_o < \tau < \tau_f$ [Ref. A-6]. Since the equation (4-5) is just a finite subsidiary condition for the differential equations (4-4) and (4-6) either the adjoint differential equation must be modified, or the constraint equation (4-5) used in the differential equations (4-4) or (4-6) to reduce the order of the state so that the adjoint differential equation applies directly. The latter course is chosen for this study. A further important observation is that the ninth and tenth elements of

$\bar{x}$ for the low torque case do not enter into consideration in forming the adjoint equations as they have been introduced only as a convenience in integrating the equations (4-4). In the light of the above comments the adjoint system will be of seventh order for both of the systems of differential equations.

The problem of a singularity in the adjoint system should be noted. In what follows, observe that x_8 appears in the denominator of a large number of terms. From (A-15) it is seen that when the total rotation approaches 180 degrees, x_8 approaches 0 . This singularity limits the present study to those trajectories which do not exceed 180 degrees of rotation.

The elements of $M(t)$ are determined by the following relationship:

$$m_{ij} = (\partial f_i / \partial x_j) \; ; \; i,j = 1,\ldots,7 \tag{A-24}$$

where f_i is the ith element in the vector $\bar{x}' = \bar{f}(\bar{x},\bar{u},\tau)$ and x_j is the jth element in the vector $\bar{x}$. The elements m_{ij} satisfy the adjoint differential equation

$$\bar{\lambda}' = -M^T(\tau)\bar{\lambda} \tag{A-25}$$

They are evaluated on the nominal trajectory $\bar{x}_n$ as discussed in Chapter II. Equation (A-25) is the adjoint system to $\bar{x}' = \bar{f}(\bar{x},\bar{u},\tau)$.

As discussed in this appendix the number of degrees of freedom of the rigid body is three; and therefore, when adding a cost functional as one element of the state, the total dimension of the state is <u>seven</u>.

i and j in (A-24) will range from one to seven, with the fourth Euler parameter x_8 eliminated from $\bar{x}' = \bar{f}(\bar{x},\bar{u},\tau)$ prior to the partial differentiation. Since x_i (i = 1,...,10) will be available for substitution in (A-24), the m_{ij} may be expressed in terms of x_8, x_9, x_{10} <u>after</u> differentiation.

Two sets of expressions for the elements m_{ij} are required: one for the low torque case, and one for the high torque case. These expressions are found below.

<u>Low Torque Case</u>

$$m_{11} = m_{12} = \ldots = m_{17} = 0$$

$$m_{21} = m_{31} = \ldots = m_{71} = 0$$

$$m_{22} = m_{33} = m_{44} = 0$$

$$2m_{23} = 2\theta' a_{33} - 2K_x(x_4 + \theta' a_{33})$$

$$2m_{24} = -2\theta' a_{23} - 2K_x(x_3 + \theta' a_{23}) \qquad\qquad (A\text{-}26)$$

$$2m_{25} = -\theta'' E_2 - 2\theta' x_3 x_5 (1 - K_x) - x_4 \theta' E_1 (1 + K_x)$$
$$\qquad - K_x \theta'(\theta' E_1 a_{33} - 2\theta' a_{23} x_5) + SK_x(a_{21}E_5 + a_{31}E_3)$$

$$2m_{26} = -\theta'' E_4 - 2\theta' x_3 x_6 (1 - K_x) - x_4 \theta' E_5 (1 + K_x)$$
$$\qquad - K_x \theta'(\theta' E_5 a_{33} - 2\theta' a_{23} x_6) + SK_x(a_{31}E_6 - a_{21}E_4)$$

<div align="right">(continued)</div>

$$2m_{27} = -\theta''E_6 - x_4\theta'E_9(1 + K_x) - K_x(\theta')^2 E_9 a_{33} \qquad \text{(A-26 cont)}$$
$$+ SK_x(a_{21}E_8 + a_{31}E_7)$$

$$2m_{32} = -2\theta'a_{33} - 2K_y(x_4 + \theta'a_{33})$$

$$2m_{34} = 2\theta'a_{13} - 2K_y(x_2 + \theta'a_{13})$$

$$2m_{35} = -\theta''E_1 + x_4\theta'E_2(1 - K_y) + 2\theta'x_2x_5(1 + K_y)$$
$$- K_y\theta'(\theta'E_2 a_{33} - 2\theta'a_{13}x_5) + SK_y a_{11}E_5$$

$$2m_{36} = -\theta''E_5 + x_4\theta'E_4(1 - K_y) + 2\theta'x_2x_6(1 + K_y)$$
$$- K_y\theta'(\theta'E_4 a_{33} - 2\theta'a_{13}x_6) - SK_y(a_{11}E_4 + 2a_{31}x_6)$$

$$2m_{37} = -\theta''E_9 + x_4\theta'E_6(1 - K_y) - K_y(\theta')^2 E_6 a_{33} + SK_y(a_{11}E_8 - 2a_{31}x_7)$$

$$2m_{42} = 2\theta'a_{23} - 2K_z(x_3 + \theta'a_{23})$$

$$2m_{43} = -2\theta'a_{13} - 2K_z(x_2 + \theta'a_{13})$$

$$2m_{45} = 2\theta''x_5 + x_2\theta'E_1(1 - K_z) - x_3\theta'E_2(1 + K_z)$$
$$- K_z\theta'(\theta'E_1 a_{13} + \theta'E_2 a_{23}) + SK_z a_{11}E_3$$

$$2m_{46} = 2\theta''x_6 + x_2\theta'E_5(1 - K_z) - x_3\theta'E_4(1 + K_z)$$
$$- K_z\theta'(\theta'E_5 a_{13} + \theta'E_4 a_{23}) + SK_z(a_{11}E_6 - 2a_{21}x_6)$$

$$2m_{47} = x_2\theta'E_9(1 - K_z) - x_3\theta'E_6(1 + K_z)$$
$$- K_z\theta'(\theta'E_9 a_{13} + \theta'E_6 a_{23}) + SK_z(a_{11}E_7 - 2a_{21}x_7)$$

$$2m_{52} = x_8$$

$$2m_{53} = -x_7$$

$$2m_{54} = x_6$$

$$2m_{55} = -x_2x_5/x_8$$

(continued)

131

$$2m_{56} = x_4 - x_2 x_6 / x_8$$

$$2m_{57} = -x_3 - x_2 x_7 / x_8$$

$$2m_{62} = x_7$$

$$2m_{63} = x_8$$

$$2m_{64} = -x_5$$

$$2m_{65} = -x_4 - x_3 x_5 / x_8$$

$$2m_{66} = -x_3 x_6 / x_8$$

$$2m_{67} = x_2 - x_3 x_7 / x_8$$

$$2m_{72} = -x_6$$

$$2m_{73} = x_5$$

$$2m_{74} = x_8$$

$$2m_{75} = x_3 - x_4 x_5 / x_8$$

$$2m_{76} = -x_2 - x_4 x_6 / x_8$$

$$2m_{77} = -x_4 x_7 / x_8$$

where

$$S = 3/(x_{10})^3$$

$$E_1 = x_8 - (x_5)^2 / x_8$$

$$E_2 = x_7 + x_5 x_6 / x_8$$

$$E_3 = x_6 + x_5 x_7 / x_8$$

$$E_4 = -x_8 + (x_6)^2 / x_8$$

(continued)

132

$$E_5 = x_7 - x_5 x_6 / x_8$$

$$E_6 = x_5 + x_6 x_7 / x_8$$

$$E_7 = -x_8 + (x_7)^2 / x_8$$

$$E_8 = x_5 - x_6 x_7 / x_8$$

$$E_9 = x_6 - x_5 x_7 / x_8$$

The ten elements of $\bar{x}$ are available, and as a result θ', θ'' and a_{ij} may be evaluated where required.

High Torque Case

The necessary expressions for the high torque case may be written for convenience in the following array:

$m_{ij} =$

i\j	1	2	3	4	5	6	7
1	0	0	0	0	0	0	0
2	0	0	$-K_x x_4$	$-K_x x_3$	0	0	0
3	0	$-K_y x_4$	0	$-K_y x_2$	0	0	0
4	0	$-K_z x_3$	$-K_z x_2$	0	0	0	0
5							
6							
7							

(A-27) *

---

* See the low torque case for the expressions for $2m_{ij}$, $i = 5,6,7$ and $j = 1,\ldots,7$.

APPENDIX B: STEEPEST-DESCENT

Equations are derived in this Appendix which describe how variations in the terminal conditions and in the initial state $\bar{x}(t_o)$ effect a change in control history, both for the conventional method where the elements of $\bar{u}$ are not bounded, and for the extended method where the u_j are bounded.

1. Conventional Method

The expression for $\delta\bar{u}(t)$ is derived here. From (5-2) it is seen that by being able to compute $\delta\bar{u}(t)$, the new control history $\bar{u}(t)$ may be found, since $\bar{u}_n(t)$ is already known. The technique that will be employed in this derivation is to minimize $V(t)$ defined in expression (5-15) subject to the $\delta\bar{\psi}$ constraint of (5-14) [Ref. 5-5]. For this purpose let $t = t_o$ in equation (5-14). For the present analysis $t_o, W(t), \delta\bar{\psi}, \delta\bar{x}(t_o), \Lambda^T(t_f,t)$ and $G(t)$ are considered known. The $\bar{\psi}$ vector here will contain, as its first element, the difference between the cost functional $\emptyset$ and its desired minimum value $\emptyset_d$; therefore, $\bar{\psi}$ becomes a $p + 1$ vector:

$$\bar{\psi} = \begin{bmatrix} \emptyset - \emptyset_d \\ \psi_1 \\ \vdots \\ \psi_p \end{bmatrix} = 0 . \tag{B-1}$$

Note that in most problems the actual value of $\emptyset_d$ will not be known beforehand. The matrix $\Lambda^T(t_f,t)$ of (5-11) now becomes a $(p + 1) \times n$ matrix since $\bar{\psi}$ has become a $(p + 1)$ vector. Since the constraint

$\overline{\psi}$ does not contain time explicity the variation in the augmented vector $\overline{\psi}$ may be written as:

$$\delta\overline{\psi} = \overline{\psi}[x(t_f)] - \overline{\psi}[x_n(t_f)] \quad , \tag{B-2}$$

where the first term on the right indicates what $\overline{\psi}$ may be equal to on the next iteration and the second term indicates the value of the constraint, resulting from the present nominal trajectory. By requiring the constraint (B-1) to be met (to a first order approximation) on the next iteration, (B-2) becomes:

$$\boxed{\delta\overline{\psi} = -\overline{\psi}[\overline{x}_n(t_f)] \quad .} \tag{B-3}$$

where $\overline{\psi}$ is as defined in (B-1).

Minimizing $V(t_o)$ subject to an integral constraint (5-14) is equivalent to an isoperimetric problem in the calculus of variations [Ref. A-6]. Therefore, mimimize the new functional V^* :

$$V^* = \int_{t_o}^{t_f} [\delta\overline{u}^T W(\tau)\delta\overline{u} - \mu^T \Lambda^T(t_f,\tau)G(\tau)\delta\overline{u}(\tau)]d\tau$$

$$+ \mu^T[\delta\overline{\psi} - \Lambda^T(t_f,t_o)\delta\overline{x}(t_o)] \tag{B-4}$$

where $\mu = $ a $p + 1$ vector of constants. The first variation in (B-4) leads to:

$$\delta V^* = \int_{t_o}^{t_f} [2\delta\overline{u}^T W(\tau) - \mu^T \Lambda^T(t_f,\tau)G(\tau)]\delta(\delta\overline{u})d\tau \tag{B-5}$$

For an extremum in V^*, $\delta V^* = 0$ for arbitrary variations $\delta(\delta\bar{u})$. The integrand of (B-5) must vanish leading to:

$$\delta\bar{u}(t) = (1/2)W^{-1}(t)G^T(t)\Lambda(t_f,t)\mu \qquad \text{(B-6)}$$

where $(\ )^{-1}$ denotes the inverse of a matrix. Substituting (B-6) into (5-14) gives

$$\delta\bar{\psi} = \Lambda^T(t_f,t_o)\delta\bar{x}(t_o) + (1/2)C(t_o)\mu \quad , \qquad \text{(B-7)}$$

with the defining relationship:

$$\boxed{C(t_o) = \int_{t_o}^{t_f} \Lambda^T(t_f,\tau)G(\tau)W^{-1}(\tau)G^T(\tau)\Lambda(t_f,\tau)d\tau \quad .} \qquad \text{(B-8)}$$

Thus the vector μ may be written from (B-7) as:

$$\mu = 2C^{-1}(t_o)[\delta\bar{\psi} - \Lambda^T(t_f,t_o)\delta\bar{x}(t_o)] \qquad \text{(B-9)}$$

Finally the desired expression for $\delta\bar{u}(t)$ is written by using (B-6) and (B-9):

$$\boxed{\delta\bar{u}(t) = W^{-1}(t)G^T(t)\Lambda(t_f,t)C^{-1}(t_o)[\delta\bar{\psi} - \Lambda^T(t_f,t_o)\delta\bar{x}(t_o)]} \qquad \text{(B-10)}$$

As stated in [Ref. 5-5] the time t_o may possess discrete values t_k, or may be a running continuous variable t if so desired.

By defining two more matrices

$$\boxed{\begin{aligned} L_1(t) &\equiv W^{-1}(t)G^T(t)\Lambda(t_f,t), \text{ an } m \times (p+1) \text{ matrix} \\ L_2(t_o) &\equiv C^{-1}(t_o)\Lambda^T(t_f,t_o) \quad , \text{ a } (p+1) \times n \text{ matrix,} \end{aligned}} \qquad \text{(B-11)}$$

136

equation (B-10) is written as

$$\delta\bar{u}(t) = L_1(t)C^{-1}(t_o)\delta\bar{\psi} - L_1(t)L_2(t_o)\delta\bar{x}(t_o)$$ (B-12)

Expression (B-12) describes how a variation in the augmented terminal constraint, $\delta\bar{\psi}$, and a variation in the state $\bar{x}_n$ at $t = t_o$ influence a change in control history.

2. Extended Method

The expression for $\delta\bar{u}(t)$ is now derived with the elements of $\bar{u}$ bounded. A similar technique from the calculus of variations is employed here as in the section above; however, equations (5-23), (5-24) and (5-25) provide the starting place in this case.

Minimize the new functional V* :

$$V^* = \sum_i [\delta\bar{u}^T T_i \delta\bar{u} - \mu^T \Lambda^T(t_f, t_i)G_i\delta\bar{u}(t_i)]$$ (B-13)

$$+ \mu^T[\delta\bar{\psi} - \Lambda^T(t_f, t_o)\delta\bar{x}(t_o)]$$

where $G_i = G(t_i)$. The first variation of V* leads to:

$$\delta V^* = \sum_i [2\delta\bar{u}^T T_i - \mu^T\Lambda^T(t_f, t_i)G_i]\delta[\delta\bar{u}(t_i)] .$$ (B-14)

For an extremum in V*, $\delta V^* = 0$ for arbitary variations in $\delta(\delta\bar{u}(t_i)$. Each term of the summation (B-14) must vanish leading to:

$$\delta u(t_i) = 1/2 T_i^{-1}G_i^T\Lambda(t_f, t_i)\mu .$$ (B-15)

Substituting (B-15) into (5-24) gives

137

$$\delta\bar{\psi} = \Lambda^T(t_f, t_o)\delta\bar{x}(t_o) + (1/2)D(t_o)\mu \qquad \text{(B-16)}$$

with the defining relationship:

$$D(t_o) = \sum_i \Lambda^T(t_f, t_i)G_i T_i^{-1}G_i^T\Lambda(t_f, t_i) \quad . \qquad \text{(B-17)}$$

Thus the vector μ may be written from (B-16) as

$$\mu = 2D^{-1}(t_o)[\delta\bar{\psi} - \Lambda^T(t_f, t_o)\delta\bar{x}(t_o)] \qquad \text{(B-18)}$$

An expression for $\delta\bar{u}(t)$ for this case may be written by using (B-15) and (B-18):

$$\delta\bar{u}(t_i) = T_i^{-1}G_i^T\Lambda(t_f, t_i)D^{-1}(t_o)[\delta\bar{\psi} - \Lambda^T(t_f, t_o)\delta\bar{x}(t_o)] \qquad \text{(B-19)}$$

By defining

$$N_1(t_i) \equiv T_i^{-1}G_i^T\Lambda(t_f, t_i), \text{ an } m \times (p + 1) \text{ matrix} \qquad \text{(B-20)}$$

$$N_2(t_o) \equiv D^{-1}(t_o)\Lambda^T(t_f, t_o) \, , \quad \text{a } (p + 1) \times n \text{ matrix}$$

the equation (B-19) is written as

$$\delta\bar{u}(t_i) = N_1(t_i)D^{-1}(t_o)\delta\bar{\psi} - N_1(t_i)N_2(t_o)\delta\bar{x}(t_o) \qquad \text{(B-21)}$$

Note the similarity between (B-12) and (B-21). Relationship (B-21) provides information as to how the switching times must be changed from their nominal values $\bar{u}_n(t_i)$ before the next iteration is begun.

138

3. Computational Techniques

A computation algorithm is presented here for application of the method of steepest-descent to systems with bounds on the control variables.

i. Guess a nominal control time history $\bar{u}_n(t)$, integrate the system differential equations forward until t_f is reached, storing the values of $\bar{x}_n(t)$ at a set of sufficiently small time intervals.

ii. Compute the matrix $\Lambda^T(t_f, t_f)$, (5-13), and integrate the adjoint system of (5-12) backward in time from t_f using the stored values of $\bar{x}_n$. Compute and store $N_1(t_i)$ at each of the switching times t_i .

iii. If so desired, set $t = t_o$ and allow t to become a running variable with discrete values and calculate the matrices $D(t_k)$ of equation (B-17) where $t_k = t_o, t_i, \ldots, t_r$ with $t_r < t_f$. In each case the summation $D(t_k)$ is performed over all values of switching times t_i where $t_k \le t_i \le t_f$. Invert the $D(t_k)$ matrices, and store these resulting matrices along with the $N_2(t_k)$ matrices.

iv. Integrate the equations forward again based upon a new control history of switching times $\bar{u}(t_i) = \delta \bar{u}(t_i) + \bar{u}_n(t_i)$ where $\delta \bar{u}(t_i)$ is calculated from (B-21). Again the variable t_o may take on discrete values $t_o, t_i, \ldots, t_r$. The $\delta \bar{x}(t_k)$ vector is calculated by (5-2) and the $\delta \bar{\psi}$ vector selected as in (B-3) for use in (B-21). No attempt is made to improve the payoff function until further iterations partially satisfy the terminal constraints. The new values of $\bar{x}(t)$, based on the new $\bar{u}(t_i)$ which has become $\bar{u}_n(t_i)$ are stored

as $\bar{x}_n(t)$. This iterative procedure of forward and backward interation and of updating the control variable and state variable nominal histories is continued until convergence to a satisfactory trajectory is achieved.

In order to simplify the simulation it has been required that the newly calculated switching times resulting from $\delta\bar{u}(t_i)$ and equation (5-23) retain their order in time for each component of the control vector and the t_i satisfy $t_o \leq t_i \leq t_k$. As an example the set of pulses for the u_i element may be changed from that of Figure B-1a to that of Figure B-1b. The pulses can expand and contract and even collapse.
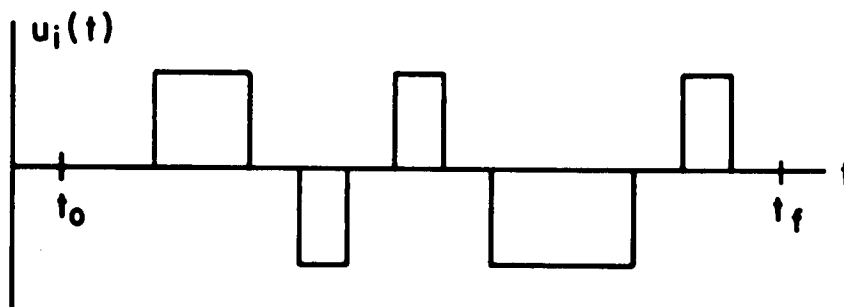
(a) ORIGINAL CONTROL
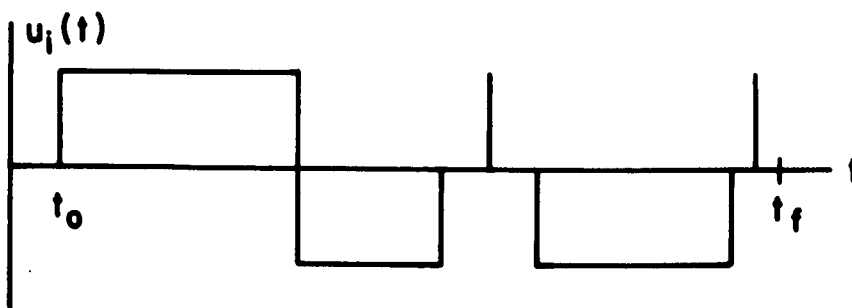
(b) SUBSEQUENT CONTROL

FIGURE B-1. INITIAL CONTROL AND SUBSEQUENT CONTROL RESULTING FROM APPLICATION OF METHOD OF STEEPEST-DESCENT

The simulations in this report were performed on the Burroughs B-5500 digital computer using Extended ALGOL as the programming language. Tapes were generated on the B-5500 for plotting on a Calcomp plotter.

Numerical integration was accomplished by a subroutine called Kutta-Merson which provides a variable step size control commensurate with required integration accuracy bounds [Ref. B-1].

REFERENCES

1-1. W. H. Foy, "Fuel Minimization in Flight Vehicle Attitude Control," IEEE Trans. on Automatic Control, AC-8, April 1963.

1-2. J. S. Meditch, "On the Problem of Optimal Thrust Programming for a Lunar Soft Landing," Conference Paper, 5th JACC, Stanford, Calif., June 1964.

1-3. M. Athans, "Fuel-Optimal Singular Control of a Nonlinear Second Order System," Conference Paper, 5th JACC, Stanford, Calif., June 1964.

1-4. H. J. Kelley, "Gradient Theory of Optimal Flight Paths," Journal of American Rocket Society, 30, 1960.

1-5. A. E. Bryson, W. F. Denham, F. J. Carroll, and K. Mikami, "Lift or Drag Programs That Minimize Re-Entry Heating," Journal of the Aerospace Sciences, 29, April, 1962.

1-6. M. Athans, P.L. Falb, R. T. Lacoss, "Optimal Control of Self-Adjoint Systems," IEEE Trans. Appl. Ind., 83, May, 1960.

2-1. L. S. Pontryagin, V. G. Boltyanskii, R. V. Gamkrelidze, E. F. Mishchenko, The Mathematical Theory of Optimal Processes, Interscience Publishers, New York, 1962.

2-2. P. C. Wheeler, "Magnetic Attitude Control of Rigid Axially Symmetric Spinning Satellites in Circular Earth Orbits," SUDAER No. 224, Department of Aeronautics and Astronautics, Stanford University, Stanford, Calif., April 1965.

2-3. I. Flügge-Lotz, H. Marback, "The Optimal Control of Some Attitude Control Systems for Different Performance Criteria", ASME Journal of Basic Engineering, 85, 2, June 1963.

2-4. C. D. Johnson, J. E. Gibson, "Singular Solutions in Problems of Optimal Control," IEEE Transactions on Automatic Control, AC-8, 1, Jan. 1963.

2-5. B. Friedland, P. E. Sarachik, "Indifference Regions in Optimum Attitude Control," IEEE Transactions on Automatic Control, AC-9, 2, April 1964.

2-6. K. A. Hales, "Comparison of Time Optimum vs. Linear Switching of a Second-Order Rate-Type Pneumatic 'Bang-Bang' Servo," S. M. Thesis, Department of Mechanical Engineering, Massachusetts Institute of Technology, Cambridge, Mass., Aug. 1961.

2-7. C. E. Hutchinson, "Minimum-Time Control of a Linear Combination of State Variables," TR No. 6311-1, Stanford Electronics Laboratories, Stanford University, Stanford, Calif., Aug. 1963.

2-8. A. Craig and I. Flügge-Lotz, "Realization of Minimum Control-Effort Optimum Control," SUDAER No. 171, Department of Aeronautics and Astronautics, Stanford University, Stanford, Calif., Oct. 1963. See also *Journal of Basic Engineering*, 87-D, 1, Mar. 1965.

2-9. D. K. Frederick, "Piecewise-Linear Switching Functions for Quasi-Minimum-Time Contactor Control Systems," SUDAER No. 178, Department of Aeronautics and Astronautics, Stanford University, Stanford, Calif., Dec. 1963.

2-10. B. B. Gragg, "Computation of Approximately Optimal Control" SUDAER No. 179, Department of Aeronautics and Astronautics, Stanford University, Stanford, Calif., Jan. 1964.

2-11. R. Sridhar et. al., "Investigation of Optimization of Attitude Control Systems," Vol I, II, JPL No. 65-185, Jet Propulsion Laboratory, Pasadena, Calif., Jan. 1965.

3-1. A. Sabroff, R. Farrenkopf, A. Frew, and M. Gran, "Investigation of the Acquisition Problem in Satellite Attitude Control," 4154-6008-RU000, TRW Space Technology Laboratories, Redondo Beach, Calif., 31 March 1965.

3-2. R. Pringle, "On the Capture, Stability, and Passive Damping of Artificial Satellites," SUDAER No. 181, Department of Aeronautics and Astronautics, Stanford University, Stanford, Calif., April 1964. See also "Bounds on the Librations of a Symmetrical Satellite," *AIAA Journal*, 2-5, May 1964.

5-1. L. A. Zadeh, C. A. Desoer, *Linear System Theory The State Space Approach*, McGraw-Hill, New York, 1963.

5-2. W. F. Denham, "Range Maximization of a Surface-to-Surface Missile with In-Flight Inequality Constraints," *Journal of Spacecraft and Rockets*, I-1, Jan. 1964.

5-3. H. J. Kelley, R. E. Kopp and H. G. Moyer, "Successive Approximation Techniques for Trajectory Optimization, "*Proceedings of Institute Aerospace Science, Symposium on Vehicle Systems Optimization*, Institute of Aerospace Sciences, New York, Nov. 1961.

5-4. A. E. Bryson and W. F. Denham, "A Steepest-Ascent Method for Solving Optimum Programming Problems," *Journal of Applied Mechanics*, 29, June 1962.

5-5. A. E. Bryson and W. F. Denham, "Multivariable Terminal Control for Minimum Mean Square Deviation from a Nominal Path", BR-1333, Raytheon Company, Sudbury, Mass., 20 Sept. 1961.

5-6. R. Rosenbaum, "Convergence Technique for the Steepest-Descent Method of Trajectory Optimization," (technical note), *AIAA J.*, I-7, July 1963.

5-7. H. J. Kelley, "Guidance Theory and Extremal Fields," IRE Transaction on Automatic Control, AC-7, 5, Oct. 1962.

5-8. W. F. Denham and A. E. Bryson Jr., "Optimal Programming Problems with Inequality Constraints II: Solution by Steepest-Ascent," AIAA J., II-1, Jan. 1964.

5-9. Capt. R. F. Vachino, "Steepest Descent with Inequality Constraints on the Control Variables", Paper presented at First International Conference on Programming and Control, USAF Academy, Colo., April 1965.

5-10. W. F. Denham, Private Correspondence, 5 Aug. 1965.

6-1. W. Hahn, Theory and Application of Liapunov's Direct Method, Prentice-Hall, Englewood Cliffs, N. J., 1963.

6-2. D. D. Otten, "OGO Attitude Control Subsystem Description, Logic, and Specification" 2313-0004-RU000, Space Technology Laboratories, Redondo Beach, Calif., 4 Dec. 1961.

6-3. "Specifications for Design Standard Requirements of an Advanced OSO," X-623-62-10, Goddard Space Flight Center, Greenbelt, Md. 10 March 1962.

7-1. K. C. Nichol, "Research and Investigation on Satellite Attitude Control," AFFDL-TR-64-168 (part IA,IB), Air Force Flight Dynamics Laboratory, Research and Technology Division, AF System Command, Wright-Patterson AF Base, Ohio, June 1965.

8-1. J. E. McIntyre, "Neighboring Optimal Terminal Control with Discontinuous Forcing Functions," AIAA Journal, IV-1, Jan. 1966.

A-1. T. R. Kane, P. M. Barba, "Attitude Stability of a Spinning Satellite in an Elliptical Orbit," Journal of Applied Mechanics, Paper No. 65-APMW-27.

A-2. H. Goldstein, Classical Mechanics, Addison-Wesley Press, Inc., Cambridge, Mass., 1950.

A-3. D. B. De Bra, "The Large Attitude Motions and Stability, due to Gravity, of a Satellite with Passive Damping in an Orbit of Arbitrary Eccentricity about an Oblate Body", SUDAER No. 126, Department of Aeronautics and Astronautics, Stanford University, Stanford, Calif., May 1962.

A-4. E. T. Whittaker, A Treatise on the Analytical Dynamics of Particles and Rigid Bodies, 4th Ed., Cambridge University Press, London, 1964.

A-5. R. H. Frick and T. B. Garber, "General Equations of Motion of a Satellite in a Gravitational Gradient Field" RM-2527, The Rand Corp., Santa Monica, Calif., 9 Dec. 1959.

A-6. I. M. Gelfand and S. V. Fomin, <u>Calculus of Variations</u>, Prentice-Hall, Inc., Englewood Cliffs, N. J., 1963.

B-1. L. Fox, <u>Numerical Solution of Ordinary and Partial Differential Equations</u>, Pergamon Press, Oxford, Eng., 1962.